
*User guide to ECMWF forecast
products*

© Copyright 2011, 2013 ECMWF

Date of original issue:	October 2011		
Author:	Anders Persson		
Version number	Date	Changed by	Change description
1.1	23/07/2013	Erik Andersson	New terminology, ENS initial perturbations

1.	Introduction.....	1
2.	The ECMWF forecasting and assimilation system.....	2
2.1.	The ECMWF global atmospheric model.....	2
2.1.1.	The model equations.....	2
2.1.2.	The numerical formulation.....	2
2.1.3.	The rationale for high resolution.....	3
2.1.4.	Topographical and climatological fields.....	3
2.1.5.	The formulation of physical processes.....	4
2.1.6.	The land surface model.....	6
2.1.7.	The ocean wave model.....	6
2.2.	The dynamic ocean model.....	7
2.3.	Data assimilation.....	7
2.3.1.	The four-dimensional data assimilation (4D-Var).....	8
2.3.2.	The ECMWF early delivery system.....	8
2.4.	Retrieving ECMWF forecasts.....	10
2.4.1.	Temporal retrieval.....	10
2.4.2.	Spatial retrieval.....	10
2.4.3.	Orography.....	10
2.4.4.	The bi-linear interpolation.....	10
2.4.5.	The subsampling procedure.....	12
2.4.6.	Interpolating land and sea points.....	13
2.5.	The relation between grid point values and observations.....	15
2.6.	Some characteristics of NWP output.....	16
2.6.1.	Forecast error growth.....	16
2.6.2.	Downstream spread of influence.....	16
2.6.3.	The relation between scale and predictive skill.....	17
2.6.4.	Forecast “jumpiness”.....	20
2.6.5.	Flip-flopping forecasts.....	21
2.6.6.	Jumpiness and forecast skill.....	22
2.6.7.	Forecast trends cannot be extrapolated.....	22
2.6.8.	Other state-of-the-art deterministic models.....	22
3.	The forecast ensemble.....	25
3.1.	The rationale behind the ensemble.....	25
3.1.1.	Qualitative use of the ensemble.....	25
3.1.2.	Quantitative use of the ENS.....	25
3.1.3.	Characteristics of a good ensemble.....	26
3.2.	Generation of the ENS.....	26

3.2.1.	Different perturbation techniques	26
3.2.2.	Quality of the individual perturbed analyses	29
3.2.3.	Quality of the individual perturbed forecasts.....	31
3.3.	The ensemble at different lead times	32
3.3.1.	The 10-day range.....	32
3.3.2.	The day 9 to 10 overlap	33
3.3.3.	The 10 to 15 day range	33
3.3.4.	Forecasts from 15 to 32 days	33
3.3.5.	Seasonal forecast	33
3.4.	Basic forecast products	33
3.4.1.	“Postage stamp maps”.....	33
3.4.2.	“Spaghetti diagrams”	34
3.4.3.	“Plumes”.....	34
3.4.4.	Ensemble mean and median.....	35
3.4.5.	Ensemble spread.....	35
3.4.6.	Probabilities.....	36
3.4.7.	Forecast expressed in terms of intervals.....	36
4.	Recommendations on categorical and probabilistic medium-range forecasting.....	37
4.1.	Relation between deterministic and probabilistic forecasts	37
4.2.	Differences between short- and medium-range operational use of NWP	37
4.3.	Medium-range forecasting <i>without the ensemble</i>	38
4.3.1.	Assessment based on the latest forecasts	38
4.3.2.	Assessment based on the two latest forecasts.....	38
4.3.3.	Assessment based on the last three or more forecasts.....	38
4.3.4.	Is it possible to compare manual and computer-generated deterministic forecasts?	39
4.4.	Medium-range forecasting based <i>only on the ENS</i>	40
4.4.1.	Use of the ensemble mean (EM).....	40
4.4.2.	Criticism of the EM.....	40
4.4.3.	A synoptic example of combining EM and probabilities.....	40
4.4.4.	Use of probabilities.....	42
4.4.5.	Probabilities over time intervals	43
4.4.6.	Probabilities over areas.....	44
4.4.7.	Probabilities of combined events.....	44
4.4.8.	Modification of the probabilities.....	45
4.4.9.	Calibration of probabilities	45
4.4.10.	Ensemble “jumpiness”	45
4.5.	Medium-range forecasting with the ENS <i>and</i> HRES	46

4.5.1.	Weather situations with good agreement between ENS and HRES	46
4.5.2.	When the ENS and HRES differ with respect to spread only	47
4.5.3.	Weather situations where agreement between the ENS and HRES is poor 48	
4.5.4.	Forecaster intervention with the ENS.....	51
4.6.	Forecasting high-impact weather in the medium range.....	52
4.6.1.	The forecaster's role.....	52
4.6.2.	Probabilities or categorical forecasts?	52
4.7.	Summary: do the opposite to the computer!	53
5.	Derived products based on the ENS.....	55
5.1.1.	Ensemble mean and spread charts	55
5.2.	EPSgrams.....	55
5.2.1.	Overview	55
5.2.2.	Ten-day EPSgrams.....	56
5.2.3.	Fifteen-day EPSgrams.....	57
5.2.4.	The weather parameters in EPSgrams	57
5.2.5.	Interpreting EPSgrams	59
5.3.	Wave EPSgrams	61
5.4.	The Extreme Forecast Index (EFI).....	63
5.4.1.	The EFI reference climate.....	63
5.4.2.	The cumulative distribution function	63
5.4.3.	Calculating the EFI	65
5.4.4.	The interpretation of the EFI.....	66
5.4.5.	EFI maps	67
5.5.	Tropical cyclone diagrams	67
5.6.	Cyclone track maps	70
5.7.	Clustering.....	71
5.7.1.	Weather scenario clustering.....	72
5.7.2.	Climatological weather regimes	73
5.7.3.	Tubing.....	74
6.	Epilogue: how to increase the public's trust in medium-range weather forecasts	75
6.1.	How can trust in medium-range forecasts be increased?	75
6.1.1.	Improving the forecast system	75
6.1.2.	Trust in individual forecasts	75
6.1.3.	When the deterministic forecast cannot be trusted.	75
6.2.	The role of the forecaster in the medium-range	76
6.3.	How the forecaster can "add value".....	76
Appendix A	Some statistical concepts to facilitate the use and interpretation of deterministic medium-range forecasts	77

Introduction.....	77
A-1 Forecast validation.....	77
A-1.1 The mean error.....	77
A-1.2 Forecast variability.....	78
A-1.3 False systematic errors.....	79
A-1.4 False model climate drift.....	80
A-2 Forecast verification.....	81
A-2.1 Measures of accuracy.....	81
A-2.2 The effect of mean, analysis and observation errors on the RMSE.....	81
A-2.3 The decomposition of MSE.....	82
A-2.4 Forecast error baseline.....	82
A-2.5 Error saturation level.....	83
A-2.6 Measure of skill - the anomaly correlation coefficient.....	83
A-3 Interpretation of verification statistics.....	84
A-3.1 Interpretation of RMSE and ACC.....	84
A-3.2 Effect of flow dependency.....	84
A-3.3 The “double penalty effect”.....	85
A-3.4 Subjective evaluations.....	85
A-4 Graphical representation.....	85
A-4.1 Forecast errors.....	86
A-4.2 Flow dependence.....	87
A-4.3 Damping of forecast anomalies.....	88
A-4.4 Forecast error correlation.....	88
A-4.5 Forecast jumpiness and forecast skill.....	89
A-4.6 Combining forecasts.....	89
A-5 The usefulness of statistical know-how.....	90
A-6 Utility verification.....	91
A-6.1 The contingency table.....	91
A-6.2 The “expected expenses”.....	91
A-7 Practical examples.....	92
A-7.1 A situation with no weather forecast service.....	92
A-7.2 The benefit of a local weather service.....	93
A-7.3 The establishment of two new weather services.....	93
A-8 An introduction to probabilistic weather forecasting.....	95
A-8.1 Uncertainty - how to turn a disadvantage into an advantage.....	95
A-8.2 Making even more use of uncertainty - probabilities.....	96
A-8.3 Towards more useful weather forecasts.....	98
A-8.4 Quality of probabilistic forecasts.....	98

A-8.5	When probabilities are not required	98
A-8.6	An extension of the contingency table – the “SEEPS” score.....	99
Appendix B	Some statistical concepts to facilitate the use and interpretation of ensemble forecasts	101
	Introduction.....	101
B-1	The reliability diagram	101
B-1.1	Reliability	103
B-1.2	Sharpness.....	103
B-1.3	Under- and overconfident probability forecasts.....	104
B-2	Rank histogram (Talagrand diagram)	105
B-3	Verification measures	107
B-3.1	The Brier score - the MSE of probability forecasts.....	107
B-3.2	Decomposition of the Brier score	107
B-3.3	The Brier score is a “proper” score	109
B-3.4	The Brier skill score	109
B-3.5	The rank probability score (RPS).....	109
B-4	The relative operating characteristics (ROC) diagram	109
B-5	Calibration of probabilities	111
B-6	Statistical post-processing – model output statistics.....	113
B-6.1	The MOS equation	113
B-6.2	Simultaneous corrections of mean error and variability	113
B-6.3	Short-range MOS	114
B-6.4	Medium-range MOS	114
B-6.5	Adaptive MOS methods	115
	References and further literature.....	119

1. Introduction

“Behind good forecast practices are often hidden good theories; equally, good theories should provide a basis for good forecast practices.” Professor Tor Bergeron, personal communication 1974

The aim of this User Guide is to help meteorologists make optimal use of the forecast products from ECMWF, develop new products and reach new sectors of society and thereby satisfy new demands. This is done by presenting the forecast system and advising on how best to use the output, not least how to build up trust in the forecast information. The emphasis is on the medium-range forecast products, since the way forecasters deal with medium-range NWP output differs in many ways from how they deal with short-range NWP on the one hand and monthly and seasonal NWP on the other. The main outline:

1. *The ECMWF forecasting system*, i.e. the dynamical model, the data assimilation and the product delivery system, are described in broad and non-technical terms.
2. *The interpretation of the NWP output* is complicated by its often counter-intuitive, non-linear behaviour. The high-resolution forecast (HRES) should therefore not be over-interpreted, in particular not in the medium-range or when extreme weather is likely. Then the use of probabilities or other risk assessments are needed.
3. *A good forecast that is not trusted is a worthless forecast.* The ECMWF forecast ensemble (ENS), which is given extensive coverage, provides a basis for formulating the most accurate categorical forecasts and the probabilities of alternative developments. Methods to combine HRES and ENS are suggested.
4. *In the medium-range the use of statistical know-how counts as much as synoptic experience*, since daily operational work is to a large extent a matter of assessing, combining and correcting NWP information. In two appendices statistical concepts for validating and verifying deterministic and probabilistic forecasts and for making the best use of NWP information are presented.
5. *The forecaster is not a computer.* Throughout the User Guide forecasters are advised not to try to imitate NWP, but to perform quite differently, with fewer details, more uncertainty and no “U-turns”.

This User Guide is the fruit of several years of discussions with scientists, forecasters and meteorologists who are interested in statistics, both from Europe and elsewhere. The interaction between these three specialized groups has been the main driving force and inspiration for this publication.

The User Guide gives only an introduction to the forecast information provided by ECMWF. Users are advised to keep themselves updated about the products through the ECMWF Newsletter and web site.

2. The ECMWF forecasting and assimilation system

The ECMWF forecasting system (the IFS) consists of several components: an atmospheric general circulation model, an ocean wave model, a land surface model, an ocean general circulation model and perturbation models for the data assimilation (EDA) and forecast (ENS) ensembles (see Chapter 3), producing forecasts from days to weeks and months ahead.

2.1. The ECMWF global atmospheric model

The atmospheric general circulation model describes the dynamical evolution on the resolved scale and is augmented by the physical parameterisation, describing the mean effect of sub-grid processes and the land-surface model. Coupled to this is an ocean wave model (Bechtold et al, 2008).

2.1.1. The model equations

The model formulation is based on a set of basic equations, of which some are **diagnostic** and describe the static relationship between pressure, density, temperature and height, and some are **prognostic** and describe the time evolution of the horizontal wind components, surface pressure, temperature and the water vapour contents of an air parcel.

Additional equations describe changes in the hydrometeors (rain, snow, liquid water, cloud ice content etc). There are options for passive tracers such as ozone. The processes of radiation, gravity wave drag, vertical turbulence, convection, clouds and surface interaction are, due to their relatively small scales (unresolved by the model's resolution), described in a statistical way as *parametrization processes* (arranged in entirely vertical columns).

2.1.2. The numerical formulation

The model equations are discretized in space and time and solved numerically by a *semi-Lagrangian* advection scheme. It ensures stability and accuracy, while using as large time-steps as possible to progress the computation of the forecast within an acceptable time.

For the **horizontal representation** a dual representation of spectral components and grid points is used. All fields are described in *grid point space*. Due to the convergence of the meridians, computational time can be saved by applying a “reduced Gaussian grid”. This keeps the east-west separation between points almost constant by gradually decreasing the number of grid points towards the poles at every latitude in the extra-tropics. For the convenience of computing horizontal derivatives and to facilitate the time-stepping scheme, a *spectral representation*, based on a series expansion of spherical harmonics, is used for a subset of the prognostic variables.

The **vertical resolution** is finest in geometric height in the planetary boundary layer and coarsest near the model top. The “ σ -levels” follow the earth's surface in the lower-most troposphere, where the Earth's orography displays large variations. In the upper stratosphere and lower mesosphere they are surfaces of constant pressure with a smooth transition in between.

2.1.3. *The rationale for high resolution*

The higher the numerical resolution, the more accurate the calculations become. A high spatial resolution also enables a better representation of topographical fields, such as mountains and coastlines, and the effect they have on the large-scale flow. It also produces a more accurate description of horizontal and vertical structures, which facilitates the assimilation of observations.

The smallest atmospheric features which can be resolved by high-resolution forecasts have wave lengths four or five times the numerical resolution. Although these atmospheric systems have a predictability of only some hours, which is about the time it takes to disseminate the forecasts, their representation is nevertheless important for energetic exchanges between different atmospheric scales.

Increasing the resolution not only benefits the analyses and forecasts of the small-scale systems associated with severe weather but also those of large-scale systems. The ability accurately to forecast the formation of large-scale blocking “omega” anticyclones and “cut-off lows” depends crucially on increasing the resolution to kilometres (Miller et al, 2010).

The interpolation technique used when forecasts are retrieved is presented in section 2.4.

2.1.4. *Topographical and climatological fields*

The **model orography** is derived from a data set with a resolution of about 1 km which contains values of the mean elevation above the mean sea level, the fraction of land and the fractional cover of different vegetation types. This detailed data is aggregated (“upscaled”) to the coarser model resolution.

The resulting *mean orography* contains the values of the mean elevation above the mean sea level. In mountainous areas it is supplemented by *sub-grid orographic* fields, to enable the parametrization of the effects of gravity waves and provide flow-dependent blocking of the air flow. For example, cold air drainage in valleys makes the cold air effectively “lift” the orography.

The **land-sea mask** is a geographical field that contains the percentage of land and water between 0 (100% sea) and 1 (100% land) for every grid point. A grid point is defined as a land point if its value indicates that more than 50% of the area within the grid-box is covered by land, see section 2.4.6.

The **albedo** is determined by a combination of background monthly climate fields and forecast surface fields (e.g. from snow depth). Continental, maritime, urban and desert **aerosols** are provided as monthly means from data bases derived from transport models covering both the troposphere and the stratosphere.

Soil temperatures and moisture in the ground are prognostic variables. There is a lack of observational data, so observed 2m temperature and relative humidity act as very efficient proxy data for the analysis.

The **snow coverage depth** is analysed every six hours from snow-depth observations, satellite snow extent and a snow-depth background field. The snow temperature is also analysed from satellite observations. They are forecast variables.

Sea surface temperature (SST) and ice concentration are based on analyses received daily from the Met Office (OSTIA, 5 km). It is updated during the model integration, according to the tendency obtained from climatology.

The **temperature at the ice surface** is variable and calculated according to a simple energy balance/heat budget scheme, where the SST of the underlying ocean is assumed to be -1.7°C .

The **sea-ice cover**, which is kept constant in the 10-day forecast integration, is relaxed towards climatology between days 10 and 30, with a linear regression. Beyond day 30 the sea-ice concentration is based on climatological values only (from the ERA 1979-2001 data).

2.1.5. The formulation of physical processes

The effect of sub-scale physical processes on weather systems is expressed in terms of resolved model variables in a technique called *parametrization*. It involves both statistical methods and simplified mathematical-physical models, such as adjustment processes. So, for example, the air closest to the earth's surface exchanges heat with the surface through turbulent diffusion or convection, which adjusts unstable air towards neutral stability (Jung et al, 2010).

The **convection scheme** does not predict individual convective clouds, only their physical effect on the surrounding atmosphere, in terms of latent heat release, precipitation and the associated transport of moisture and momentum. The scheme differentiates between deep, shallow and mid-level convection. Only one type of convection can occur at any given grid point at one time (see Figure 1).

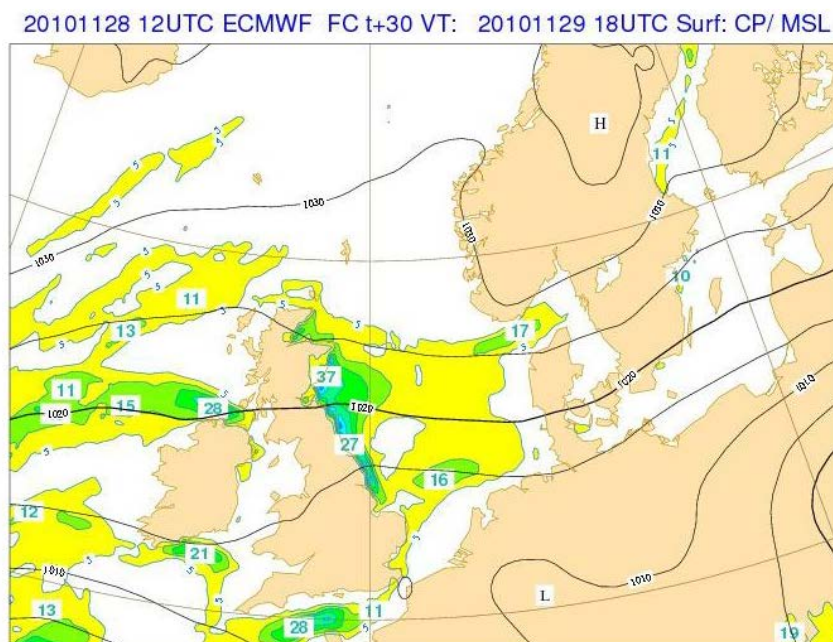


Figure 1: The ECMWF total convective rainfall forecast from 28 November 2010 12 UTC + 30h. The convection scheme has difficulty in advecting wintery showers inland over Scotland and northern England from the relatively warm North Sea. The convection scheme is diagnostic and works on a model column, so cannot produce large amounts of precipitation over the relatively dry and cold

(stable) wintery land areas. In nature these showers succeed in penetrating inland through a convectively induced upper-level warm anomaly leading to large-scale lifting and saturation.

Clouds, both convective and non-convective, are handled by explicit equations for cloud water, ice and cloud cover. Liquid and frozen precipitation are strongly coupled to other parametrized processes, in particular the convective scheme and the radiation. The scheme also takes into account important cloud processes, such as cloud-top entrainment and the evaporation of water. Fog is represented in the scheme as clouds that form in the lowest model level.

The **radiation** spectrum is divided into a long-wave part (thermal) and a short-wave part (solar radiation). Since it has to take the cloud-radiation interaction into account in considerable detail, it makes use of a cloud-overlap algorithm, which calculates the relative placement of clouds across levels. For the sake of computational efficiency, the radiation scheme is called less frequently than the model time step on a reduced grid. Nevertheless, it accounts for a considerable fraction of the total computational time.

For **the precipitation and hydrological cycles** both convective and stratiform precipitation are included in the ECMWF model. *Evaporation* of the precipitation, before it reaches the ground, is assumed not to take place within the cloud, only in the cloud-free, non-saturated air beside or below the model clouds. The *melting* of falling snow occurs in a thin layer of a few hundred metres below the freezing level. It is assumed that snow can melt in each layer, whenever the temperature exceeds 0°C. The cloud-overlap algorithm is also important for the “life history” of falling precipitation: from level-with-cloud to level-with-clear-sky and vice versa.

The **near-surface wind forecast** displays severe weaknesses in some mountain areas, due to the difficulty in parametrizing the interaction between the air flow and the highly varying sub-grid orography (see Figure 2). As with many other sub-grid-scale physical processes that need to be treated in simplified ways, this problem will ultimately be reduced when the air-surface interaction can be described explicitly, thanks to a higher and appropriate resolution. The system also produces wind-gust forecasts as part of post-processing (Balsamo et al, 2011).

20110302 12UTC ECMWF FC +12 VT: 20110303 00UTC Surf: 10U/ 10V/ MSL

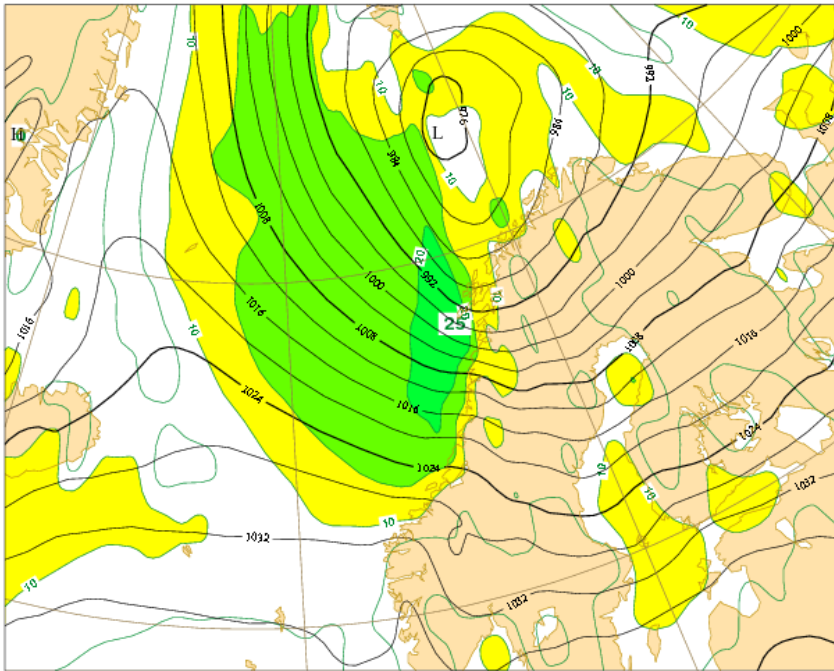


Figure 2: MSLP and 10 m wind forecast from 2 March 2011 12 UTC + 12 h. The 10 m winds are unrealistically weak over the rugged Norwegian mountains. Values of 10 m/s might be realistic in sheltered valleys, but not on exposed mountain ranges.

2.1.6. The land surface model

In the H-TESSSEL scheme (Hydrology-Tiled ECMWF Scheme for Surface Exchange over Land) the main types of natural surfaces found over land are represented by a "mosaic" approach. In other words, each atmospheric model grid-box is in contact and exchanges energy and water with up to 6 different types of parcel or "tile" on the ground. These are: bare soil, low and high vegetation, water intercepted by leaves, and shaded and exposed snow.

Each land-surface tile has its own properties, describing the heat, water and momentum exchanges with the atmosphere; particular attention is paid to evaporation, as near-surface temperature and humidity are very closely related to this process.

The soil (with its four layers) and the snow-pack (with one layer) have dedicated physical parametrizations, since they represent the main land reservoirs that can store water and energy and release them into the atmosphere in lagged mode.

Finally, the vegetation seasonality is described by the leaf area index (LAI) from climatological data. The LAI describes the growing, mature, senescent and dormant phases of several vegetation types in H-TESSSEL (four types of forests and ten types of low vegetation).

2.1.7. The ocean wave model

The wave model at ECMWF is called the "WAM". It describes the rate of change of the 2-dimensional wave spectrum, in any water depth, caused by advection, wind input, dissipation due to white capping and bottom friction and non-linear wave interactions. It is set up so as to allow the two-way interaction of wind and waves with the atmospheric model. It is also incorporated in the medium-range, monthly and seasonal ensembles.

Radar altimeter wave-height data are assimilated from satellites. Buoy wave data are not assimilated; instead, they serve as an independent check on the quality of modelled wave parameters. The propagation of swell in the wave model is handled by a simple scheme that gives rise to a smoothing of the wave field. At present the effects of surface currents on the sea state are not taken into account. In particular areas, such as the Gulf Stream or Agulhas current, the current effect may give rise to localised changes of up to one metre in the wave height.

The representation of the sea-ice fields is not as accurate as would be needed to handle waves near the ice edge. Due to the present model resolution, wave products near the coasts and, to a lesser extent, in small enclosed basins (e.g. the Baltic Sea) may be of lower quality than the open-ocean products.

2.2. The dynamic ocean model

The three-dimensional general circulation ocean model can reproduce the general features of the circulation and the thermal structure of the upper layers of the ocean and its seasonal and inter-annual variations. It has, however, systematic errors, some of which are caused by the coarse vertical and horizontal resolution: the model thermocline is too diffuse; the Gulf Stream does not separate at the right location.

The ocean analysis is performed every 10 days, down to a depth of 2000 m. Observational input comes from all around the globe, but mostly from the tropical Pacific, the tropical Atlantic and, to an increasing degree, from the Indian Ocean. In places where the ocean floor is below 2000 m the information from above 2000 m is “propagated” downwards by statistical vertical influence functions, similar to those in the atmospheric data assimilation.

The *ocean-atmosphere coupling* is achieved by a two-way interaction: the atmosphere affects the ocean through its wind, heat and net precipitation (precipitation-evaporation), whilst the ocean affects the atmosphere through its SST.

For the seasonal forecasts the interaction is once a day, while for the ENS it is every hour. This high-frequency coupling may have some positive impact on the development of some synoptic-scale systems, such as tropical cyclones.

2.3. Data assimilation

The observations used for the analysis of the atmosphere can be divided roughly into conventional, in-situ observations and non-conventional, remote-sensing observations.

The *conventional observations* consist of direct observations from surface weather stations, ships, buoys, radiosonde stations and aircraft, both at synoptic and, increasingly, at asynoptic hours. All surface and mean sea-level-pressure observations are used, with the exception of cloud cover, 2 m temperature and wind speed (over land). 2 m temperature and dew point observations are used in the analysis of soil moisture. Observed winds are used from ships and buoys but not from land stations, not even from islands or coastal stations.

The *non-conventional observations* are achieved in two different ways: *passive technologies* sense natural radiation emitted by the earth and atmosphere or solar radiation reflected by the earth and atmosphere; *active technologies* transmit radiation and then sense how much is

reflected or scattered back. In this way surface-wind vector information is, for example, derived from the influence of the ocean capillary waves on the back-scattered radar signal of scatterometer instruments (Hersbach and Janssen, 2007).

2.3.1. *The four-dimensional data assimilation (4D-Var)*

The increasing availability of asynoptic data and non-conventional observations has necessitated the use of advanced analysis procedures, such as four-dimensional variational data assimilation (4D-Var), where the concept of a continuous feedback between observations and model data is put on a firm mathematical foundation (Andersson and Thépaut, 2008).

The 4D-Var analysis uses the model dynamics and physics to create, over a time window, (currently 12 hours), a sequence of model states that fits as closely as possible with the available observations and background, i.e. a short-range forecast that serves to bring the information forward from the previous cycle. These states are consistent with the dynamics and physics of the atmosphere, as expressed by the equations of the model. The correction of one model variable generates physically and dynamically consistent corrections of other variables. For instance, a sequence of observations of humidity from a satellite infrared instrument that shows a displacement of atmospheric structures will entail a correction not only of the moisture field but also of the wind and temperature fields.

The impact of the observations is determined by the assumed accuracy of the observations and the model short-range forecasts. While the former can be regarded as more or less static, the latter are flow-dependent; the uncertainty may be larger in a developing baroclinic low than in a subtropical high-pressure system. The background-error accuracy is also dependent on the local observation density. To estimate the flow-dependent uncertainty, a set of 3-hour forecasts, valid at the start of the 4D-Var time window, is computed from ten perturbed, equally likely analyses. They differ because of small variations imposed on the observations, the sea surface temperature and model error parameterization. These variations reflect the uncertainties in the observations, the SST and the forecast evolution. The perturbations produced using this *ensemble of data assimilations* (EDA) are also used for the construction of the perturbations in the forecast ensemble (see chapter 3, in particular Section 3.2.1. For further detail on the EDA see Isaksen et al, 2010).

The 4D-Var system handles all observational data similarly, including radiances from satellites. It compares the actual observations with what would be expected, given the model fields. For satellite radiances the variational scheme modifies the model fields of temperature, wind, moisture and ozone in such a way that the simulated observations are brought closer to the observed values.

2.3.2. *The ECMWF early delivery system*

The 4D-Var analysis uses observations from a 12-hour time window, either 21 - 09 UTC (for the 00 and 06 UTC analyses) or 09 - 21 UTC (for the 12 and 18 UTC analyses). To provide the best initial condition for the next analysis a full resolution 3-hour forecast is run, based on the previous 4D-Var analysis (see Figure 3).

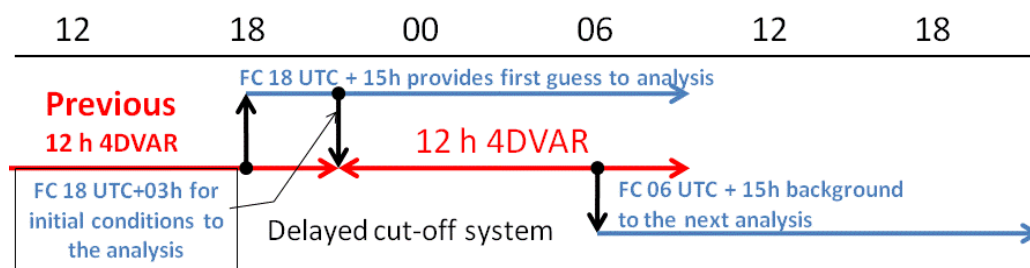


Figure 3: The 00 UTC cycle of the delayed cut-off 4D-Var analysis covering 21 – 09 UTC starts with a 15-hour forecast from the previous 18 UTC 4D-Var delayed cut-off analysis (the 09 - 21UTC assimilation). Waiting for most of the available observations to arrive, the delayed cut-off analysis starts at 14:00 UTC using the 3-hour forecast as initial condition. The rest of the 15-hour forecast is used as background (“first guess”) for the 12-hour delayed cut-off 4D-Var analysis (and similarly for the next 12 UTC analysis cycle).

To ensure the most comprehensive global data coverage, including southern hemisphere surface data and global satellite-sounding data, the 4D-Var analysis waits about 5 hours to ensure that almost all available observations have arrived.

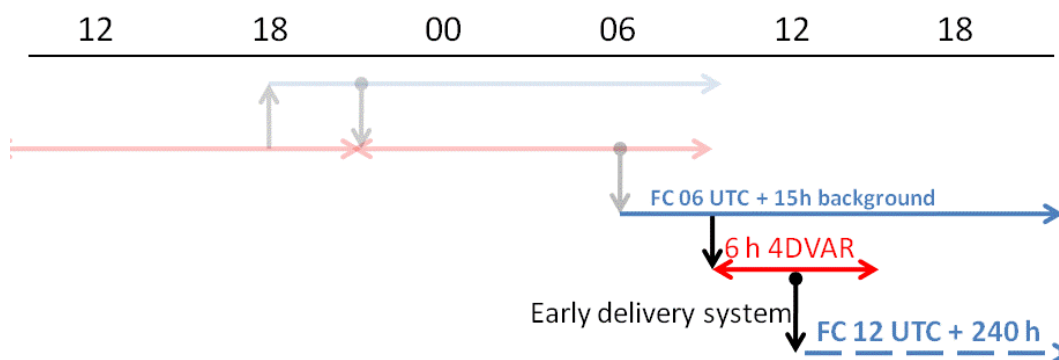


Figure 4: The 12 UTC cycle of the early delivery analysis also starts from a 3-hour forecast, now from 06 UTC, which is used as the background (“first guess”) for a 6-hour early delivery 4D-Var analysis covering the time interval 09 - 15 UTC. The operational ten-day forecast then starts from the 12 UTC analysis at about 16:30 UTC. The early delivery cut-off 12 UTC analysis starts at 16:00 UTC.

Although waiting for later data benefits the quality of the analysis and its subsequent forecast, it adversely affects product timeliness. To overcome this problem, ECMWF has introduced its *early delivery system*, which allows the 00 and 12 UTC operational analyses to be produced significantly earlier, without compromising the operational quality of the forecast products (see Figure 4).

To achieve this, an early cut-off analysis is made, relying on observations arriving during the first four hours, which accounts for about 85% of the available global observations. Since 80 - 85% of the value of each 4D-Var analysis stems from the background (“first guess”) information and only 15-20% from the latest observations, not making use of the remaining 15% of the observations reduces the predictive skill by a few hours. Since this enables ECMWF to disseminate its forecasts 10 hours earlier, there is an operational gain of 4 - 6 hours in effective predictability. It is important to note that the background information always comes from the 12-hour 4D-Var where, thanks to the late cut-off, almost all available observations have been used.

2.4. Retrieving ECMWF forecasts

The exact value of the forecast parameters can be affected by the way the data is retrieved, interpolated and presented.

2.4.1. Temporal retrieval

All forecast parameters, both surface and upper air, based on 00 and 12 UTC HRES and ENS, are available at 3-hourly intervals up to +144 hours and at 6-hourly intervals from +150 to +240 hours. The parameters are available hourly up to +90 hours to members of the Boundary Conditions (BC) optional programme. Also available to BC programme members are two additional cycles, at 06 and 18 UTC, with all forecast parameters, both surface and upper air available hourly up to +90h.

Precipitation forecasts are provided as values accumulated from the start of the forecast integration. The range of the daily variation of the forecast 2 m temperature and wind gust is best estimated by retrieving the forecast maximum and minimum values. In both cases the valid time is defined as the time at the end of the period. The combination of accumulated and instantaneous forecast information can occasionally lead to inconsistencies, for instance, during the passage of a cold front: whereas there might be almost cloud-free conditions at the *end* of the interval, they will be timed together with significant precipitation amounts accumulated over the *whole* time interval.

2.4.2. Spatial retrieval

ECMWF forecast products can be retrieved at a wide range of spatial resolutions, from regular and rotated lat-lon grids to the original regular and reduced Gaussian grid. The data can be retrieved from model, pressure, isentropic or iso-potential vorticity (PV) levels, depending on the parameter.

Temperature, wind and geopotential forecast information is stored in spectral components but can be interpolated to any specified latitude-longitude grid. This interpolation can also be applied to near-surface parameters, although direct use of the original reduced Gaussian grid point values is strongly recommended, especially for precipitation and other surface fluxes to avoid the undesired effects of interpolation.

2.4.3. Orography

Because valleys and mountain peaks are smoothed out by the model orography the direct model output of 2 m temperature may represent an altitude significantly different from the real one. A more representative height might be found at one of the nearby grid points. Any remaining discrepancy can be overcome by a correction using the Standard Atmosphere lapse rate or statistical adaptation (see Appendix B-6).

2.4.4. The bi-linear interpolation

Since 1979 ECMWF has used a bi-linear interpolation technique because of its efficiency. It uses the 2 x 2 grid points closest to the selected interpolation location and takes a weighted average to arrive at the interpolated value (see Figure 5).

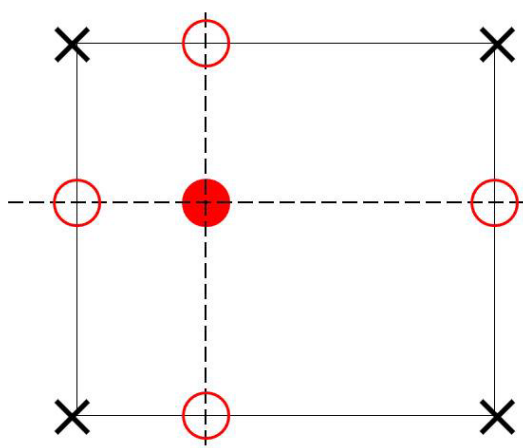


Figure 5: Bi-linear interpolation of four model grid points (black crosses) starts by linear interpolation between each pair of grid points (red circles). These two, in either the latitudinal or longitudinal direction, are then used for interpolation to the requested location (filled circle), weighted according to their distance from each of the model grid points.

The weights are based on the distance of the interpolated location from each of the model grid points. Although linear in both directions, the bi-linear interpolation is not linear but quadratic, except along lines which connect the model grid points (see Figure 6).

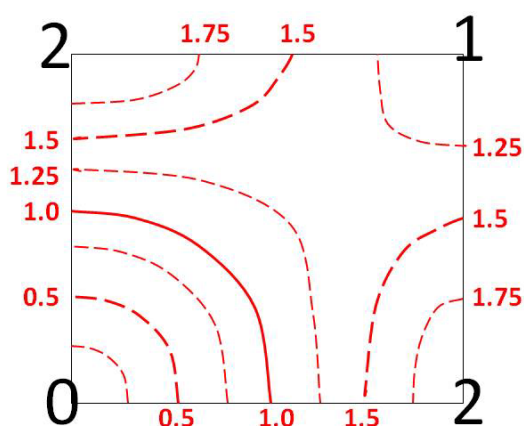


Figure 6: Example of bilinear interpolation for any location within the grid box. The interpolated value for the centre is 1.25, but may take any value between 0 and 2 elsewhere.

Every interpolation technique has its advantages and disadvantages. When the interpolation grid length is significantly coarser than the model grid, small-scale variability might misleadingly appear to represent larger scales. If, for example, the interpolation is made to a location close to one of the grid points, it will more or less take this value, even if it happens to represent a small-scale extreme. Only if the interpolation point is in the centre, does an interpolated value represent the mean over the grid-box area.

For the dissemination, all fields are bi-linearly interpolated to a 0.125° lat/lon grid, corresponding to a 13.5 km resolution in the meridional direction.

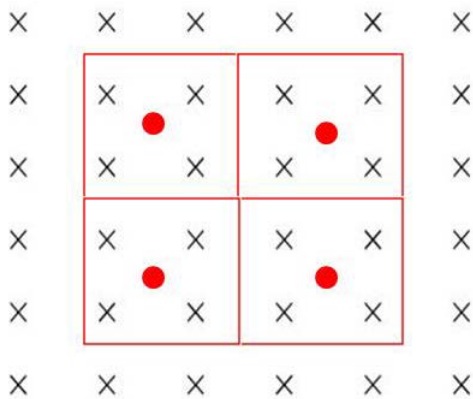


Figure 7: For a given interpolation grid (red circles) the proportion of model information taken into account depends on the model grid resolution (black crosses). When the interpolated grid is twice the model grid length (or less), all model grid values will be used in the interpolation.

When the model grid is *less* than half the interpolation grid length, the proportion of used grid points decreases (see Figure 7). If, for example, the model grid length is a quarter of the interpolation grid, only a quarter of the model grid points are taken into account. This has the undesired effect of not conserving area totals, which makes it unacceptable for use for surface fields, such as precipitation.

2.4.5. The subsampling procedure

Data may be requested on grids much coarser than 0.125° or 13.5 km. Then a subsample of the 0.125° resolution grid points is selected. If, for example, interpolated values in 0.5° , 1.0° or 1.5° resolutions are requested, every 4th, 8th or 12th interpolated value will be selected and disseminated (see Figure 8).

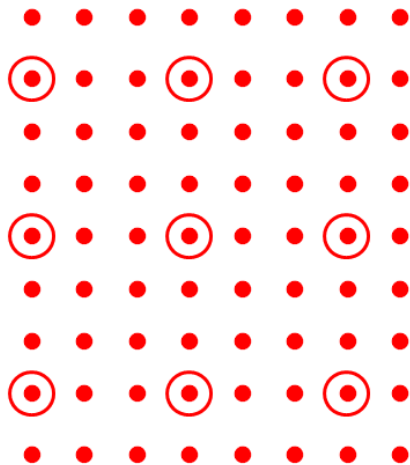


Figure 8: When the requested interpolation grid length is, for example 0.5° , every 4th of the bi-linearly interpolated values (red circles) in a 0.125° resolution is selected.

This will have the undesired effect that model grid point values which, essentially represent small scales, may by chance appear to represent much larger scales (see Figure 9).

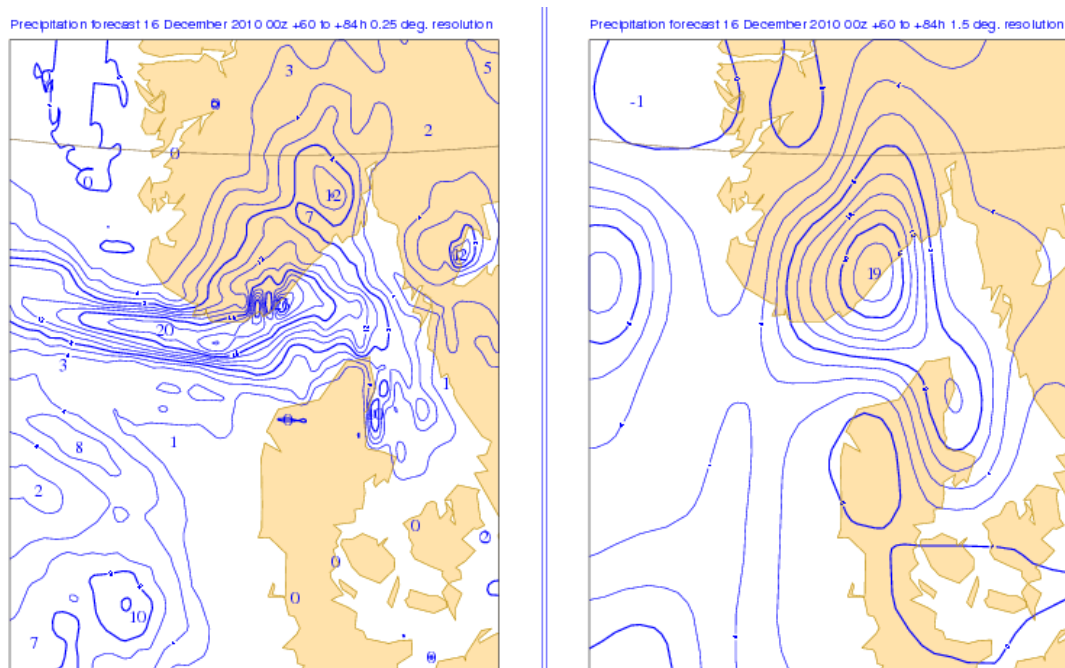


Figure 9: Example of the effect of inappropriate interpolation of precipitation fields. To the left the forecast is interpolated in a $0.25 \times 0.25^\circ$ grid, to the right in a $1.5 \times 1.5^\circ$ grid.

2.4.6. Interpolating land and sea points

When the interpolation of the 2 m temperature or 10 m wind takes place over or near a coast line, the interpolation makes use of the land-sea mask (see Section 2.1.4) to decide whether the four grid points are land or sea points (see Figure 10). This determines whether the interpolated value should be regarded as a land or sea point. In this way there will be no undesired smoothing of gradients along coast lines.

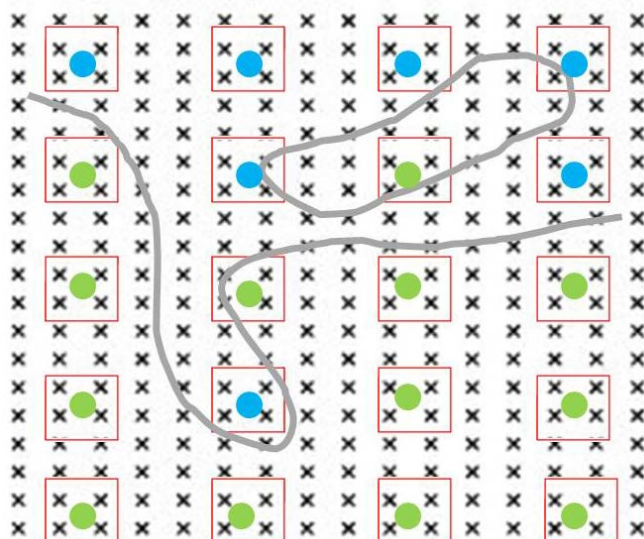


Figure 10: A rather detailed coast line (grey line) is defined by the model high-resolution grid (crosses). In the interpolation to a coarser grid, only the four nearest grid points to the interpolated position are used. Depending on whether they are predominantly of land or sea character, they will unambiguously define an interpolated land (green) or sea (blue) point.

Systematic differences between HRES and ENS (see chapter 3) can, for example, occur in connection with strong gradients along coasts, small islands or in mountainous regions. Any such discrepancy is most clearly apparent during the first few days, when the spread is normally small (see Figure 11 and Figure 12).

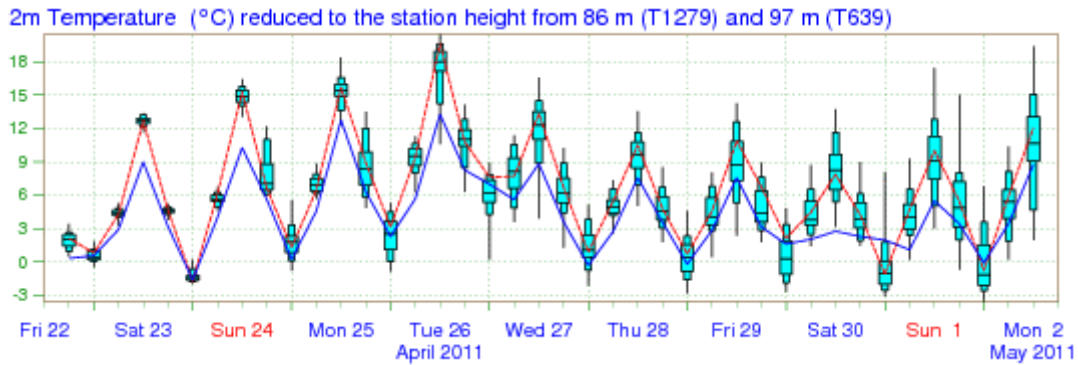


Figure 11: EPSgram for Kontiolahti in eastern Finland, 22 April 2011 12 UTC. The systematic difference between the HRES (blue line) and the ensemble Control forecast (red line) is around 5°C. Kontiolahti lies close to a small lake resolved in HRES but not in the ENS (for more details about EPSgrams see Section 5.2).

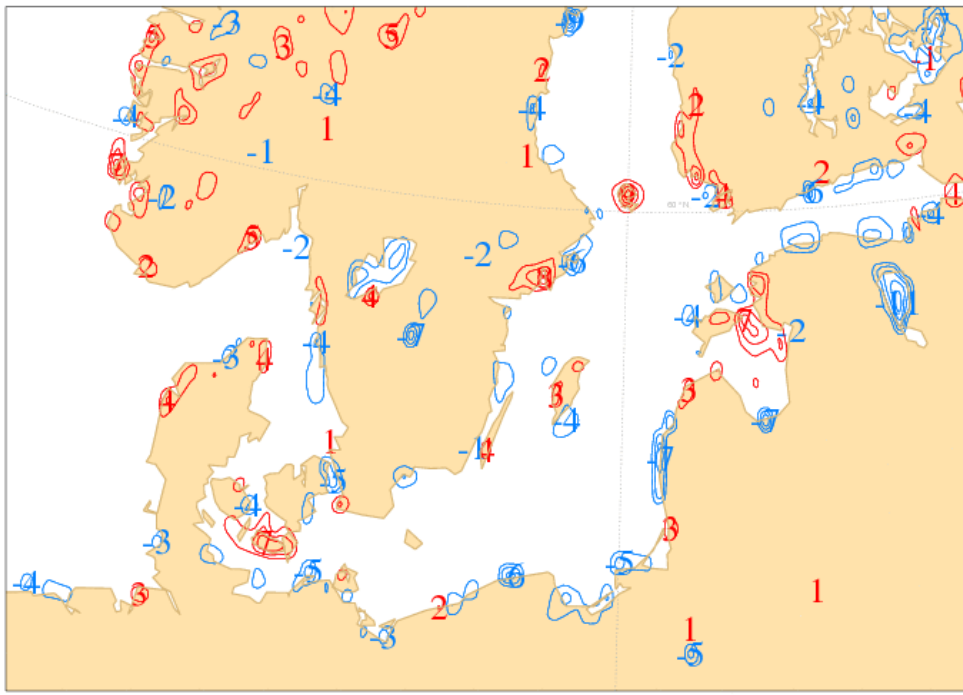


Figure 12: The difference in 2 m temperature between the HRES and the ensemble Control forecast for 23 April 2011 00 UTC + 12h. The maximum and minimum differences are indicated as integers. The interval is 2°C. The differences are largest where the discrepancy between the HRES and ENS land-sea mask or orography is largest.

At grid points along coastlines the marine influence may be overestimated and statistical interpretation schemes can be beneficial, in particular for temperature forecasts (see Appendix B-6).

2.5. The relation between grid point values and observations

The reduced Gaussian grid values, like all other grid values, should not be considered as representing the weather conditions at the exact location of the grid point, but as a time-space average within a two- or three-dimensional grid box (Göber et al, 2008). The discrepancy between the grid-point value and the verifying observed average can be both systematic and non-systematic. The systematic errors reflect the limitations of the model's ability to simulate the physical and dynamic properties of the system; the non-systematic errors reflect synoptic phase and intensity errors (see Figure 13).

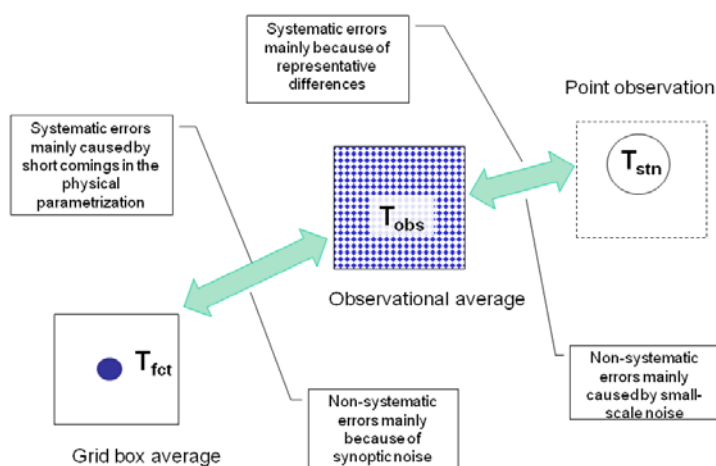


Figure 13: The comparison between NWP model output and observations ought ideally to follow a two-step procedure: first from grid-point average to observation area average. The systematic errors are then due to model shortcomings; the non-systematic stem from synoptic phase and intensity errors. In the next step, the systematic errors between observation average and point observation result from station representativeness and the non-systematic from sub-grid scale variability.

When the NWP model output is compared with point observations, additional systematic and non-systematic errors are introduced, due to the unrepresentativeness of the location and the observations' sub-grid variability (see Figure 14).

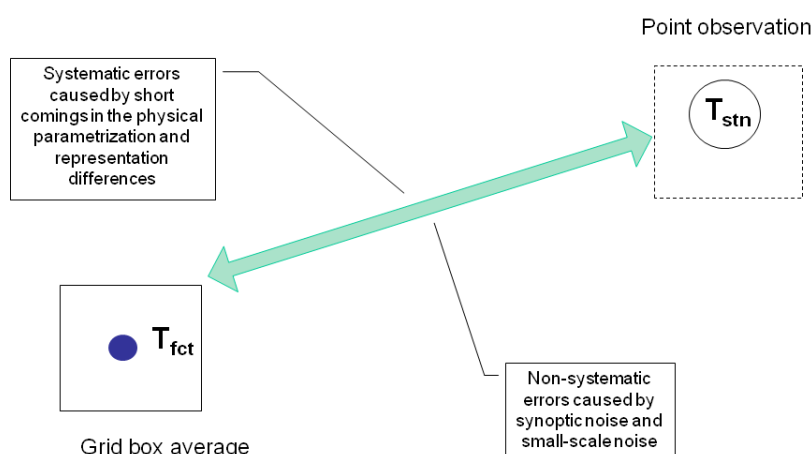


Figure 14: In reality, the comparison between NWP and observations must for simplicity bypass the area average stage. This results in the systematic and non-systematic errors emanating from distinctly different sources.

Systematic errors due to model deficiencies and/or observational representativeness can be partly corrected by statistical means (see Appendix B-6). Non-systematic synoptic errors can be dampened by different ensemble approaches (see Chapter 4), but the errors due to sub-grid variability can only be remedied by new model versions with higher numerical resolutions. A model-independent estimate of the sub-grid “noise” can be made by verifying the observations from one observing station as “forecasts” for a neighbouring observing station. A typical value for homogenous terrain is about 1°C with typical distances of 50-150 km.

2.6. Some characteristics of NWP output

Output from NWP models does not behave in a simple or regular way due to the non-linear nature of the forecast system.

2.6.1. Forecast error growth

Forecast error growth is, on average, largest at the beginning of the forecast. At longer forecast ranges it levels off asymptotically towards the error level of persistence forecasts, pure guesses or the difference between two randomly chosen atmospheric states (see Figure 15). This error level is significantly higher than the average error level for a simple climatological average used as a forecast (see Appendix A-2 for details).

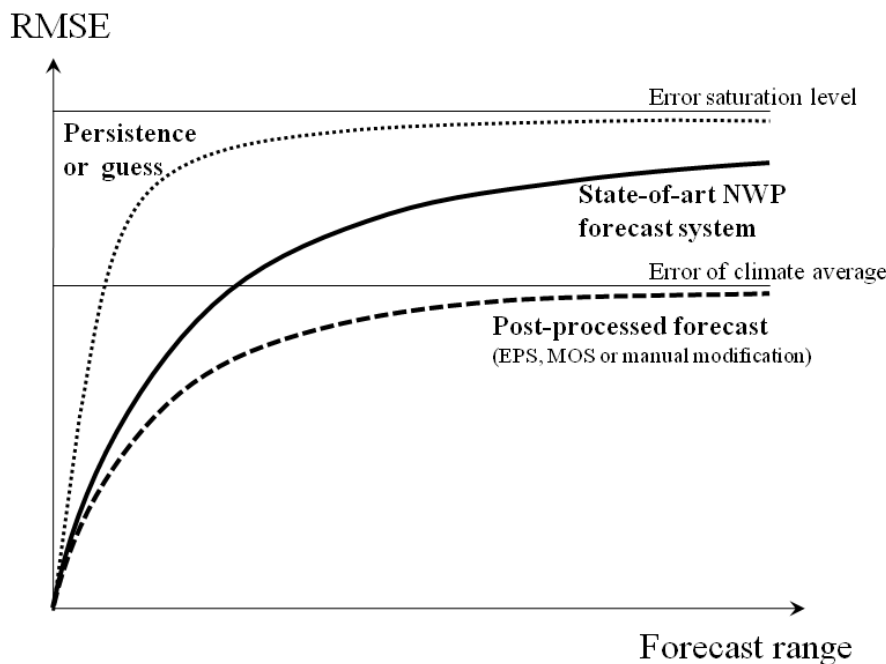


Figure 15: A schematic illustration of the forecast error development of a state-of-the-art NWP (full curve), persistence and guesses (dotted curve), whose errors converge to a higher error saturation level than modified forecasts, which converge at a lower level (dashed curve).

2.6.2. Downstream spread of influence

Influences in the forecasts, both good and bad, often travel faster downstream than the synoptic systems themselves. A two-day forecast over Europe may be affected by the initial conditions over most of the North Atlantic, a five-day forecast also by the initial conditions over the North American continent and easternmost North Pacific. There is also an ever

present influence from the subtropical and tropical latitudes, particularly when a subtropical depression, tropical storm or hurricane enters the westerlies (see Figure 16).

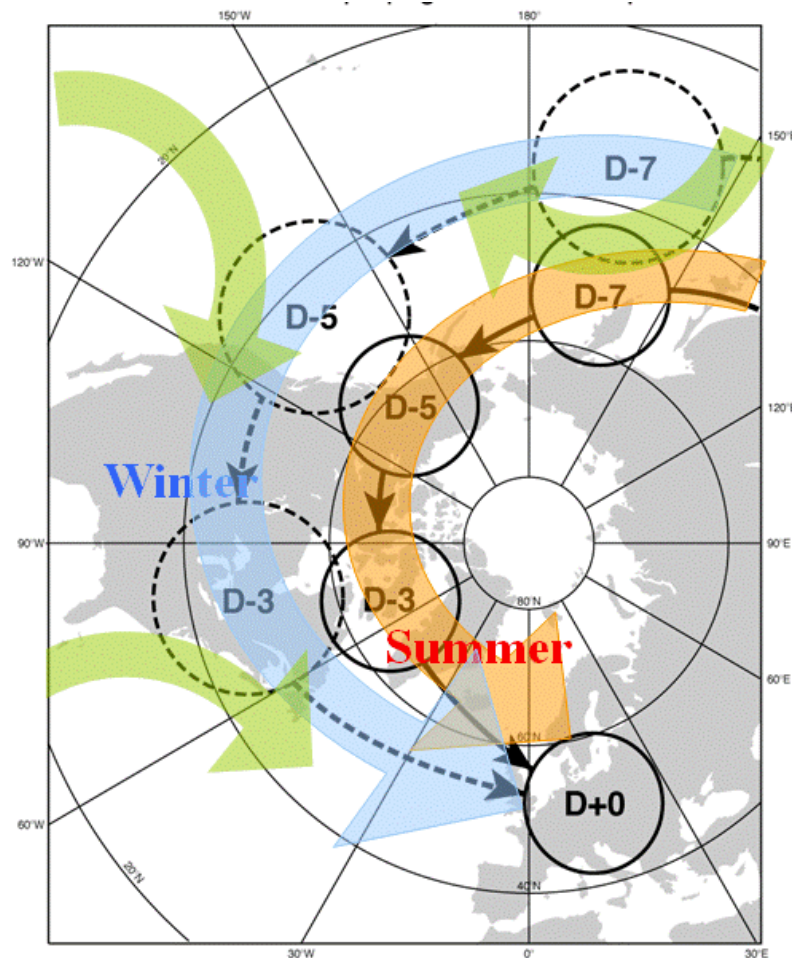


Figure 16: Schematic illustration of the typical propagation of forecast errors over the northern hemisphere towards Europe in situations with generally zonal flow. The errors propagate mainly along the storm track, which during the warm season is displaced polewards. Forecast errors or “jumpiness” at D+3 typically have their origin over the eastern part of the North American continent, at D+5 over the western part or the eastern part of the North Pacific. In rare cases, forecast failures at D+7 have been traced back even further. During all seasons, but in particular during the summer and autumn, forecast errors associated with disturbances in the tropics or subtropics can move into the zonal westerlies.

Hence, if the short-range forecast is initially poor (good) over the area of interest, this does not mean that the medium-range forecast for the same area is necessarily poor (good). Any attempt to judge the medium-range performance a priori from the short-range performance ought to be made over large upstream areas and also involve the upper-air flow (Bright and Nutter, 2004).

2.6.3. The relation between scale and predictive skill

It is known from theory and synoptic experience that the larger the scale of an atmospheric system, the longer its timescale and the more predictable it normally is (see Figure 17).

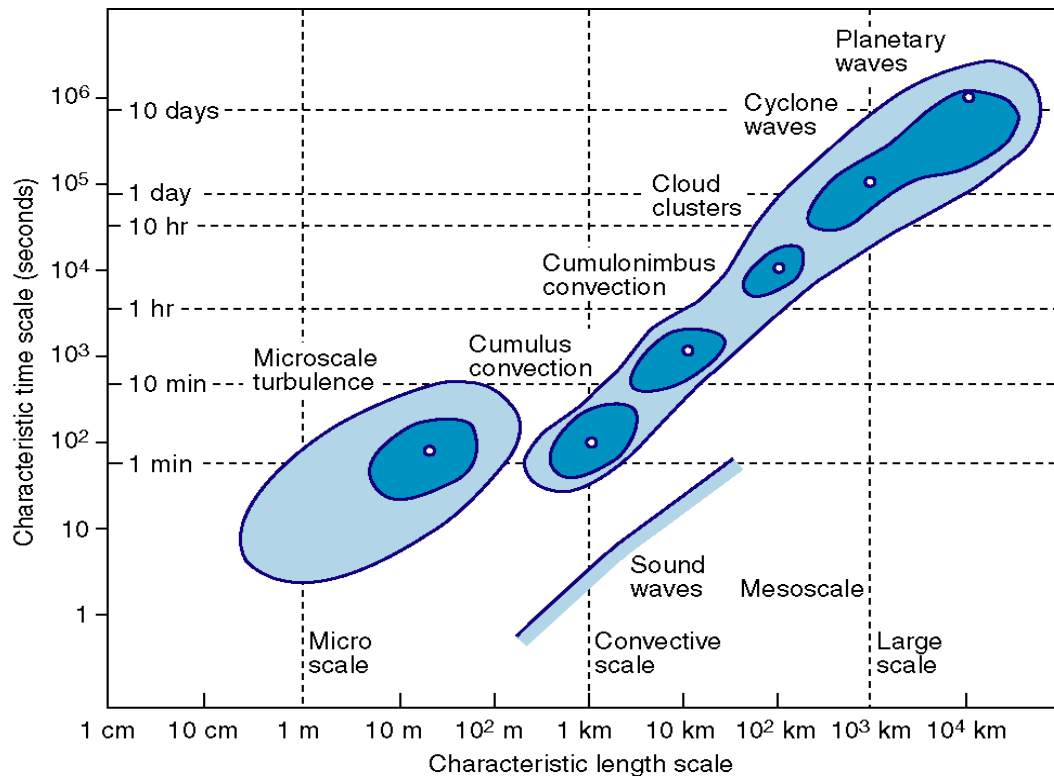


Figure 17: A schematic illustration of the relationship between atmospheric scale and timescale. The typical predictability is currently approximately twice the timescale, but might ultimately be three times the timescale

Small baroclinic systems or fronts are well forecast to around D+2, cyclonic systems to around D+4 and the long planetary waves defining weather regimes to around D+8. Exceptions are features that are coupled to the orography, such as lee-troughs, or to the underlying surface, such as heat lows. The predictable scales also show the largest consistency from one run to the next.

Figure 18 shows 1000 hPa forecasts from the operational model. The forecast details differ between the forecasts but large-scale systems, such as a low close to Ireland, a high over central Europe and a trough over the Baltic States are common features.

The +144 h forecast from 14 August predicted a south-westerly gale over the British Isles six days later. It would, however, have been unwise to make such a detailed interpretation of the forecast, considering the typical skill at that range. Only a statement of windy, unsettled and cyclonic conditions would have been justified. Such a cautious interpretation would have avoided any embarrassing forecast “jump”, when the subsequent +132 h and +120 h runs showed a weaker circulation. The same cautious approach would have minimized the forecast “jump” with the arrival of the +108 h forecast.

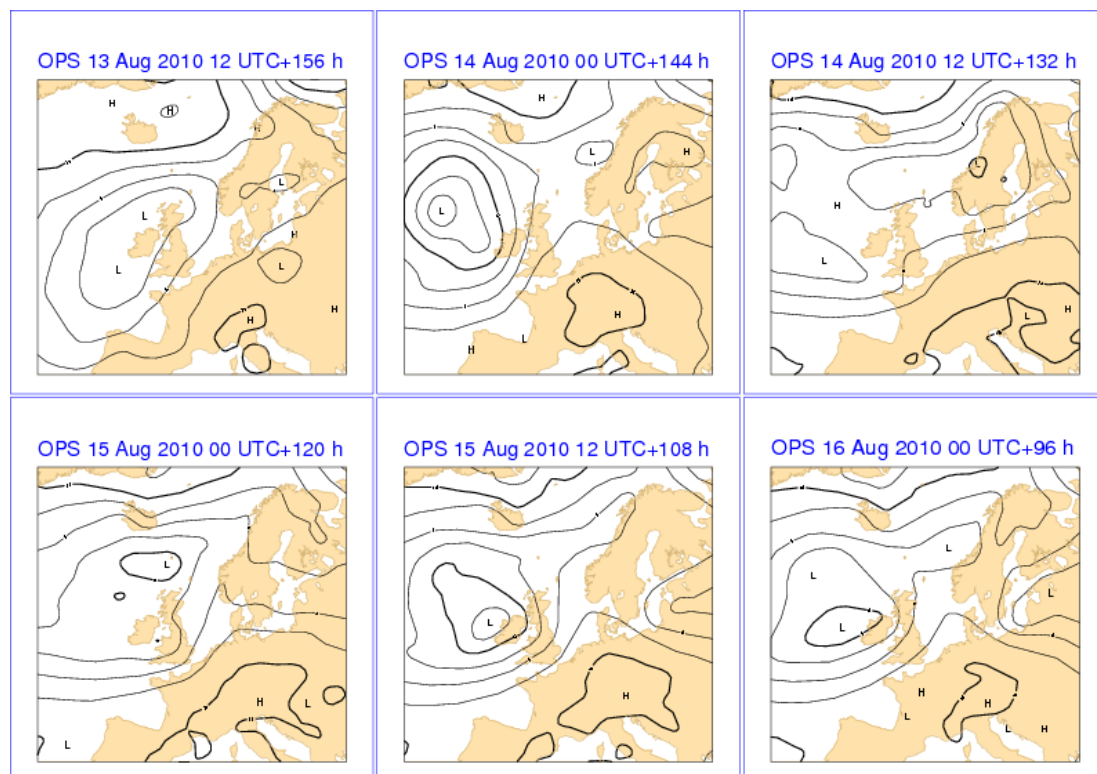


Figure 18: A sequence of 1000 hPa forecast maps ranging from +156 h to +96 h, all verify on 20 August 2010, 00 UTC.

Smoothing out or, more correctly, filtering away small-scale details, in order to highlight the predictable scale, does not necessarily have to be done subjectively (“by eye”). There are also various convenient ways to do it objectively. For example, retaining only the first 20 spectral components filters away all scales smaller than 1000 km and brings out the more predictable large-scale pattern (see Figure 19).

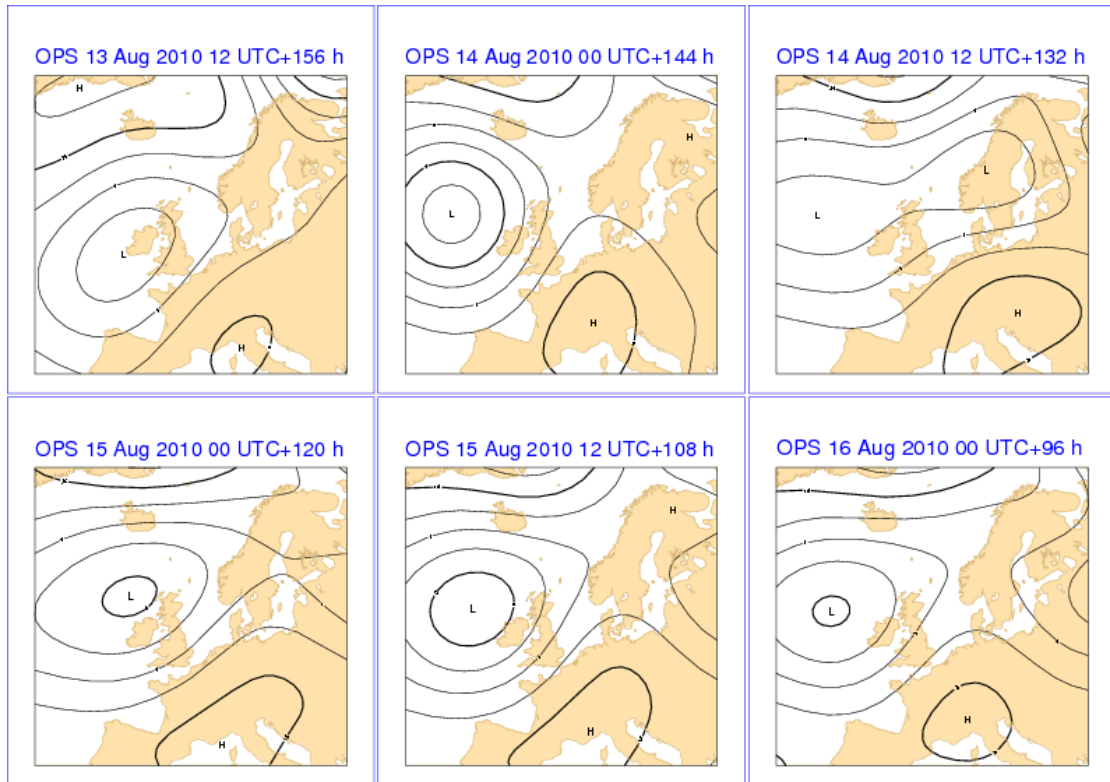


Figure 19: Same as Figure 18 but based on the 20 largest spectral components.

Five of the six forecasts now show much larger coherence, with a cyclonic feature approaching the British Isles and a stationary high pressure system over central Europe.

Spectral filtering does not take into account how the predictability varies due its flow dependency: a small-scale feature near Portugal might be less predictable than an equally sized feature over Finland. Section 4.4.3 shows how the ensemble forecasting system would treat the same synoptic situation in a more consistent and optimal way.

2.6.4. Forecast “jumpiness”

Since every new forecast run is, *on average*, better than the previous one, it is also different. These differences occur because of new observations that modify previous analyses of the atmospheric state and thereby the subsequent forecasts generated from these analyses. Usually, the differences in the forecasts are small or moderate but can occasionally be quite large and appear as “forecast jumps”. This “jumpiness” is an unavoidable consequence of a non-perfect dynamical forecast system and not a problem *per se*. Only when the forecasts are perfect will there never be any “jumpiness” (Persson and Strauss, 1995).

Just because the most recent forecast is, on average, better than the previous one, does not mean that it is *always* better. A more recent forecast can, as shown in Figure 20, frequently be worse than a previous one; with increasing forecast range it becomes increasingly likely that the 12 or 24 hours older forecast is the better one. Chapter 4 describes how forecasters can handle forecast “jumpiness” by combining previous forecasts with the most recent one.

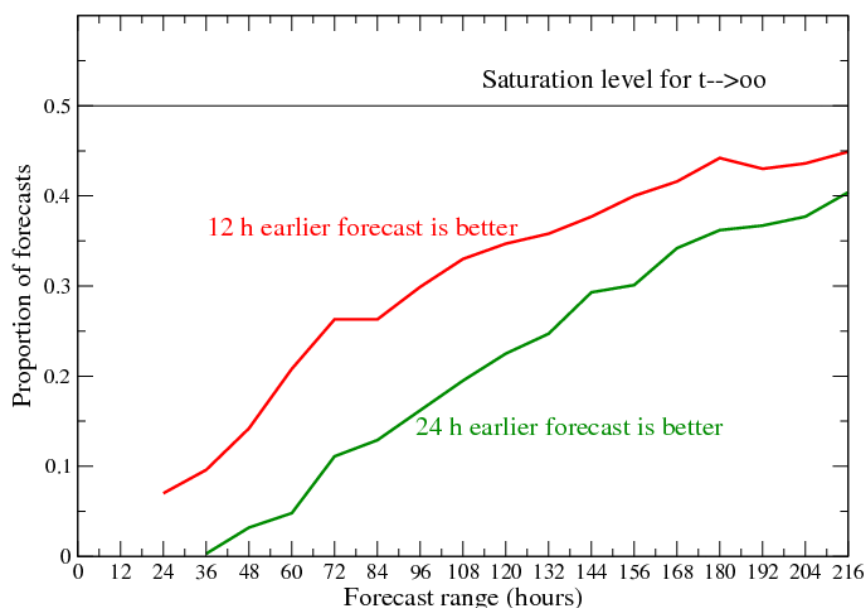


Figure 20: The likelihood that a 12-h or 24-h forecast is “better” (in terms of RMSE) than today’s forecast. The parameter is the MSLP for N Europe and the period October 2009-September 2010. The result is almost identical, if ACC is used as the verification measure.

2.6.5. Flip-flopping forecasts

The order in which the “jumpiness” occurs can provide additional insights. According to Table 1 the likelihood that precipitation occurs seems to be about equal for the last two forecasts being consistent (R R -) or the last three “flip-flopping” (R - R).

Last 3 forecasts 84,96,108h	Numerical probability	Observed frequency	Number of forecasts
- - -	0%	6%	598
- - R	33%	15%	66
- R -	33%	22%	46
R - -	33%	36%	59
- R R	67%	30%	43
R - R	67%	44%	27
R R -	67%	47%	43
R R R	100%	74%	157

Table 1: The percentage of cases when > 2mm/24 h has been observed, when up to three consecutive ECMWF runs (+84, +96 and +108h) have forecast >2mm/24 h for Volkel, Netherlands October 2007-September 2010. Similar results are found for other west and north European locations and for other NWP medium-range models.

This might be because, although the last two forecasts are more skilful than the earliest forecast, they are also, on average, more correlated. What the earliest forecast might lack in forecast skill, it compensates for by being less correlated with the most recent forecast. The agreement between two on average less correlated forecasts carries more weight than two on average more correlated.

2.6.6. *Jumpiness and forecast skill*

It is intuitively appealing to assume that a forecast is more reliable, if it has not changed substantially from the previous run. Objective verifications, however, show a very small correlation between forecast “jumpiness” and the quality of the *latest* forecast (see Figure 21). The “jumpiness” relates rather to the skill of the average of the forecasts (see Appendix A-5).

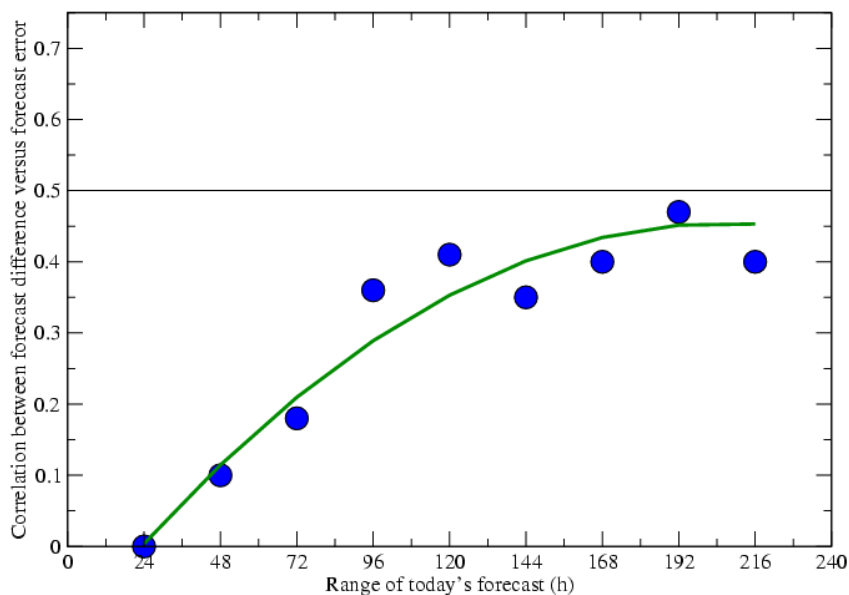


Figure 21: The correlation between 24 hour forecast jumpiness and forecast error for 2 m temperature forecasts for Heathrow at 12 UTC, October 2006 - March 2007. While the relationship between jumpiness and error is low in the short range, it increases with forecast range and asymptotically approaches the 0.50 correlation.

2.6.7. *Forecast trends cannot be extrapolated*

Trends in the development of individual synoptic systems over successive forecasts do not provide any indication of their future development. If, during its last runs, the NWP has systematically changed the position and/or intensity of a synoptic feature, it does not mean that the behaviour of the next forecast can be deduced by simple extrapolation of previous forecasts (Hamill, 2003).

2.6.8. *Other state-of-the-art NWP models*

What has been said so far applies, in principle, to all major state-of-the-art NWP models, spectral- or grid-point-based, global or limited area, hydrostatic or non-hydrostatic. The differences in their average forecast quality are less significant than the daily variability of the scores. Hence, the best NWP model, on average, is not necessarily the best on a particular

day. An NWP model that has recently performed significantly better (or worse) than other models (of about the same average skill), is not likely to continue to do so.

However, as mentioned in Section 2.6.2 and further discussed in Section 4.2, it is as difficult to determine the “model of the day” from one of several NWP model forecasts as it is from consecutive forecasts from the same model. Forecasters are advised to treat forecasts from different NWP models as a “multi-model ensemble” whose members differ slightly in their initial conditions and model characteristics. The better forecasters learn to handle the NWP output in this way, the better they will be able to manage the ensemble forecasts, where these problems are more consistently addressed (see Chapter 4).

3. The forecast ensemble

The value of NWP forecasts would be greatly enhanced if the quality of the forecasts could be assessed a priori; consequently, in parallel with improving the observational network, the data assimilation system and the models, methods of providing advance knowledge on how certain (or uncertain) a particular forecast is and what possible alternative developments might occur are being developed.

3.1. The rationale behind the ensemble

The ECMWF forecast ensemble is based upon the notion that erroneous forecasts result from a combination of initial analysis errors and model deficiencies, the former dominating during the first five days or so. Analysis errors amplify most easily in the sensitive parts of the atmosphere, in particular where strong baroclinic systems develop. These errors then move downstream and amplify and thereby affect the large-scale flow. To estimate the effect of possible initial analysis errors and the consequent uncertainty of the forecasts, small changes to the 4D-Var analysis are made, creating an ensemble of many (currently 50) different, “perturbed”, initial states. Model deficiencies are represented by a stochastic process. In order to save computational time, the ensemble members are run with a lower resolution version of the IFS.

3.1.1. *Qualitative use of the ensemble*

If forecasts starting from these perturbed analyses agree more or less with the forecast from the non-perturbed analysis (the ensemble Control forecast), then the atmosphere can be considered to be in a predictable state and any unknown analysis errors would not have a significant impact. In such a case, it would be possible to issue a categorical forecast with great certainty.

If, on the other hand, the perturbed forecasts (the ENS) deviate significantly from the Control forecast and from each other, it can be concluded that the atmosphere is in a rather unpredictable state. In this case, it would not be possible to issue a categorical forecast with great certainty. However, the way in which the perturbed forecasts differ from each other may provide valuable indications of which weather patterns are likely to develop or, often equally importantly, not develop.

3.1.2. *Quantitative use of the ENS*

The ENS provides the ensemble mean (EM) forecast (or the ensemble median) where the less predictable atmospheric scales tend to be averaged out. The accuracy of the EM can be estimated a priori by the spread of the ensemble: the larger the spread, the larger the expected EM error, on average.

More importantly, the ENS provides information from which the probability of alternative developments is calculated, in particular those related to risk of extreme or high-impact weather.

3.1.3. Characteristics of a good ensemble

- a) The ensemble forecasts should display no mean errors (bias), otherwise the probabilities will be biased as well.
- b) The forecasts should have the ability to span the full climatological range, otherwise the probabilities will either over- or under-forecast the risks of anomalous or extreme weather events.
- c) Any systematic errors with respect to mean error or variability can be detected by the deterministic verification methods discussed in Appendix A. They can, however, also be measured through the probabilistic verification methods outlined in Appendix B.

3.2. Generation of the ENS

3.2.1. Different perturbation techniques

The small perturbations added to the Control analysis to create 50 perturbed initial conditions are computed by a combination of three methods:

- a) A *singular vector* (SV) technique seeks perturbations on wind, temperature and pressure that will *maximize* their impact on a 48 hour forecast, measured by the total energy over the hemisphere outside the tropics. The maximization does not mean that the SV only intensifies weather systems; equally often it weakens them. In addition, the systems can be slightly displaced. Since SV calculations are quite costly, they have to be run at a low, T42, resolution corresponding to almost 500 km.

To specifically address uncertainties in the moisture processes typical of low latitudes, in particular of tropical cyclones, a special version of the SV is created using a linearised diabatic version of the model. These *tropical SVs* may also influence forecasts of extra-tropical developments, when, for example, tropical cyclones enter the mid-latitude some days into the forecast and interact with the baroclinic developments in the westerlies.

- b) The perturbations are modified by using differences between the members of an *ensemble of data assimilations* (EDA). The EDA is an ensemble of independent 4D-Var data assimilations where the main analysis error sources (observation, model and boundary conditions errors) are represented by perturbing the relative quantities (observations, forecast model and sea surface temperature, respectively) according to their estimated accuracy.
- c) Model uncertainty is represented by two different stochastic perturbation techniques. One, “stochastic physics”, randomly perturbs the tendencies in the physical parametrization schemes. The other, “stochastic backscatter”, models the kinetic energy in the unresolved scales by randomly perturbing the vorticity tendencies. The whole globe is perturbed, including the tropics. The Control forecast is run without stochastic physics.

In the idealized schematics Figure 22, one can see how the 4D-Var 12-hour assimilation window (left part of the diagram) modifies the initial trajectories of the EDA members (in yellow) to reflect the information from the assimilated observations (black dots with error bars). The analysis trajectories (in green) show the impact of the new observations on the

3. The forecast ensemble

ensemble: the spread of the ensemble has been reduced and a bias has been corrected by reducing the magnitude of some of the highest values.

At the end of the assimilation window the EDA is used to provide (a) background error information for the successive deterministic analysis update and (b) the initial perturbations of the ensemble around the control analysis.

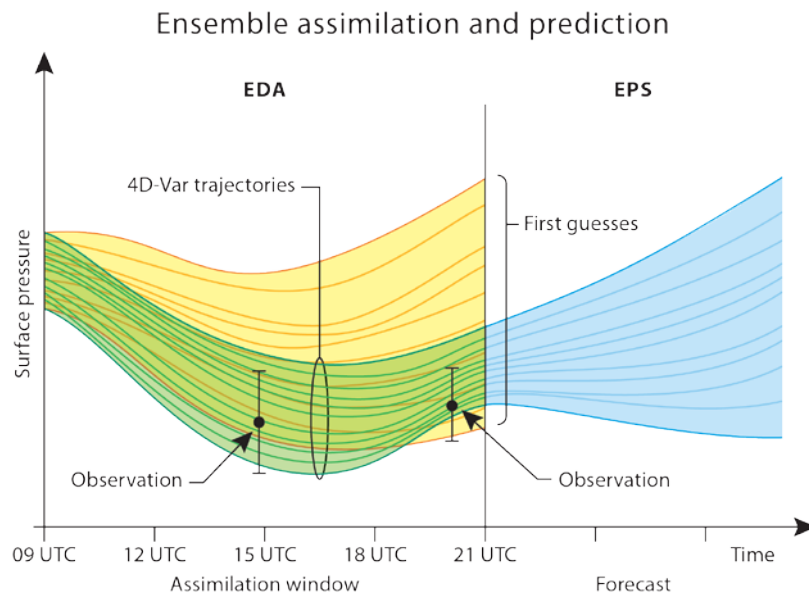


Figure 22 Schematic representation of the ensemble of assimilations (EDA, green) and its link with the forecast ensemble (ENS, blue). The yellow area represents the spread of forecasts starting from the previous EDA analyses 12 hours earlier.

Once the different sets of SVs have been separately calculated over the northern and southern hemispheres and over the tropics between 30° N and 30° S, they are linearly combined (using coefficients randomly sampled from a Gaussian distribution) and added to the EDA perturbations to make a set of 25 global perturbations. The signs of these 25 global perturbations are then reversed to obtain another set of 25 “mirrored” global perturbations. This yields a total of 50 global perturbations for 50 alternative analyses and forecasts.

Consecutive members therefore have, pair-wise *anti-symmetric* perturbations. The anti symmetry may, depending on the synoptic situation and the distribution of the perturbations, disappear after one day or so, but can occasionally be noticed 3-4 days into the perturbed forecasts (see Figure 23 and Figure 24).

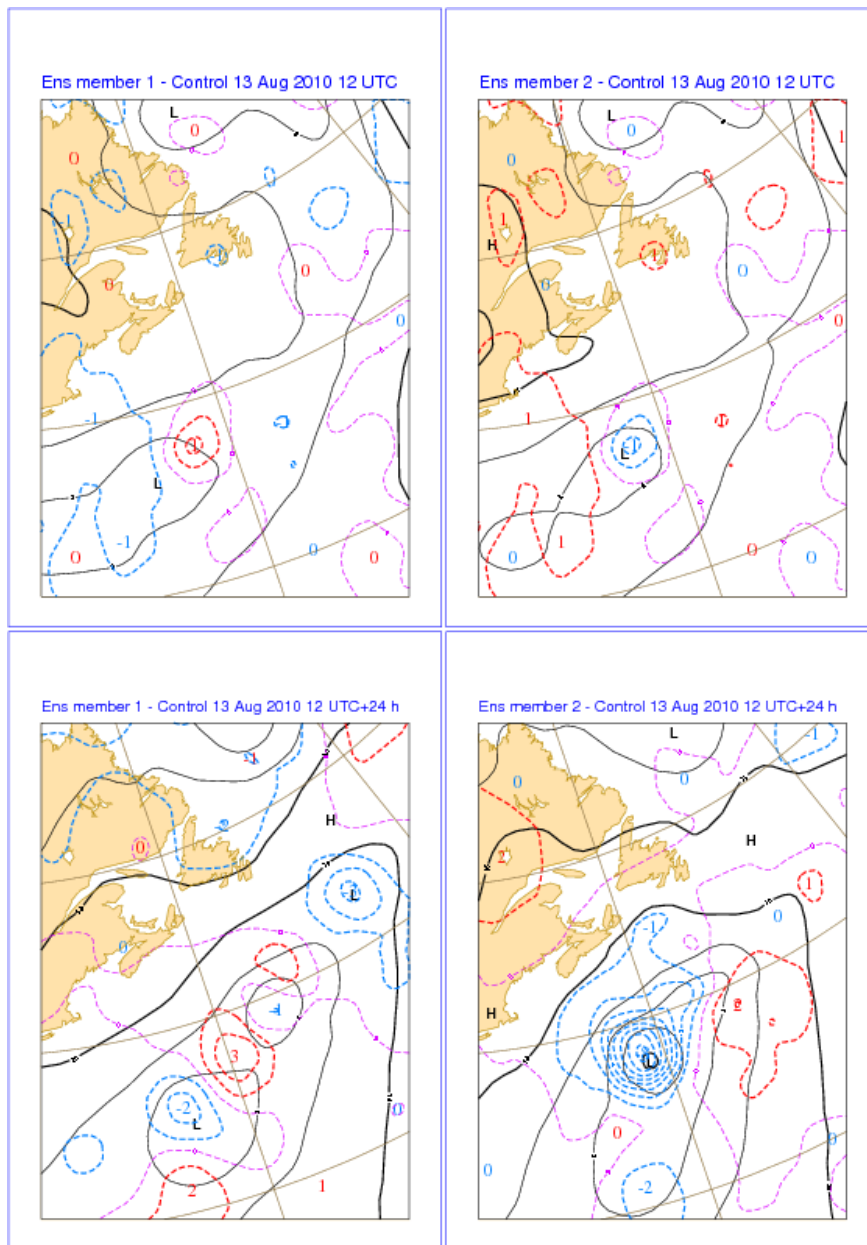


Figure 23: 1000 hPa perturbed analyses and forecasts of members 1 and 2 from 15 August 2010, 12 UTC; the positive and negative perturbations in red and blue dashed lines respectively. At initial time the perturbations are pair-wise anti symmetric, weakening or deepening a shallow low-pressure system on the westernmost Atlantic (upper images). 24 hours into the forecast, the perturbations in member 1 have led to the low splitting into two cyclonic pressure systems, in member 2 to a significant deepening of the single low pressure system.

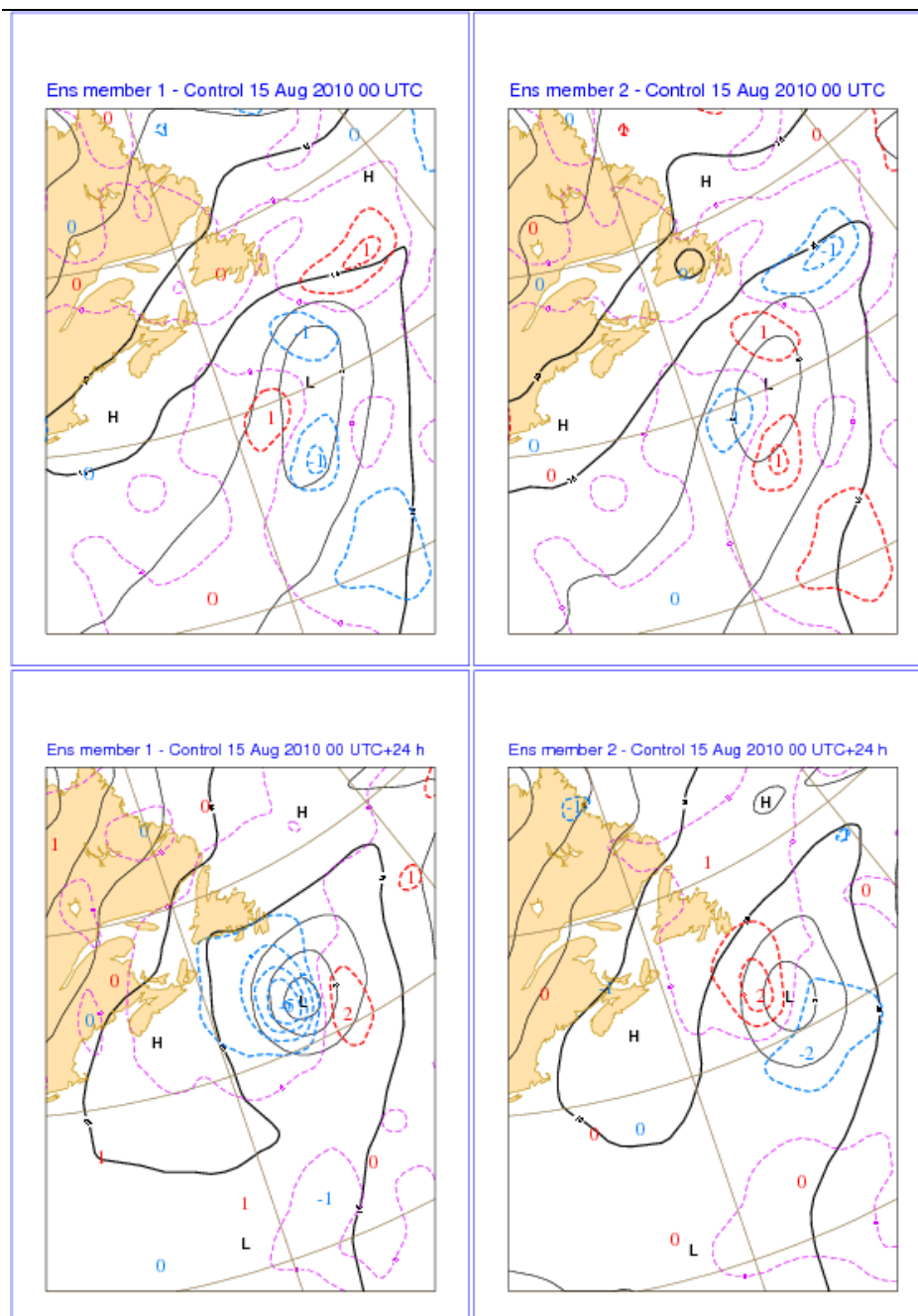


Figure 24: Same as Figure 23 but for 15 August 2010 00 UTC. In this case the anti symmetry is still clearly seen 24 hours into the forecast, member 1 having the low deepened and displaced into a slightly more westerly position, member 2 having the low weakened and displaced into a slightly more easterly position.

3.2.2. Quality of the individual perturbed analyses

An unavoidable consequence of modifying the initial conditions around *the most likely* estimate of the truth, the 4D-Var analyses, is that the perturbed analysis is on average slightly degraded. The RMS distance from truth for a perturbed analysis is, in the ideal case, on average $\sqrt{2}$ times the RMS distance of the unperturbed analysis from the truth (see Figure 25).

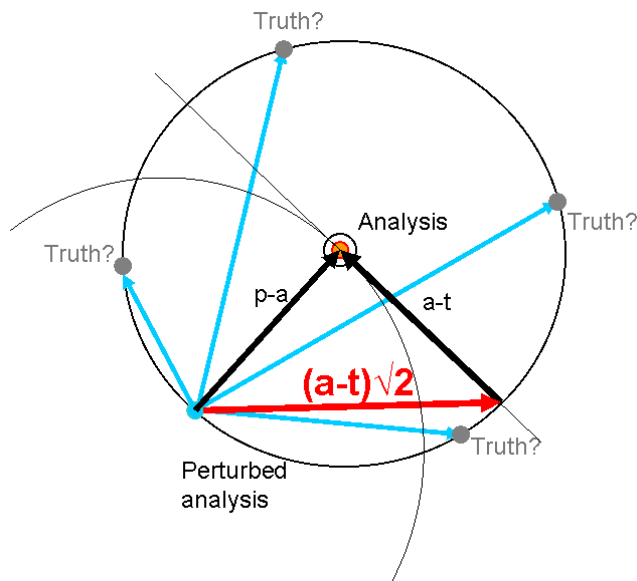


Figure 25: A schematic illustration of why the perturbed initial conditions will, on average, be further from the true state than the Control analysis is. The analysis is known, as well as its average error, but not the true state of the atmosphere (which can be anywhere on the circle). Any perturbed analysis can be very close to the truth, but is in a majority of the cases much further away: in the ideal case the average distance is the analysis error times $\sqrt{2}$

Consequently, the proportion of the perturbed analyses that are better than the Control analysis for a specific location and for a specific parameter, such as the 2 m temperature or MSLP, is only 35% (see Figure 26); considering more than one grid point lowers the proportion even further.

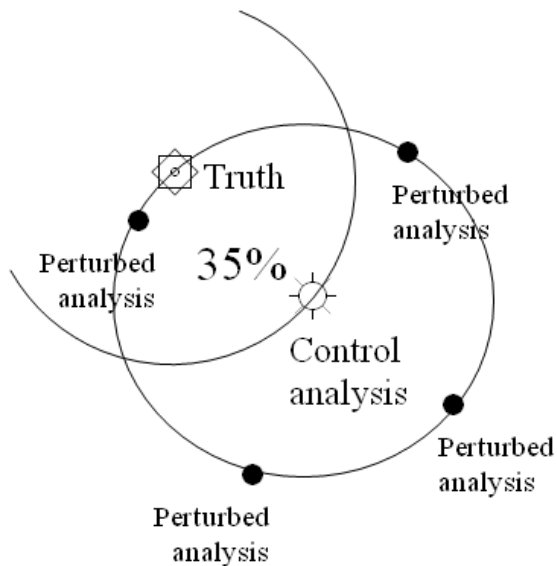


Figure 26: Although the perturbed analyses differ on average from the Control analysis as much as Control from the truth, for a specific gridpoint only 35% of the perturbed analyses are closer to the truth than the Control analysis.

If an ensemble member is closer to the truth than to the Control in, for example, Paris, it might not be so in Berlin. Indeed, the larger the area, the less likely that any of the perturbed

members are better than the non-perturbed Control analysis (Palmer et al, 2006). For a region the size of a small ECMWF Member State, only about 7% of the perturbed analyses are, on average, better than the Control analysis, for the larger Member States this decreases to only 2% (see Figure 27).

With respect to the forecasts, in the short range only a small number of the perturbed forecasts are, on average, more skilful than the Control forecast. However, with increasing forecast range the average proportion of perturbed forecasts that are better than the Control forecast increases, eventually asymptoting to 50%.

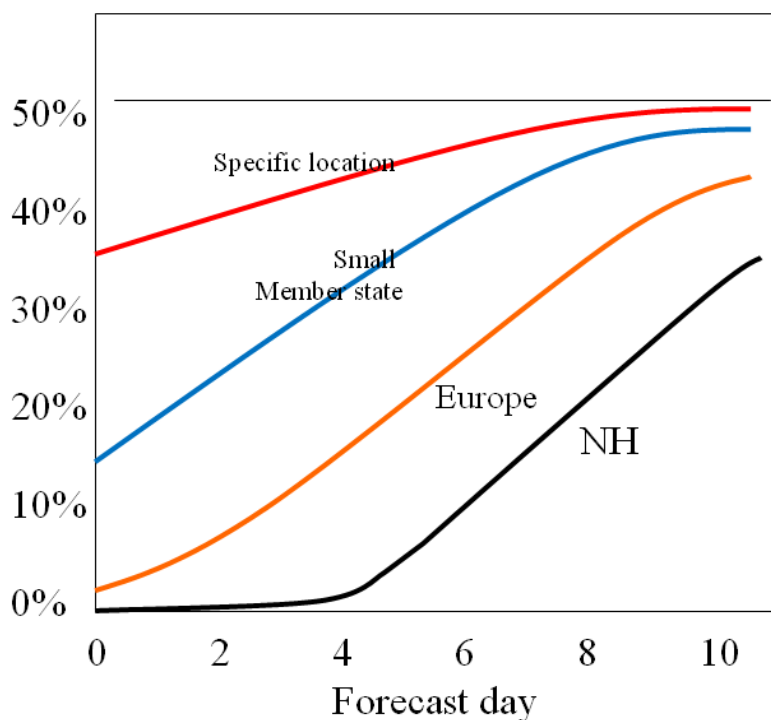


Figure 27: Schematic representation of the percentage of perturbed forecasts with lower RMS error than the Control forecast for regions of different sizes: northern hemisphere, Europe, a typical “small” Member State and a specific location. With increasing forecast range, fewer and fewer perturbed members are worse than the Control (from Palmer et al 2006).

3.2.3. Quality of the individual perturbed forecasts

Since the perturbed analyses have, ideally on average, 41% larger analysis errors than Control, this makes the individual ensemble forecasts on average less skilful than the unperturbed Control forecast. The difference in predictive skill varies with season and geographical location, but is about one day (see Figure 28).

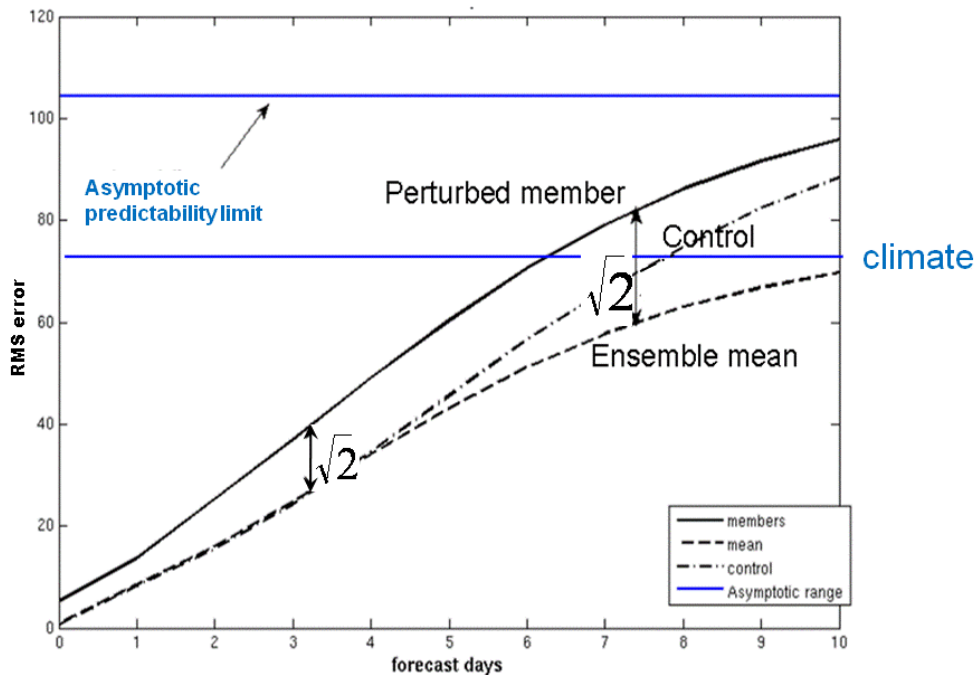


Figure 28: Schematic image of the RMS error of the ensemble members, ensemble mean and Control forecast as a function of lead-time. The asymptotic predictability limit is defined as the average difference between two randomly chosen atmospheric states. In a perfect ensemble system the RMS error of an average ensemble member is $\sqrt{2}$ times the error of the ensemble mean.

However, what the perturbed forecasts may lack in individual skill, they compensate for by their large number, their ability to form good median or ensemble mean values and reliable probability estimations. The information should therefore be used in its totality, i.e. from all the members in the ensemble. The low proportion of perturbed forecast members “better” than the Control in the short range makes the task of trying to select the “member of the day” very difficult and, perhaps, impossible. There are no known methods to a priori identify the “best” ensemble member beyond the first day or so (see Sections 2.6.2 and 4.2).

3.3. The ensemble at different lead times

To use computer resources cost-efficiently, the horizontal resolution of the ensemble is reduced at day 10, and the remainder of the forecast (out to 15 or 32 days) is run at half the horizontal resolution of the first 10 days.

3.3.1. The 10-day range

In spite of its coarser resolution, which is half that of HRES, the ensemble Control forecast performs very similarly to HRES with respect to synoptic patterns. Differences are most noticeable for small-scale extreme weather events, where HRES is able to generate, for example, stronger winds and higher precipitation values.

There is no ocean coupling for the first 10 days of the forecasts.

3.3.2. *The day 9 to 10 overlap*

It is worth noting that the ENS resolution becomes coarser at day 10. Between day 9 and day 10 there is a 24-hour overlap period, to reduce the “shock” of the change, in particular for the parameters that are most sensitive, for example convection and large-scale precipitation. Accumulations of precipitation (and other fluxes) for periods that span the resolution change (day 10) need to use low-resolution data from the overlap period and such data is therefore available via dissemination. An example showing how to make use of these extra fields and how to obtain them in dissemination can be found in the [Meteorological Bulletin M3.1](#):

http://www.ecmwf.int/services/dissemination/3.1/Meteorological_Bulletin_M3_1_50.html

3.3.3. *The 10 to 15 day range*

From day 10 onwards the atmospheric model is coupled with the ocean model. To account for initial uncertainties, the oceanic Control temperature analysis, including the SST and the deep ocean temperature, is complemented by four alternative analyses. They are produced by adding randomly chosen wind perturbations to the ocean data assimilation, driven by five slightly different meteorological fields based on the Control analysis, slightly and randomly perturbed. The resulting five ocean analyses are then distributed among the Control and ensemble members.

3.3.4. *Forecasts from 15 to 32 days*

The treatment of the ensemble members between day 15 and day 32 is the same as for the 10-15 day range described earlier. In order to estimate and compensate for any model drift, a five-member ensemble is integrated from the same calendar date for the last 18 years. This results in “back statistics”, based on a 90-member ensemble of re-forecasts from which systematic errors can be calculated. Systematic errors are then corrected during post-processing, after the forecast is run.

3.3.5. *Seasonal forecast*

Seasonal forecasts (SEAS) are run once a month, based on a slightly different version of the IFS, at an even coarser resolution than the 32-day forecast. The SST and the atmospheric analyses are globally perturbed to form 40 members, using only SV and stochastic physics (See References for further details).

3.4. Basic forecast products

The multitude of products created by the IFS can be separated into basic products and derived products. Basic products display only the raw data, without any particular modification or post-processing. (For derived products see Chapter 5.)

3.4.1. *“Postage stamp maps”*

All the ensemble members, individually plotted as charts with MSLP and 850 hPa temperature, are displayed, together with the HRES and the Control, as “postage stamp maps”. The charts are intended to be used for reference, for example to explain the spread in synoptic terms, in particular the reasons for extreme weather (see also Section 5.6, Cyclone track maps). Any attempt to determine a “Member of the Day” is difficult, since the

performance of any member during the first 12 hours of the forecast has little relevance to its skill beyond + 48 hours in the same area (see Sections 2.6.2 and 4.2).

3.4.2. “Spaghetti diagrams”

Spaghetti diagrams display certain pre-defined isolines (for a specific value of geopotential or temperature at 850 hPa or 500 hPa, for example) drawn for each member. While the isolines are initially very tightly packed, they spread out more and more with increasing lead time, reflecting the flow-dependent increase in forecast uncertainty.

Being visual images, “spaghetti diagrams” are sensitive to gradients. In areas of weak gradient they can show large isoline spread, even if the situation is highly predictable. On the other hand, in areas of strong gradient they can display a small isoline spread, even if there are important forecast variations.

3.4.3. “Plumes”

Plumes are a collection of curves from the HRES, Control and ENS for ten days for 850 hPa temperature, 500 hPa geopotential and 12-hourly accumulated precipitation, for different locations in Europe. The colouring indicates the proportion of members within $\pm 2^\circ\text{C}$ (see Figure 29).

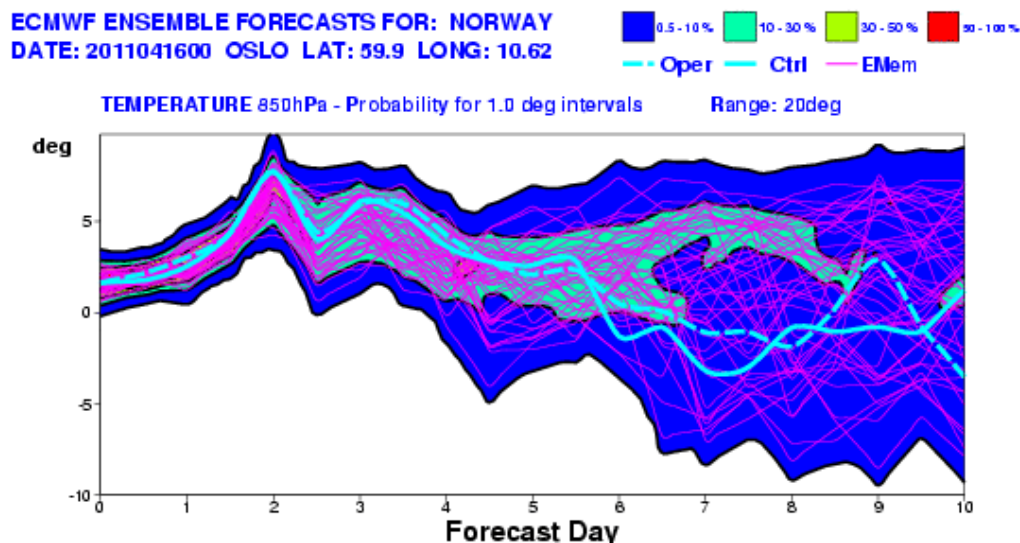


Figure 29: A plume diagram for Oslo 16 April 2011 00 UTC. The ensemble forecast indicates a bi-modal distribution between days 5 and 7, whereas the HRES and the Control follow one branch.

In contrast to EPSgrams (see Figure 44), plumes can display “bi-modal” characteristics. One part of the ensemble might, for example, favour a transition to blocking, while the rest shows a zonal regime. Such “large-scale bi-modality”, should be distinguished from “local bi-modality”, when, for example, a front or minor low is forecast by different members either upstream or downstream of a particular location, resulting in quite different local weather forecasts.

3.4.4. Ensemble mean and median

The ensemble mean (EM) forecast is a simple but effective product. The averaging serves as a filter to reduce or remove atmospheric features that vary amongst the members and are therefore likely to be regarded as less predictable *at the time*. Such non-predictable features are effectively removed from the EM. Significant high-impact events are often weakened or absent in the EM. Use of probabilities is therefore essential in conjunction with the EM.

The EM is most suited to parameters like temperature and pressure, which usually have a rather symmetric Gaussian distribution. It is less suitable for wind speeds and precipitation because of their skewed distributions. For these parameters, the *median* might be more useful. It is defined as the value of the middle ensemble member, if the members are ordered according to rising (ranked) values. Due to the anti-symmetry of the initial perturbations, the EM is very similar to the Control (or HRES) in the short range.

The EM tends to weaken gradients: all members might forecast an intense low-pressure system with 15-20 m/s winds in different positions. These differences in position lead to a rather shallow low in the EM, which gives the impression of weak average winds.

3.4.5. Ensemble spread

The ensemble spread is a measure of the difference between the members and is represented by the standard deviation (Std) *with respect to the EM*. On average, small spread indicates high a priori forecast accuracy and large spread low a priori forecast accuracy. The ensemble spread is flow-dependent and varies for different parameters. It usually increases with the forecast range, but there can be cases when the spread is larger at shorter forecast ranges than at longer. This might happen when the first days are characterized by strong synoptic systems with complex structures but are followed by large-scale “fair weather” high pressure systems.

The spread around the EM as a measure of a priori accuracy applies only to the EM forecast error, not to the median, the Control or HRES, even if they happen to lie mid-range within the ensemble. The spread of the ensemble, relative to a particular ensemble member is, for example, about 41% larger than the spread around the EM. The spread with respect to the Control is initially the same as for the EM, but gradually increases, ultimately reaching the same 41% excess as any member (see Figure 30).

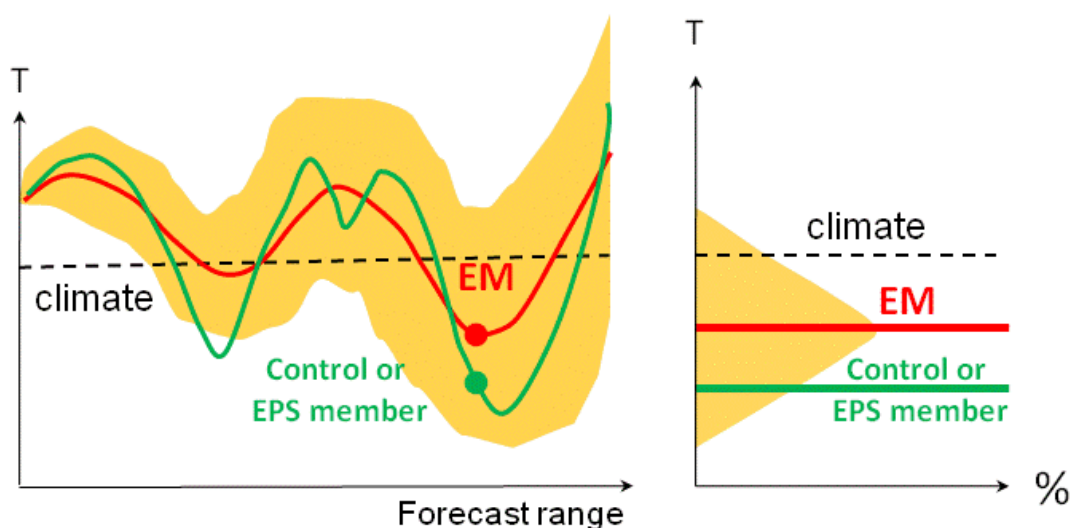


Figure 30: The diagram to the left shows schematically the relation between the spread of the ensemble for the whole forecast range (orange shaded area) and an individual forecast and the EM. The EM (red line) lies in the middle of the ensemble spread whereas any individual ensemble member (green line), can lie anywhere within the spread. The Control, which does not constitute a part of the plume, can even on rare occasions (theoretically on average 4% of the time) be outside the plume.

The ensemble spread should reflect the diversity of all possible outcomes, in particular when the deterministic forecasts are “jumpy”, which might indicate that different weather developments are possible (see Section 4.5).

Two similar-looking forecast maps may display large differences in geopotential if they contain systems with strong gradients that are slightly out of phase. On the other hand, two synoptically rather different forecast maps will display small differences if the gradients are weak. This is clearly reflected in maps of ensemble spread.

3.4.6. Probabilities

The most consistent way to convey forecast uncertainty information is by the probability of the occurrence of an event. The event can be general or user-specific representing the exceedance of a threshold. The event threshold often corresponds to the point at which the user has to take some action to mitigate for the potential damage of a significant weather event.

Probabilities can be instantaneous, such as 10 m wind probabilities. They can also be calculated over a time interval, for instance precipitation, because the values are themselves originally computed as values accumulated over some time interval. Probabilities for extreme wind gusts are computed as probabilities over 24 hours because it is considered more important to know that an extreme wind gust might occur than to know exactly when within a 24 h interval.

3.4.7. Forecast expressed in terms of intervals

Forecast intervals, such as “temperatures between 2° and 5°C” or “precipitation between 5 and 8 mm/24h”, can be used as a hybrid between categorical and probabilistic forecasts. The standard deviation of a normal distribution corresponds approximately to 63% of the members centred around the ensemble mean or median and can be chosen as a suitable interval. With 50 members, this corresponds to the central 31-32 members.

4. Recommendations on categorical and probabilistic medium-range forecasting

The ECMWF forecast products can be used at different levels of complexity, from categorical, single-valued forecasts to probabilistic, multi-valued forecasts. They can be used as guidance to forecasters but also to provide direct input to elaborate decision-making systems. The choice largely depends on user demands but is also influenced by the traditions, and constraints of the particular meteorological service. The emphasis here will be on a combined use of HRES and ENS. The use of ECMWF products for categorical and probabilistic forecasting will be discussed.

4.1. Relation between deterministic and probabilistic forecasts

Issuing reliable categorical weather forecasts is of crucial importance for any meteorological service during normal weather conditions. It builds up trust with the public. If they have confidence in the weather service's ability to 'get it right' in normal weather conditions, they will of course be more likely to trust its forecasts, even probabilistic ones, in cases of extreme weather. The provision of categorical and probabilistic forecasts to the public and end-users therefore support and complement each other.

However, the categorical forecasts should also be fairly consistent over time. Nothing undermines the public's confidence more than "jumpy" forecasts, in particular in connection with anomalous or extreme weather events. A bad five-day forecast will be identified as such only after five days; a "jumpy" forecast will be identified immediately. Although NWP must, by necessity, be "jumpy" to some extent (see Section 2.6.4), there is no reason to convey this "jumpiness" to the public by basing one's forecast on the very latest deterministic NWP output. This can best be avoided by making active use of uncertainty information.

In Appendix A-7 it will be shown not only that probability forecasts convey more information than simple deterministic statements, but also that weather forecasters may, paradoxically, sometimes aid their end-users more by *not* issuing a very uncertain forecast.

4.2. Differences between short- and medium-range operational use of NWP

There are some fundamental differences between how forecasters work in the short range and the medium range.

- In the *short range* forecasters use real-time observations, which have not been used by the NWP (e.g. due to their late arrival), to determine which NWP guidance is "on track" (the "Model of the Day" approach). They then use their meteorological knowledge and experience to determine to what degree the NWP needs to be modified. Due to upstream influences (see Section 2.6.2) this "Model of the Day" approach cannot, however, be applied in the *medium range*. Instead, forecasters have to choose between or, rather, combine information from different NWP sources (Bright and Nutter, 2004).
- In the *medium range* forecast errors are usually dominated by non-systematic errors related to the positions and intensities of atmospheric systems, rather than systematic errors. Whereas in the *short range* forecasters rarely have to question the existence of

predicted synoptic systems, in the *medium range* such systems might not come into existence at all.

- Finally, whereas *short-range* forecasts must first of all show their skill versus persistence, the main objective in the *medium range* is to be more skilful than climate.

Weather forecasting involves the application of meteorological and statistical knowhow. Whereas the former is most important in the *short range*, the latter is most important in the *medium range*.

4.3. Medium-range forecasting *without the ensemble*

It will be assumed that ensemble forecast material is not available, only the latest HRES. The main strategy is to avoid over-interpreting non-predictable features. The most recent forecast should, therefore, not be used in isolation. The forecast “jumpiness” can on the one hand be tackled as something negative that has to be dampened, on the other hand as something positive which can enrich the forecast information.

4.3.1. *Assessment based on the latest forecasts*

By making use of the relationship between scale and predictability, forecasters may disregard the smaller and unpredictable scales and concentrate on the larger and predictable ones. As mentioned in Section 2.6.3, small baroclinic systems or fronts are well forecast up to around D+2, large cyclonic systems up to around D+4 and the long planetary waves, defining weather regimes, up to around D+8. Exceptions to these rules are meteorological features that are coupled to the underlying surface, for example lee-troughs or heat lows.

4.3.2. *Assessment based on the two latest forecasts*

Use of the scale-predictability relation will normally highlight similarities in the latest two NWP forecasts, reduce the error, dampen any “jumpiness” and thereby make the final forecast more trustworthy. The scale-predictability relation also applies when the latest two NWP forecasts are highly consistent. Paradoxically, it is in cases of high consistency that forecasters might be lured into unfounded over-interpretation of non-predictable synoptic features.

4.3.3. *Assessment based on the last three or more forecasts*

One way to take advantage of the skill of previous forecasts is to combine them, together with the latest forecast, into a consensus forecast. Together, they can be regarded as a mini-ensemble that has started from slightly different initial conditions (“lagged average forecast”).

A consensus forecast will preserve those synoptic features which the individual NWP forecasts have in common and can, therefore, be considered more reliable and predictable. The spread of the lagged “mini-ensemble” will define the degree of uncertainty and indicate possible alternative developments. It might even be possible to infer crude but realistic probabilities with respect to weather parameters. The “mini-ensemble” technique will train forecasters to manage the fully fledged ensemble forecasts, where these problems are more consistently addressed (see Sections 4.4 - 4.6).

4. Recommendations on categorical and probabilistic medium-range forecasting

4.3.4. Is it possible to compare manual and computer-generated deterministic forecasts?

Forecasts from NWP models and human forecasters cannot really be compared, because they play different games: NWP modellers strive to provide forecast systems with optimum accuracy, the overriding proviso being that the atmospheric motions contain all scales, irrespective of whether they are predictable or not. (see Figure 31). Weather forecasters do the opposite, they disregard and damp unpredictable features, in order to improve the accuracy and reduce the ‘jumpiness’ of their categorical forecasts (see Figure 32).

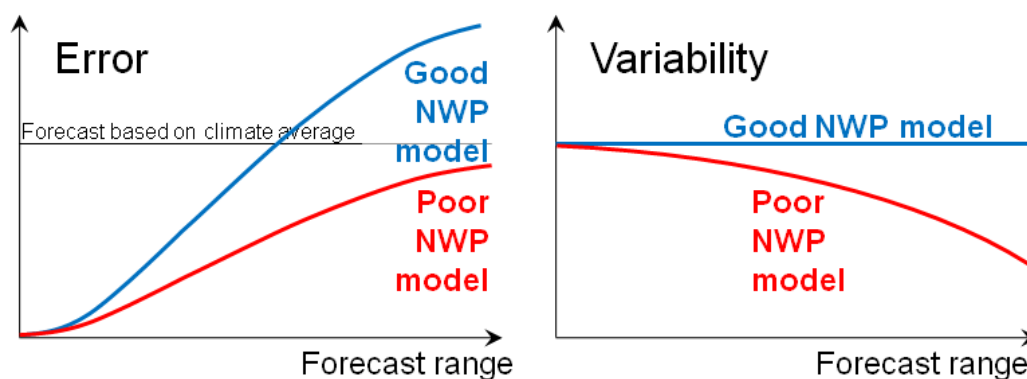


Figure 31: The root-mean-square error and variability of two NWP systems: one a good state-of-the-art high-resolution NWP model (blue curve in left figure), the other a poor NWP model due to excessive diffusion or coarse numerical resolution (red curve in left figure). The errors of the good model approach a high error level because it is able to represent the whole spectrum of resolvable atmospheric scales throughout the forecast (straight blue line in the right figure), while the errors of the bad model approach a lower level because it suffers from a gradual reduction of the scales and thereby the variability (red curve in the right figure).

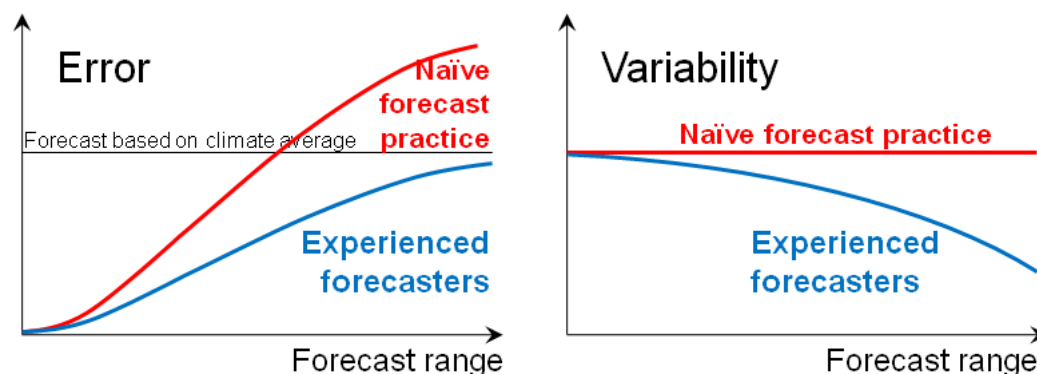


Figure 32: The same as figure 30 but for two different forecast practices: one experienced practice which disregards or damps less likely synoptic features, the other which naïvely reads off the raw output from a state-of-the-art NWP model. The errors of the experienced practice (blue curve in the left figure) approach a low error level because of a gradual reduction of the less predictable scales and thereby the forecast variability (blue curve in the right figure), while the errors of the naïve practice approach a higher error level (red curve in the left figure) because the forecasts maintain the whole spectrum of resolvable atmospheric scales for all lead times irrespective of whether they are predictable or not (straight red line in the right figure).

To summarise: “Good” deterministic forecast performance cannot be judged with the same yardstick as NWP modellers, forecasters and end-users: “what looks bad might be good, what

looks good might be bad”. If the reduction in categorical forecast errors occurs *during* the forecast integration, due to deficiencies in the NWP model, then it is “bad”; if it happens *after* the forecast integration, by some subjective or objective post-processing of the NWP output, then it is “good”. Any “competition” between NWP modellers and forecasters is without relevance outside the meteorological community. Besides the NWP models would easily be beaten, in particular in the medium range! (see also Section 2.6.1, Figure 14 and Appendix A).

4.4. Medium-range forecasting based *only on the ENS*

The ensemble prediction system offers the most consistent method of achieving what was mentioned above: identifying the predictable scale and dampening forecast jumpiness, estimating the overall confidence and drawing attention to possible alternative developments, in particular those which involve extreme or hazardous weather events.

4.4.1. *Use of the ensemble mean (EM)*

Generally, whether the ensemble spread is small or large, the EM (or median) will, beyond the short range, exhibit higher accuracy than the Control (and the high-resolution forecast); this is particularly true for “dry” parameters, such as MSLP and temperature. With increasing spread, the forecast information will depend more heavily on the probabilities; this is particularly true for “wet” parameters, such as precipitation and cloud amounts. The EM will also display a higher degree of day-to-day consistency. *The relative dampening of forecast “jumpiness” is, on average, about three times larger than the reduction in error.*

4.4.2. *Criticism of the EM*

Although EM forecasts and, similarly, averages of forecasts from the same or different models provide more accurate and considerably less “jumpy” deterministic forecasts, meteorologists are somewhat apprehensive about using them. This reluctance derives mainly from three reasons:

- a) *Ensemble averages do not constitute genuine, dynamically three-dimensional representations of the atmosphere.*
- b) *Ensemble averages are less able to represent extreme or anomalous weather events.* Use event probabilities or the EFI instead.
- c) *Ensemble averages might lead to inconsistencies between different parameters.* For example, the ensemble cloud average (or median) might not be consistent with the average (or median) of the precipitation.

4.4.3. *A synoptic example of combining EM and probabilities*

To avoid over-interpreting the EM, in particular underestimating the risk of extreme weather events, it should preferably be presented together with a measure of the ensemble spread or event probabilities; these will convey an impression complementary to the EM.

Since the EM and the probabilities relate naturally to each other, they should be presented together. So, for example, the EM of the MSLP (or 1000 hPa) presented together with gale

4. Recommendations on categorical and probabilistic medium-range forecasting

probabilities will put the latter into a synoptic context that will facilitate interpretation (see Figure 33).

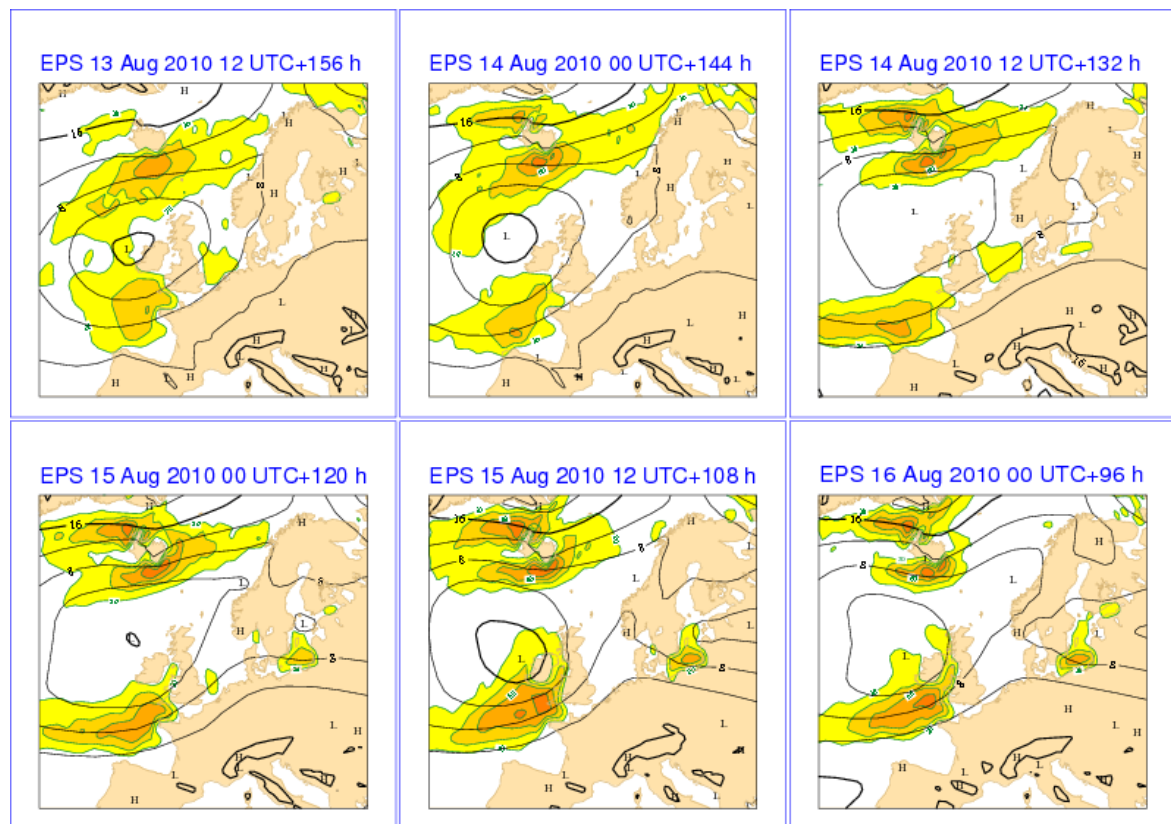


Figure 33: 1000 hPa forecast from 13 August 12 UTC +156 h to 16 August 00 UTC + 96 h, all valid at 20 August 00 UTC. Full lines are the 1000 hPa geopotential EM overlaid by the probabilities of wind speeds > 10 m/s. Probabilities are coloured in 20% intervals starting from 20%. Compare with Figure 18 and Figure 19.

Figure 17 and Figure 18 (Section 2.6.3) showed an example, from 20 August 2010, of how filtering less predictable synoptic scales can increase the accuracy and reduce the jumpiness of forecasts. This filtering is much better accomplished through the ensemble. Thanks to its flow dependency, it serves as a superior dynamic filter. The +12 h ensemble forecast is used as an analysis proxy for the verification (see Figure 34).

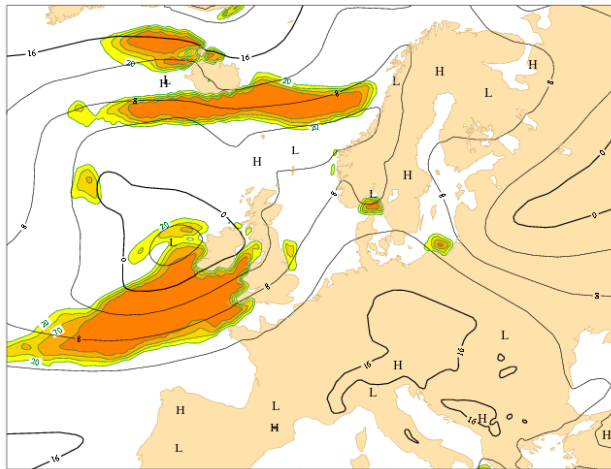


Figure 34: 1000 hPa EM 19 August 12 UTC +12 h valid at 20 August 00 UTC may serve as a proxy analysis for verification because of the small forecast range and the fact that the EM, thanks to the initial anti-symmetric nature of the perturbations, is almost identical to the Control. The probabilities essentially show where the verifying wind speed was > 10 m/s.

In retrospect, it can be seen that some of the HRES medium-range forecasts in Figure 18 (+96, +108 and perhaps +144 h) were quite good with respect to strong winds over Britain and Ireland but *at the time* the ENS indicated that gale force winds were not certain.

4.4.4. Use of probabilities

Probabilities give no indication of the physical nature of the uncertainty. A 25% probability of precipitation >5 mm/24h might be related to a showery regime or to the uncertainty of the arrival of a frontal rain band. A 25% risk forecast for temperatures < 0°C might be related to the possible early morning clearing of low cloud cover or the possible arrival of arctic air.

Probability forecasts cannot be linearly extrapolated into the future. If an event was assigned a 10% probability in the forecast two days ago, 20% in yesterday's forecast and 30% in today's, there is no reason that it will necessarily further increase in tomorrow's forecast; it could equally well remain at its current level or decrease (see Figure 35).

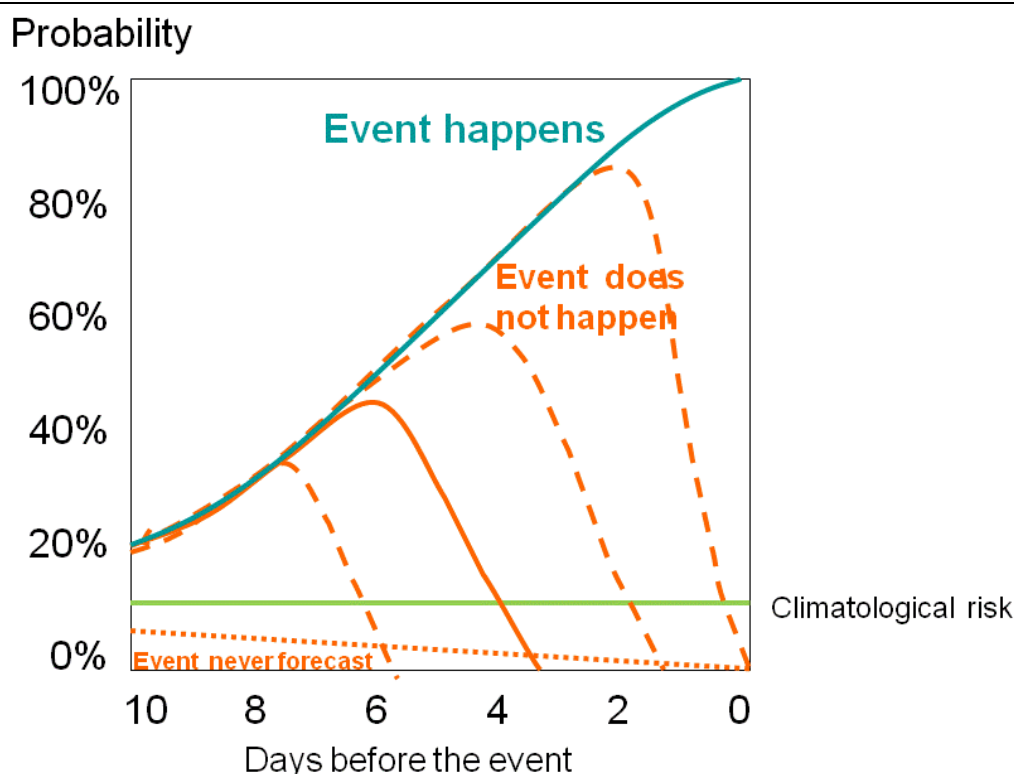


Figure 35: A schematic illustration of an average event probability development for a specific location over ten days. The climatological probability of the event (lime green line) is the event probability in the absence of other information. If very few or no ensemble members forecast the event the event probability gradually reduces to zero with time (orange dotted line). On the other hand, if day by day the ensemble forecasts the event with increasing frequency, the event probability increases (turquoise line). However, at any lead time, the increase may stop and fall back to the lower levels or to zero (dashed orange line). In this particular scenario, at day 6 there is a 40% chance that the event will verify and, consequently, a 60% probability that the event will not occur and that the probabilities will later decrease to zero (continuous orange line).

4.4.5. Probabilities over time intervals

Increased certainty in forecasting an *occurrence* is gained by sacrificing knowledge of exactly *when* the event will occur: the longer the time interval over which event probabilities are calculated, the higher their values. The uncertainty in *individual* rain forecasts for days 5, 6 and 7 is always higher than for the *whole* three-day interval. A high probability statement, such as “70% risk of precipitation > 40 mm/24 h any time during Friday - Sunday”, may convey a stronger message than a low, 30% risk that it will occur on each of the days separately.

Probabilities cannot easily be combined: if the probability for an event in one time interval is 40% and for the next time interval 20%, there is normally no straightforward way to find out the probability over both time intervals together, except when the events are uncorrelated. Depending on the correlation between the two time intervals, the combined probability that it will rain in *either* period might be anything between 40% and 60% and the probability that *both* periods will have rain can vary between 0% and 20% (see Figure 36).

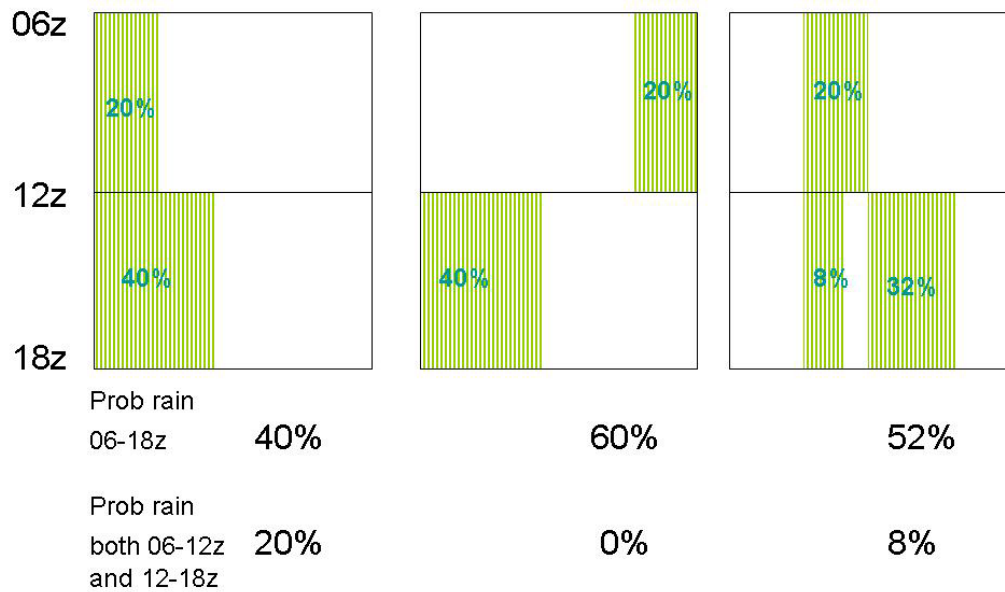


Figure 36: If the events in the two adjacent time intervals are non-correlated, the combined probability is $(1 - (1 - 0.4)(1 - 0.2)) = 52\%$ (far right figure). If they are correlated, so that rain in the first interval is followed by rain in the second, the probability for rain at any time during the whole period is 40% (far left figure). If they are anti-correlated, so that rain in the first period is followed by dry conditions in the second, and dry in the first period is followed by rain in the second, then the total probability is 60% (centre figure).

The only way to get a correct probability for combined time intervals is to go to the original ensemble data and count the proportion of members having rain in *either* or *both* of the time intervals.

4.4.6. Probabilities over areas

Probabilities are normally calculated for individual locations. Calculating probabilities with respect to several grid points within a certain geographical area increases the event probability for the same reason as increasing the time windows. Similarly, a probability statement, such as “a 70% risk of precipitation >40 mm/24 somewhere in Belgium”, may convey a stronger message than a forecast of 10% probability at an individual location.

Since heavy rainfall has hydrological consequences far away from its immediate location, there are also practical advantages in calculating the probabilities of rain over a river’s catchment area as a whole, rather than for individual grid points in the area.

4.4.7. Probabilities of combined events

As with probabilities over longer time intervals or larger areas, probabilities for combined events such as “cloud cover <6/8 *and* temperatures >20°C” or blizzards (combination of heavy snowfall and strong winds) cannot be made from the separate probabilities but can be calculated from the ensemble data.

4.4.8. *Modification of the probabilities*

As mentioned in Section 3.4.6, ECMWF calculate event probabilities from the proportion of members exceeding a certain threshold. If, for example, 34% of members forecast 2 mm/12h or more, then the probability for this event is considered to be 34%. Since the number of ensemble members is limited, the probability of an event is not necessarily 0% just because no member has forecast it; nor is it necessarily 100% because all members have forecast the event. Depending on the underlying mathematical-statistical assumptions and the size of the ensemble, probabilities such as 1-2% and 98-99% could be assigned to situations when no or all members forecast an event, with intermediate probabilities adjusted slightly upwards or downwards accordingly.

4.4.9. *Calibration of probabilities*

Forecast probabilities often show systematic deviations from the observed frequencies (see Appendix B-5). Low probabilities are often too low, high probabilities often too high. Calibration (see Appendix B-5) or statistical post-processing (see Appendix B-6) can improve the reliability of the probability forecasts. This might affect the internal consistency between parameters. If an over-prediction of rain is coupled to an over-prediction of cloud and perhaps under-prediction of temperature, ideally all the parameters would have to be calibrated jointly, in order to maintain a physical consistency.

4.4.10. *Ensemble “jumpiness”*

As with HRES, in order to improve, the ENS must develop from one run to the next, but in contrast to HRES, these “forecast jumps” should be fairly regular with no “zigzagging” or “flip-flopping”. Although this is generally the case, the ENS is still occasionally affected by some undesirable “jumpiness”.

At very short range, the EM is almost identical to the Control (and to HRES) and about equally “jumpy”. With increasing uncertainty (increasing forecast range), the “jumpiness” increases in HRES but decreases in the EM. Zsótér et al, 2009 found that from about T+72 hours, the EM provides more consistent forecasts than the control and this benefit gradually increases with forecast range to day 15. Another aspect of the higher consistency of the EM is that, although the flip frequencies (single jumps) are very similar for both the control and the EM, zigzagging occurs clearly less frequently with the EM. This suggests that the forecast uncertainty is not sufficiently well sampled in the two ENSs. This could be because the ensemble size is not large enough or because the perturbations do not adequately represent all sources of uncertainty.

Like Persson and Strauss (1995), Zsótér et al. (2009) found that the connection between forecast inconsistency and forecast error is weak. There is a more substantial relationship between ensemble spread and EM forecast error.

Forecasters should always check whether the EM and probabilities are fairly consistent with previous runs. If not, forecasters should consider creating a “grand ensemble” of the last two or three ENSs, comprising two or three times the number of members (see Section 4.5.3).

4.5. Medium-range forecasting with the ENS and HRES

The main problem for forecasters is how to react when the information from the ENS and the latest HRES and/or other forecast guidance appear to diverge. The ENS should ideally reflect the characteristics of the latest HRES. So, for example, during periods of “jumpy” HRES, the spread should ideally be larger than normal and reflect the difference between consecutive HRES. When the spread is small, the HRES should ideally develop along similar synoptic lines. What should forecasters do, when this does not seem to be the case?

The HRES and ENS Control synoptic flow predictions have almost the same skill and are usually very similar. In the following discussion, they are considered to be identical.

4.5.1. Weather situations with good agreement between ENS and HRES

The most common scenario is when the two latest HRES fall within the spread of the ensemble. In cases of *small spread* and correspondingly good run-to-run consistency, the latest HRES can be trusted. Since there might still be large uncertainties in the weather details, however, forecasters should be careful not to over-interpret synoptic details and should use their experience of what is predictable (see Figure 37).

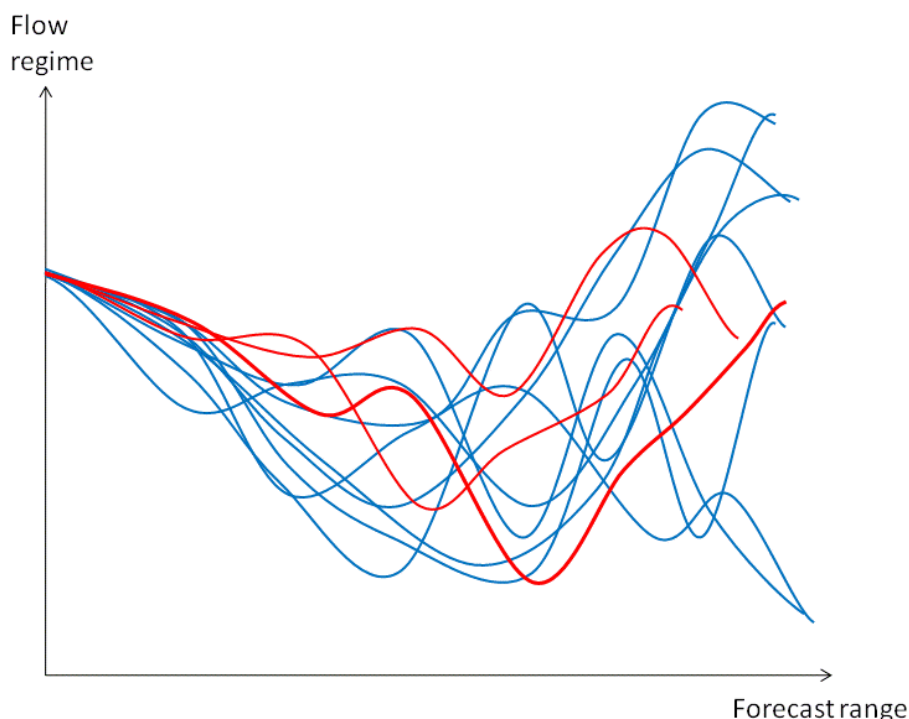


Figure 37: Schematic illustration of the relation between the ENS (blue lines) and the three latest HRES (red lines) for the common case of general agreement. Since the order in which the forecasts have arrived might be significant, the thick, longest red line denotes the latest HRES, the thinnest, shortest red line the earliest.

In cases of *large spread* and correspondingly large run-to-run “jumpiness”, the latest HRES cannot add much information. For any categorical forecast, the safest strategy is to rely on the

4. Recommendations on categorical and probabilistic medium-range forecasting

EM and use the ENS to indicate the uncertainty of this forecast, particularly if there are significant probabilities of extreme weather events.

4.5.2. When the ENS and HRES differ with respect to spread only

It is assumed here that the average development of the few latest HRES agrees fairly well with the average ENS development but that the spread does not agree with the forecast “jumpiness” of the latest HRES.

In cases of *large spread* and good HRES run-to-run consistency (see Figure 38) there may be high sensitivity to initial conditions. The latest HRES can be trusted but forecasters should be careful to use their experience of what is predictable and not over-interpret synoptic details. They should consider alternatives and probabilities as indicated by the ENS, in particular if they involve extreme weather developments.

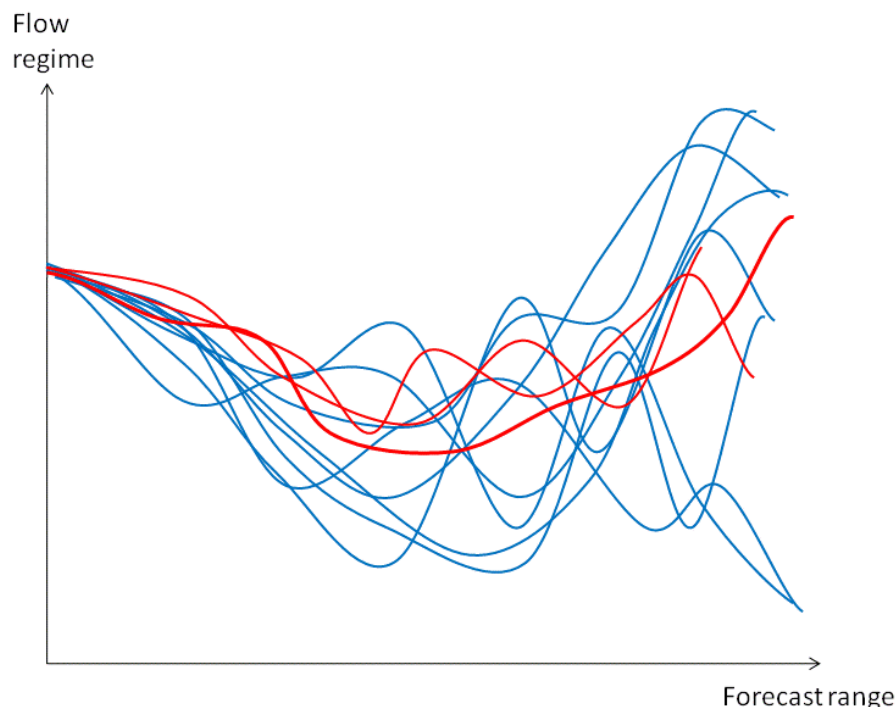


Figure 38: The same as Figure 37 for the case when the latest HRES are consistent, with smaller spread than the ENS.

In cases of *small spread* but poor HRES run-to-run consistency the ensemble has obviously not been able to identify some sensitive regions and/or not been able to perturb the analysis appropriately (see Figure 39).

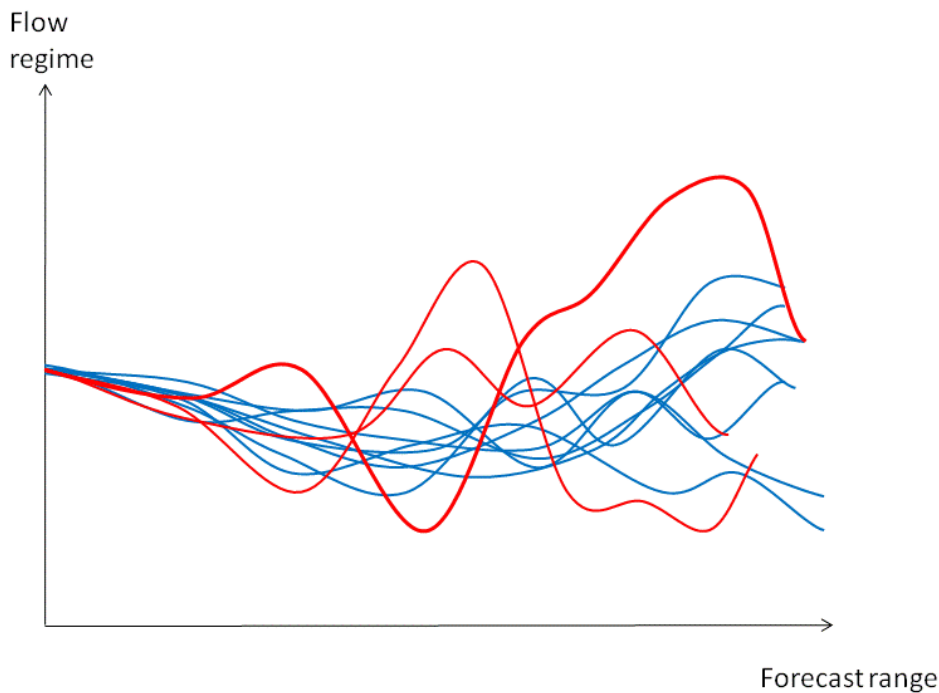


Figure 39: Same as Figure 37 for the situation with large forecast “jumpiness”, in spite of small spread.

Forecasters are in a difficult position; they are recommended not to trust the latest HRES but, rather, to base their categorical forecast on the EM. The uncertainty of this forecast should, however, be regarded as larger than indicated by the spread. If the HRES contains extreme weather events not covered by the ENS, or only covered by a few members, the information from HRES should be used to upgrade the probabilities.

4.5.3. Weather situations where agreement between the ENS and HRES is poor

The problem becomes even more difficult for forecasters when, irrespective of the agreement between the spread and “jumpiness”, there is a clear divergence between the developments in the EM and the latest HRES, the latter being outside the spread (see Figure 40).

Flow regime

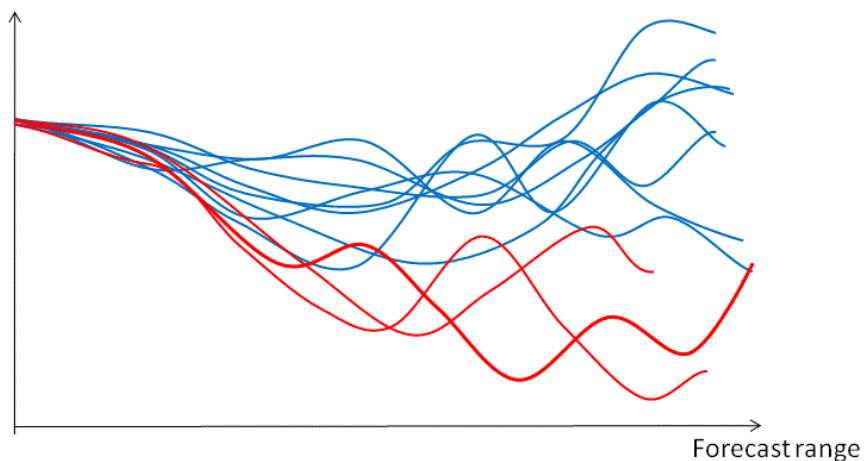


Figure 40: Same as Figure 37, for the case when the latest few HRES are not contained in the ENS

Forecasters can try to synthesise or merge the ensemble with the latest HRES (see Figure 41).

Flow regime

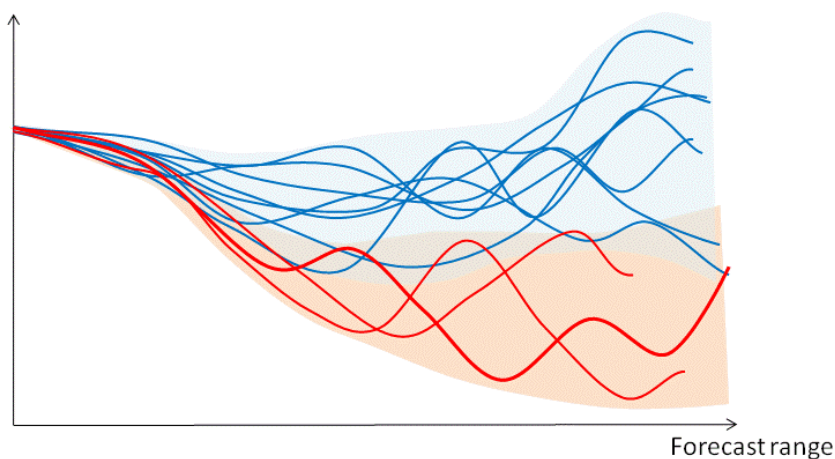


Figure 41: Same as Figure 40; an illustration of the combination of the ENS with the latest few HRES, as if they were two independent ensembles (blue and red shading).

This can be achieved either by combining them as equal ensembles or by weighting them, if there are reasons to assume that one of them is more likely than the other (see Figure 42).

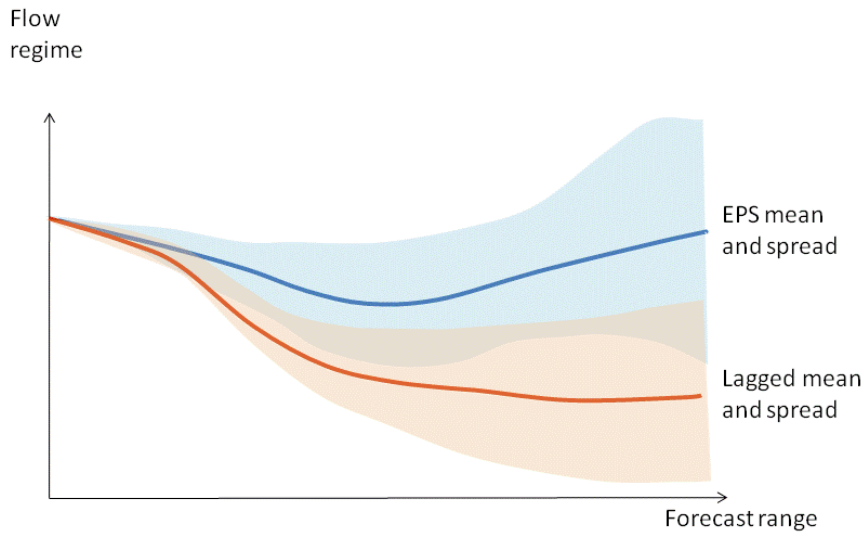


Figure 42: A schematic illustration of the combination of two ensemble forecasts with different EM (full lines).

Another possible approach would be to consult the previous ensemble forecasts. If the latest ENS have been “jumpy” - normally they should not be (Zsótér et al, 2009) - it enables us to see whether they favour the last ENS or the HRES solution (see Figure 43).

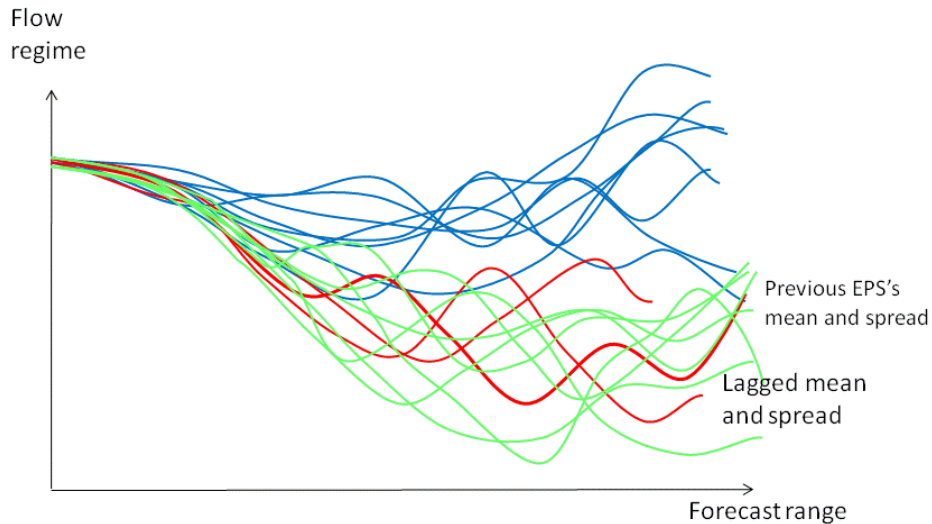


Figure 43: A schematic illustration of a case where the previous ENS (green lines) is in good agreement with the latest HRES (red lines).

If the latter is the case, forecasters might consider combining the ENS and the HRES in an extended ensemble (see Figure 44).

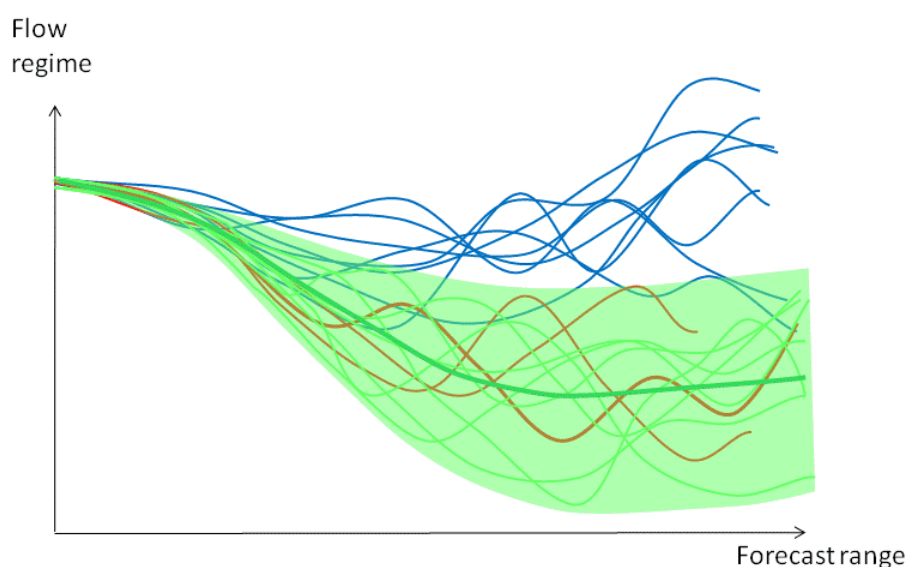


Figure 44: A schematic illustration to show how the latest few HRES (red lines) are combined with the previous ENS (green lines, the thick line being the EM).

A third possibility is to combine both ensemble forecasts into a “grand ensemble” which would include the HRES (Figure 45).

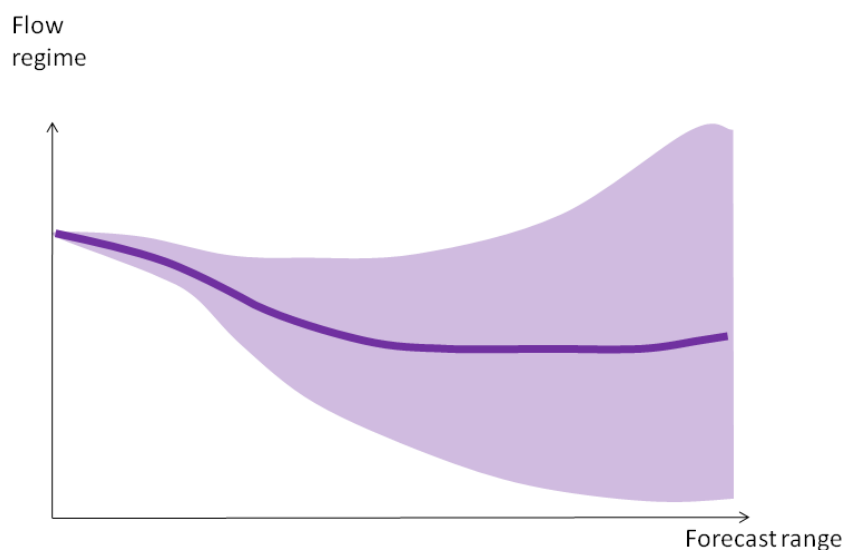


Figure 45: The resulting expanded ensemble, where the EM is the average of the two systems' EMs and the spread their combined spread.

4.5.4. Forecaster intervention with the ENS

It is often taken for granted that forecasters cannot improve on the ENS. Forecasters can manually intervene and, from their experience for a certain location or guided by verification, correct tendencies to over- or under-forecast probabilities. Unless the ENS is the only source of forecast information, forecasters may consider information from other sources, primarily higher-resolution forecasts. It is not unusual for forecasters to have to weigh a 50% probability from the ENS against a 30% value from a different, but equally reliable, statistical

or ensemble system, while taking account of the fact that five of the last six HRES and/or other state-of-art models have forecast the event.

4.6. Forecasting high-impact weather in the medium range

“Extreme” or “severe” weather is coupled to both the small and large atmospheric scales and is mainly of three types:

- large-scale cold outbreaks or heat waves lasting for three days or more
- intense synoptic-scale dynamic precipitation and extreme synoptic-scale winds
- strong and organized sub-grid-scale convection

The ENS is well equipped to forecast the first two types of anomalous events with the current resolution. Sub-grid-scale features can, to some extent, be added by experienced forecasters or statistical interpretation schemes (see Appendix B-6). The *Extreme Forecast Index* (see Section 5.4) has been developed to help forecasters relate the probabilities to the climatological conditions at every location.

4.6.1. *The forecaster’s role*

What has been said above about the forecaster’s role applies in particular to extreme weather forecasting. Calibrating or otherwise applying statistically based modifications to extreme weather events is very difficult because of their rarity. However, forecasters can accumulate some experience of the models’ ability from extreme weather events in neighbouring areas.

Complementary information, in particular forecasts from different models and/or runs, might motivate forecasters to upgrade or downgrade the probabilities. Forecasters also have a unique role in supplying probability forecasts of events not explicitly covered by the ECMWF forecasting system, such as fog and thunderstorms.

Perhaps the most important task is to help end-users, such as regional and national authorities, to make the optimal decision about protective action.

4.6.2. *Probabilities or categorical forecasts?*

Since severe or extreme weather is often characterized by low protective costs, compared to high potential losses, relatively low probabilities become highly decisive (see Appendix A-7.2). Protective action might be prompted at a level as low as 10% event probability, often even lower.

Forecasters’ advice does not have to be probabilistic; if they are very familiar with their customer’s decision process and preferences, purely categorical forecasts may be generated. In cases of extreme weather, the necessary actions may be obvious - evacuating the area or taking shelter.

4.7. Summary: do the opposite to the computer!

General advice could be summarized in a rather unexpected manner: weather forecasters should not try to “compete” with the NWP output on its own terms but, rather, do the opposite:

1. Deterministic NWP output provides highly detailed synoptic scenarios, irrespective of how predictable they are. **Forecasters are advised not to do the same.** With increasing forecast range, they should not try to add detailed information to the NWP, but rather *remove* information, providing fewer and fewer unreliable details in their own forecasts.
2. Deterministic NWP must change run by run. These changes can be quite profound, in particular in the medium-range. **Forecasters are advised to dampen any forecast “jumpiness”**, in order to increase the end-user’s confidence in the deterministic forecast. Forecast “jumpiness” can also be used constructively, by indicating possible alternative developments.
3. Deterministic NWP gives an impression of very high certainty. **Forecasters are advised to make use of uncertainty.** The public and end-users are better served by having an uncertain weather forecast presented as such, rather than with misleading certainty. This will not only make the weather forecast service much more beneficial for decision-makers, but also make the difficult task of weather forecasting more gratifying for the forecasters themselves.

These three rules apply *in particular* to extreme weather events, such as cold outbreaks, heat waves, heavy rainfall and strong winds, which are more susceptible to unrealistic details and “forecast jumps” and for which uncertainty indices or probabilities are the most appropriate ways to convey forecast information.

5. Derived products based on the ENS

A wide range of products is specially derived from the ENS: the EM and spread charts, EPSgrams, the Extreme Forecast Index, tropical cyclone charts, clusters and extra-tropical cyclone charts.

5.1.1. Ensemble mean and spread charts

Special composite maps have been created to facilitate comparisons between EM and HRES. Such maps normally show great consistency from one forecast to the next and can help forecasters judge how far into the future the EM can carry informative value for large synoptic patterns. The spread refers to the uncertainty of the values of mean sea-level pressure, geopotential height, wind or temperature, not necessarily to the flow patterns.

The ensemble spread tends to show a strong geographical dependence. For geopotential and pressure it takes low values at low latitudes and high values at mid-latitudes, where the variability is higher. Since this latitude dependence tends to obscure the particularities of today's current situation, a normalised spread (Nstd) has been defined as

$$\mathbf{Nstd} = \mathbf{Std/Mstd}$$

where Mstd (the mean spread) is a field that represents the mean of the spread of the 30 most recent 00 UTC ENS. It is a function of lead time and geographical location. The **Nstd** highlights geographical areas of unusually high or low spread, where the uncertainty is larger or smaller than over the last 30 days.

If the spread in a particular area, for example at day 5, seems to be large but has recently tended to be equally large in the same area, then the Nstd is ≈ 1 . Conversely, if the spread exceeds the spread that has been seen recently, then the Nstd is > 1 .

5.2. EPSgrams

The EPSgram provides a probabilistic interpretation of the ENS for specific locations. It displays the time evolution of the distribution of several meteorological parameters from the ensemble at each forecast range by a box and whisker plot.

5.2.1. Overview

EPSgrams come in several flavours: a 10-day medium-range plot for weather and wave forecast use and a 15-day extended-range version for weather only.

- a) The medium-range version provides meteorological information every 6 hours throughout the first 10 days.
- b) The extended-range version displays the *daily* average evolution of the meteorological parameters for a 15-day forecast period at a coarser resolution.
- c) The 15-day extended EPSgram has a version where the typical climatological values and variance are included, to help in the assessment of useful predictability and to highlight how anomalous a forecast is.

- d) The 10-day EPSgram has a wave version with the directions, strengths and periods of waves.

Common to all versions is the title section, which gives the name (unless overwritten by the user) and height of the chosen location and the co-ordinates of the grid point used, based on the ENS resolution.

When creating an EPSgram for a specific location, the four surrounding grid points are considered. If there is at least one land grid point within these four, then the nearest land point will be chosen. Otherwise, if only sea points are available, the nearest sea grid point will be chosen. This situation is noted in the EPSgram title section by the words “EPS sea point”.

5.2.2. Ten-day EPSgrams

For each 6-hour time interval, forecast distributions are displayed using a box and whisker plot (see Figure 46) which shows the median (short horizontal line), the 25th and 75th percentiles (wide vertical box), 10th and 90th percentiles (narrower boxes) and the minimum and maximum values (vertical lines). The HRES is interpolated onto the ENS grid (meteorological fields and the model orography) from the four nearest grid points in this model to the location of the selected grid point (see Figure 10 in Section 2.4.6).

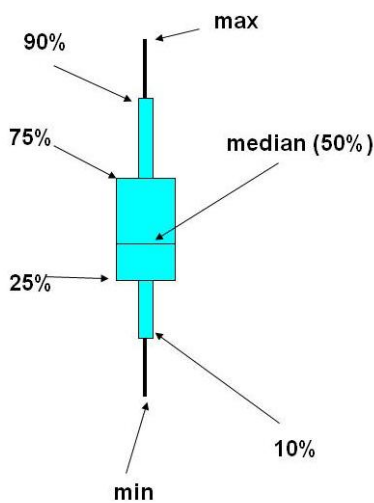


Figure 46: The box and whisker plot used in the ECMWF 10- and 15-day EPSgrams

The HRES and ENS Control are included in the 10-day EPSgram for reference (see Figure 47).

EPS Meteogram
 Strassbourg 48.48°N 7.6°E (EPS land point) 141 m
 Deterministic Forecast and EPS Distribution Tuesday 12 July 2011 12 UTC

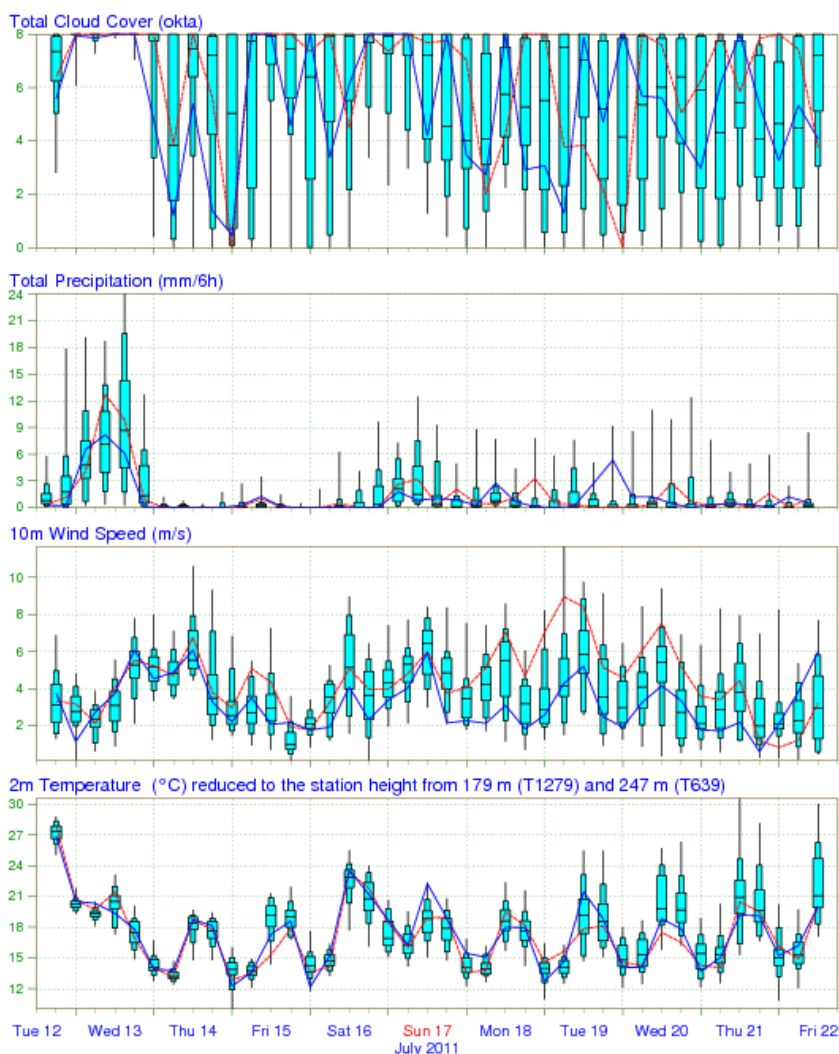


Figure 47: The 10-day EPSgram for Strassbourg, based on the ENS from 12 July 2011, 12 UTC. The expected 6-hourly rain on Wednesday 13 and Sunday 17 July cannot easily be converted into 24-hourly values. Blue lines indicate HRES, the dashed red lines the ENS Control forecast.

5.2.3. Fifteen-day EPSgrams

To provide a consistent product throughout the 15-day forecast period, the fields from the first 10 days are interpolated onto the coarser grid used for the forecast integrations beyond day 10 (see Section 3.3 for details).

The 15-day EPSgram displays the probability distribution from 00 UTC to 00 UTC, i.e. for each calendar day. Consequently, for the 12 UTC forecast the first and last 12 hours are excluded and only 14, instead of 15, daily distributions are generated (see Figure 48).

5.2.4. The weather parameters in EPSgrams

- a) **Total cloud cover** in the 10-day EPSgram is the instantaneous forecast value in oktas (eighths of the sky covered by cloud); in the 15-day EPSgram, the daily average. When all members have 0 cloudiness (clear sky) or 8 oktas cloudiness (overcast), there is no line

or box at all. Be aware that when the forecast is very uncertain and all cloud amounts are more or less equally likely, the blue columns cover almost the whole range from 0 to 8, which gives a misleading visual impression of “overcast”. An alternative display has a circle divided clockwise into eight arcs, each arc representing 1/8 cloud cover. So, for example, the arc covering 45°-90° represents 2/8 cloud cover. The shading within each arc is proportional to the number of members that forecast this particular degree of cloud cover or more.

- b) **Total precipitation** in the 10-day EPSgram is accumulated precipitation (sum of convective and large-scale) over six-hour periods (00-06 UTC, 06-12 UTC, etc); accumulated over 24-hour periods (00-24 UTC) in the 15-day extended EPSgram. Probabilities for intervals longer than the 6- and 24-hour time intervals cannot be deduced from the EPSgram (except in dry weather, when all members repeatedly forecast no rain). Be aware that periods of probabilities >0% in every interval can give a visual impression of uninterrupted rain. Conversely, if one looks only at the median, one can sometimes get the false impression that protracted dry spells are likely. Because of its higher resolution, the HRES is generally better able to generate realistic precipitation amounts than the ENS.

The y-axis range is chosen separately for each EPSgram, so that at least 90% of the predicted values are covered; consequently, the y-axis range commonly varies in steps from one location to the next and, for the same location, from one forecast to the next. When the top of the distribution is beyond the scale maximum in the 10-day EPSgram, the largest 6-hourly totals are shown at the top as red numbers.

- c) **10m wind speed** is shown as an instantaneous forecast value in m/s in the 10-day EPSgram; as the 24-hour wind-speed average in the 15-day extended EPSgram. As with extreme precipitation, in cases of strong small-scale wind systems, the maximum wind can be considerably stronger in HRES than in the ENS. The peaks of the whiskers should not be interpreted as wind gusts. Users are referred to the special products related to gusts, such as probability maps (see Section 5.4.5).
- d) **10m wind direction** is shown only in the 15-day EPSgram. It is presented as daily distributions, by taking each 6-hourly forecast step (06-12-18-24 UTC) and allocating it to the relevant octant. The size and the shading of the octants are proportional to the number of forecasts falling in each octant. To aid visualisation, each wind rose is scaled to the size of the most populated octant.
- e) **2m temperature** is shown as instantaneous forecast values at 6-hourly intervals in the 10-day EPSgram; as daily maximum and minimum temperatures in °C in the 15-day EPSgram. The forecast temperature is adjusted by the 6.5°K/km difference between the station height (as displayed in the title) and the ENS or HRES orography, as displayed in the title of the temperature panel.

At longer lead times, the EM and the median will display a tendency to gravitate asymptotically towards the model’s climate. This is most clearly seen when the first ten days of the forecast are anomalous. For example, after an initial spell of cold and rainy weather, the

ensemble tends to indicate a return to milder and drier conditions at longer forecast ranges. This follows logically from the fact that at an infinite range, when predictive skill is completely lost, a climatological value constitutes the optimal forecast.

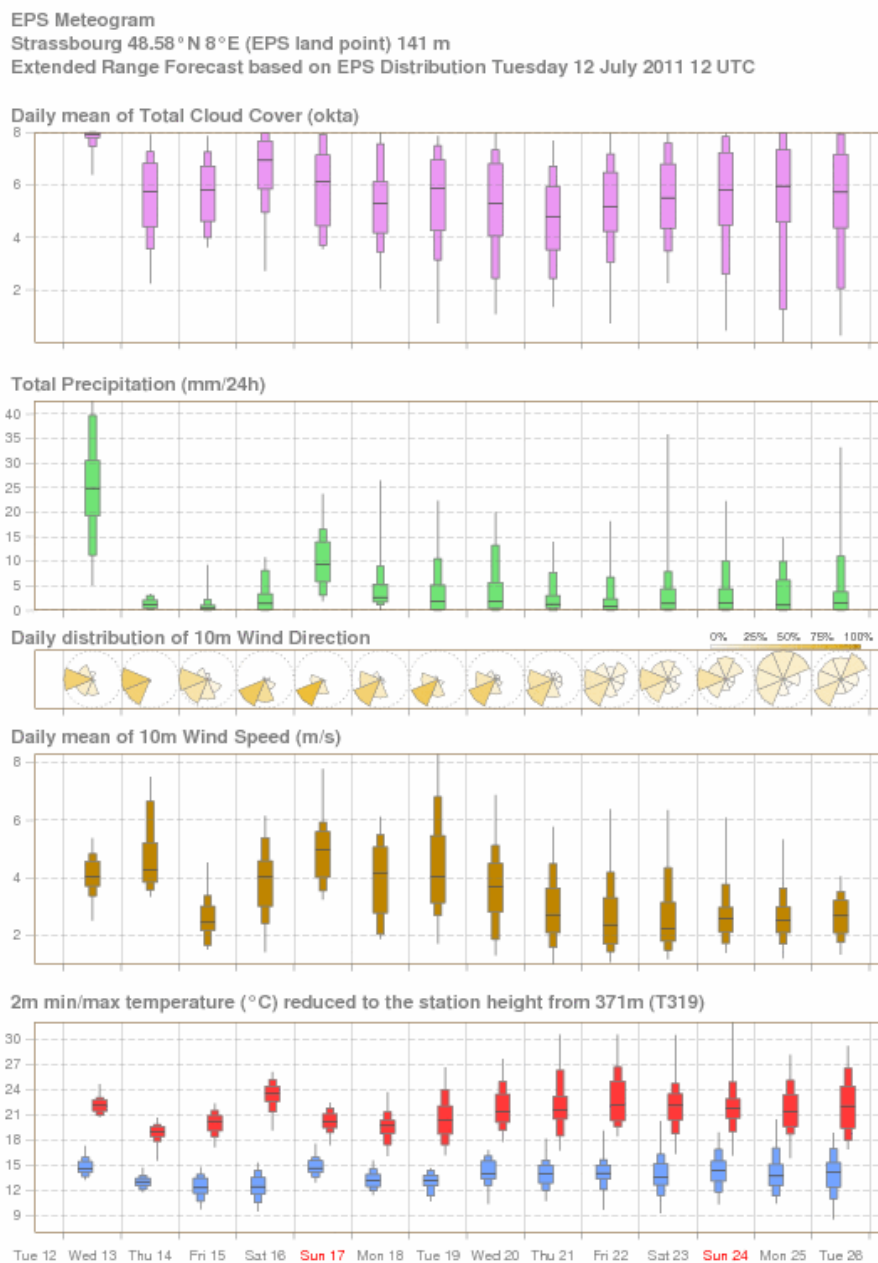


Figure 48: The 15-day EPSgram for Strassbourg, based on the ENS from 12 July 2011, 12 UTC. Here, 24-hourly rainfall probabilities are computed, showing a significant risk of 10 - 15 mm, information that was not obvious from the 6-hourly values in the previous EPSgram.

5.2.5. Interpreting EPSgrams

In EPSgrams the occurrence of a bi-modal distribution will not be detected and users are referred to “plume diagrams” (see Section 3.4.3). If a majority of the members forecast temperatures below zero and, at the same time, a large number of members forecast substantial precipitation, there is no way to determine the likelihood of snowfall from the

diagram alone: the precipitating members might all have temperatures well above zero; as with the probability of combined events (see Section 4.4.7), this can only be calculated from the original ENS data.

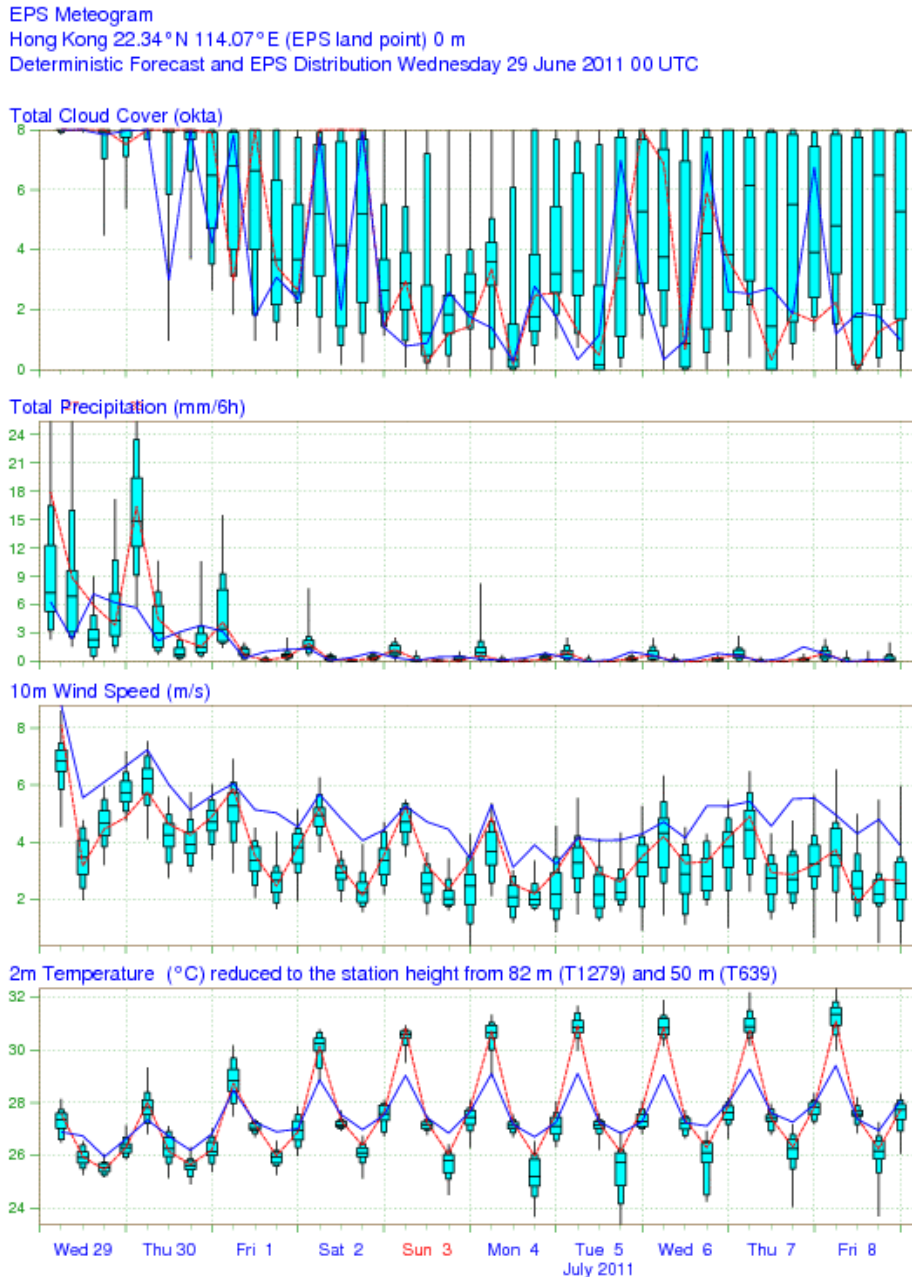


Figure 49: The 10-day EPSgram for Hong Kong, based on ENS from 29 June 2011, 00 UTC. The discrepancy between HRES (blue line) and the EBS Control (red dotted line) is due to the grid-point definitions. The closest HRES grid point is fairly close to Hong Kong, whereas the closest ENS grid point is situated on mainland China, with its warmer and less windy climate.

The relative forecast spread may vary considerably between one parameter and another in the same forecast step. During a high-pressure blocking event, there may be a relatively small spread in precipitation and wind, but a large spread in clouds and temperature. Conversely, in

a zonal regime, there might be a large spread in the precipitation and wind and a small spread in the temperature and cloudiness.

The ensemble can only predict severe weather events of the kind that the model can resolve. The HRES has a small advantage over the ENS with respect to rainfall rate or wind speed. This is another good reason to consider the last HRES together with the ENS in a mini-ensemble.

When the HRES deviates systematically from the ENS, forecasters, relying on their experience or local knowledge, have to decide which information is the more realistic or representative and, if necessary, adjust one to the other. In such circumstances, it may be appropriate to give more weight to HRES (see Figure 49).

5.3. Wave EPSgrams

The data are based on the resolution of the wave model (WAM) HRES and ENS. All ensemble members use the unperturbed wave analysis as the initial condition. The divergence between the ensemble members with respect to ocean waves is, therefore, due only to different wind forcing, if the coupled atmospheric ensemble members develop in different directions (see Figure 50).

10 m wind direction (“wind rose”) is divided into eight main directions or octants, each covering 45° (N, NE, E, SE etc) e.g. the northerly octant is between 337.5° and 22.5°. The length of the radius of an octant is proportional to the probability of that wind direction (i.e. to the proportion of forecasts falling in that octant). The exact probability of each octant is indicated by shading, obtained using a continuous colour scale from light to dark blue (see colour scale in the upper right corner).

10 m wind speed (m/s) is given as the mean of the instantaneous forecast wind speed in m/s. The length of the whiskers should not be interpreted as likely wind gusts.

Significant wave height is given as an instantaneous forecast value in metres. It is an estimate of the mean height of the highest 1/3 of the waves, corresponding with international conventions.

Mean wave direction is the mean direction of propagation of the waves, based on a weighted average of the wave spectrum. Distribution roses for wave direction are created similarly to those for wind direction (see above). Directions are shown in accordance with oceanographic convention, i.e. the direction *towards* which waves are propagating, the *opposite* to the way in which wind direction is displayed: e.g. zero means waves propagating *towards* the north, wind blowing *from* the north.

The instantaneous distribution is shown for the first 12 hours into the forecast and then for all subsequent 24 hour intervals. In order to relate wave height to direction, each octant is coloured, based on the distribution of the significant wave height associated with each mean wave direction. The straight red and blue lines are the mean direction of the control and deterministic forecasts.

Mean wave period is given as an instantaneous value in seconds. The mean period presented corresponds to the “energy period”. The key point for users is that more weight is given to low frequency waves containing swell than to high frequency waves.

Note also that waves might appear unrealistic near small islands that are not represented by at least one land point: in this case, the model’s wave energy will pass the location undisturbed rather than, as in reality, being partly blocked by the island. Similarly, coastlines are represented differently in the ENS and HRES owing to the difference in their resolutions. Moreover, wave data are always selected from the closest sea point in the relevant grid. For these reasons, care should be taken when using wave EPSgrams for points very near complicated coastlines.

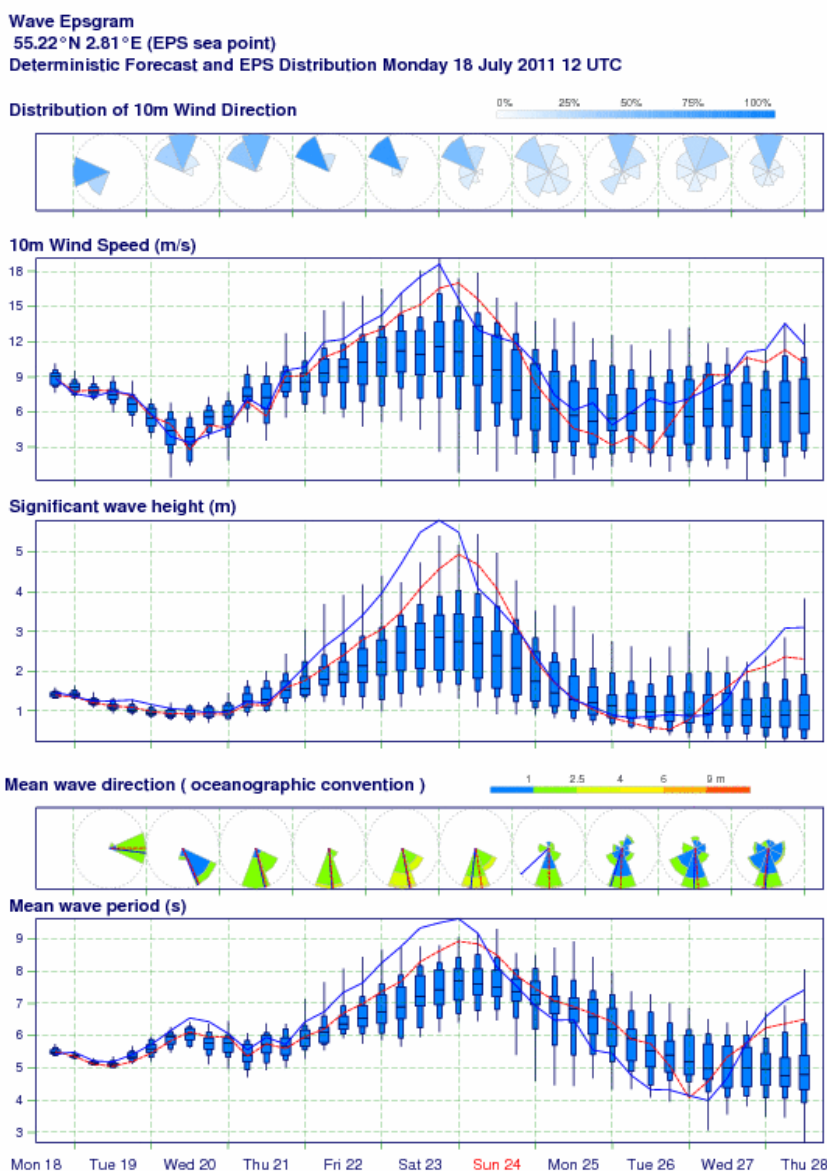


Figure 50: An example of a wave EPSgram for the North Sea 18 July 2011, 12 UTC. A north-westerly wind is forecast to increase over the location, giving rise to amplified waves with increasing periods. The mean wave direction indicates that during the weekend the waves travel mainly to the south with a higher proportion of large waves.

5.4. The Extreme Forecast Index (EFI)

The extraction of extreme weather-related information from the ensemble is not always straightforward. For example, the probabilities themselves do not reveal whether a certain value is unusual or even extreme. A 30% probability of >20 mm rainfall in 6 hours in July would not be “extreme” in New Delhi, but would be in Cairo. The *Extreme Forecast Index* (EFI) has been developed to alert forecasters to anomalous or extreme events by relating the forecast probability distribution to the climatological one (Lalurette, 2003; Zsótér, 2006).

5.4.1. The EFI reference climate

In EFI the forecast probability distribution is compared to the model climate (M-climate) distribution for the chosen location, time of year and lead time. The underlying assumption is that, if a forecast is anomalous or extreme with respect to the M-climate, the real weather is also likely to be anomalous or extreme compared to the real climate.

The M-climate is based on five consecutive weekly 32-day re-runs of the ENS, with four perturbed and one unperturbed initial conditions and started from ERA-Interim re-analyses from each of the last 20 years. The resolution decreases with forecast range exactly as in the ENS. This procedure allows seasonal variations and model changes to be taken into account, as well as model drift. By construction the EFI compensates for systematic errors in the model climate.

The model climate for the EFI calculations on Sunday 31 October 2010 at 12 UTC is, for example, prepared from five re-runs of forecast from five Thursdays, centred on the 28 October, i.e. 14, 21 and 28 October and 4 and 11 November, for all the 20 years, totalling 500 re-forecasts (see Figure 51).

5.4.2. The cumulative distribution function

The EFI value is computed from the difference between two cumulative distribution function (CDF) curves: one for the M-Climature, and the other for the current ENS forecast distribution. The calculations are made so that more weight is given to differences in the tails of the distribution (see Figure 51).

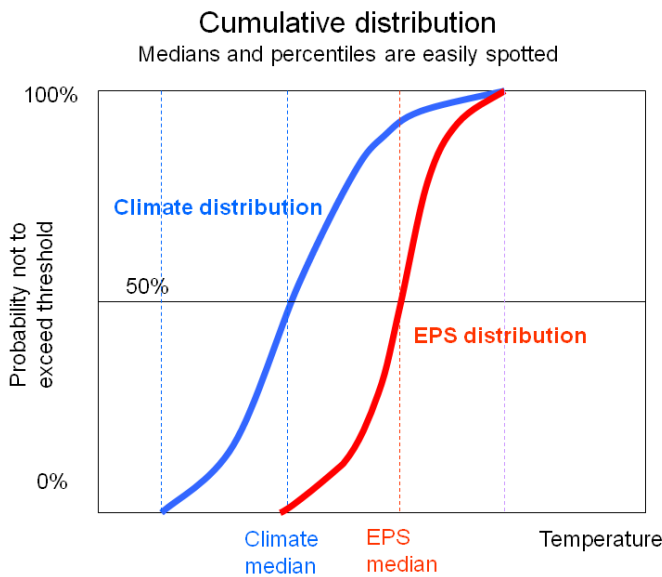


Figure 51: A schematic explanation of the principle behind the Extreme Forecast Index, measured by the area between the cumulative distribution functions (CDFs) of the M-Climate and the ensemble members. The CDF shows the probability (y-axis) against the exceedance threshold value (x-axis). The EFI is, in this case, positive (red line to the right of the blue), indicating higher than normal probabilities of warm anomalies.

From a CDF curve it is also easy to determine the median and any other percentiles as the point on the x-axis where a horizontal line intersects the curve. The most likely values are associated with those where the CDF is steepest. Another way to assess it is by the probability density function (pdf), which is a derivative of the CDF (i.e. the gradient of the curve). The highest probability intervals are easily recognised as the peaks in a pdf (see Figure 52).

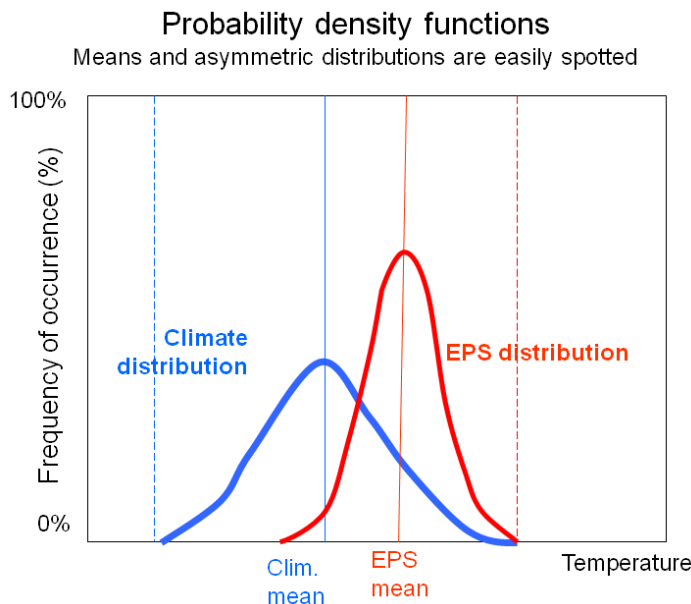


Figure 52: The temperature climatology (blue curve) and the forecast distribution (red curve) presented as probability density functions corresponding to the CDF curves in Figure 51. The pdf is the derivative of the CDF. Here the forecast pdf is to the right (red curve) of the M-climate pdf (blue

curve), indicating that the forecast predicts warmer than normal conditions with high probability, consistent with the conclusions on positive EFI from Figure 51.

The EFI can be understood and interpreted with both the CDF and pdf in mind; the former relates to the EFI value, the latter clarifies the connection to probabilities.

5.4.3. Calculating the EFI

The Extreme Forecast Index is calculated according to the formula

$$EFI = \frac{2}{\pi} \int_0^1 \frac{p - F_f(p)}{\sqrt{p(1-p)}} dp$$

where $F_f(p)$ denotes the proportion of EPS members lying below the p quantile of the climate record. The EFI is computed for many weather parameters, for different forecast ranges and accumulation periods. Charts are accessible via the ECMWF web pages.

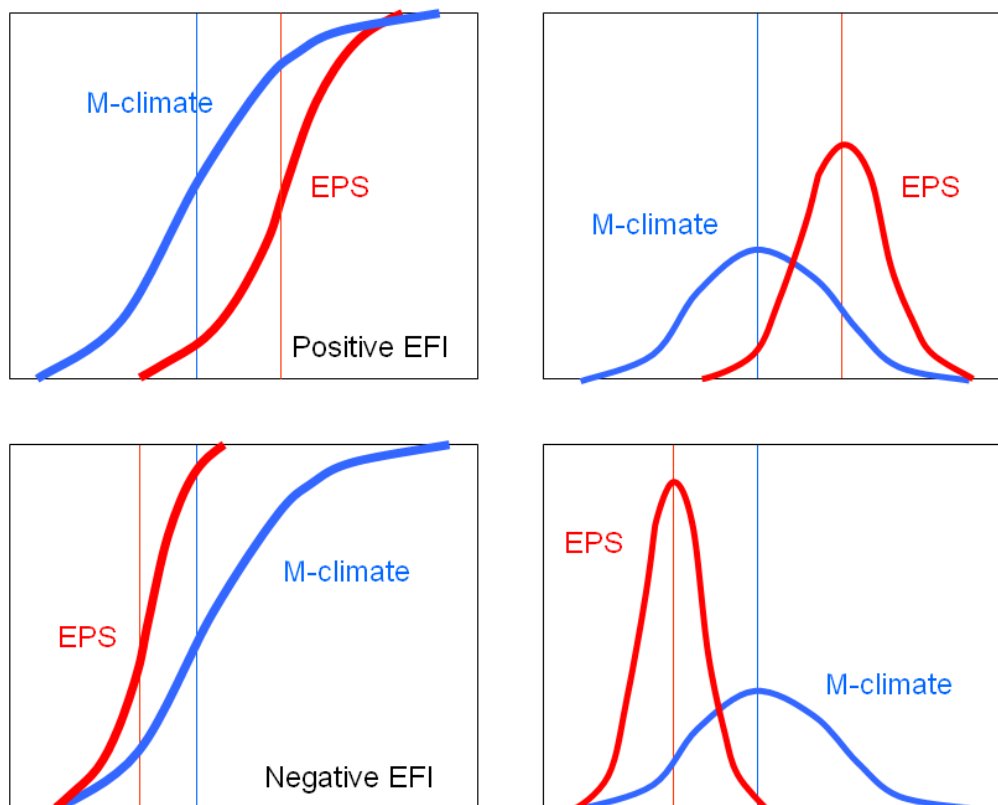


Figure 53: The EFI can have both negative and positive values: positive for positive anomalies (upper figures) and negative for negative anomalies (lower figures).

If the forecast probability distribution agrees with the M-climate distribution then $EFI = 0$. If the probability distribution (mean, spread and asymmetry) does not agree with the climate probability distribution, the EFI takes non-zero values. In the special case where all the members forecast values above the absolute maximum in the M-climate, the $EFI = +1$; if they all forecast values below the absolute minimum in the M-climate the $EFI = -1$ (see Figure 53).

Experience suggests that EFI values of 0.5 - 0.8 (irrespective of sign) can be generally regarded as signifying that “unusual” weather is likely and values above 0.8 as usually signifying that “very unusual” or extreme weather is likely.

A convenient way to depict the current forecast together with previous runs verifying at the same time (“lagged ensembles”) is to depict the CDF from previous runs (see Figure 54).

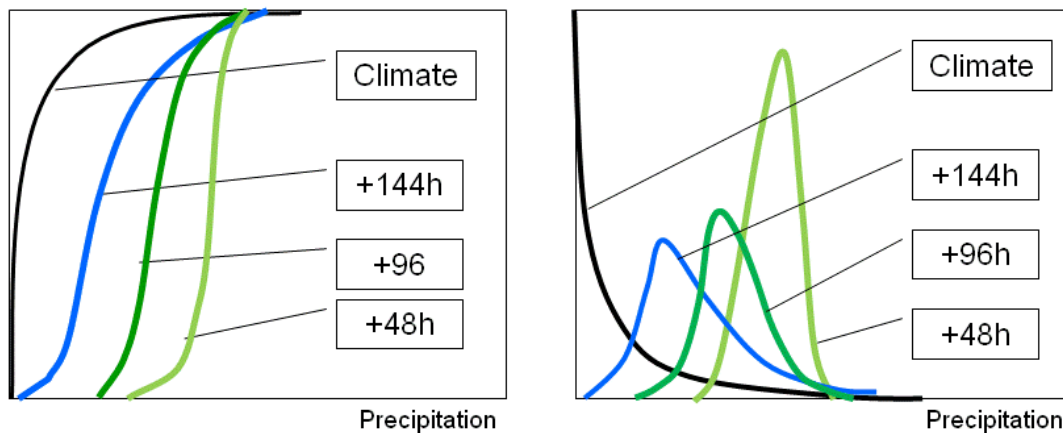


Figure 54: A schematic illustration of the CDF (left) and pdf (right) for forecasts of 12-hour accumulated precipitation. The last EPS forecast +48 hour ahead (light green curves) is presented together with the climate (black curves) and the EPS forecasts four (dark green) and six days back (blue curves).

5.4.4. The interpretation of the EFI

Although a high EFI value indicates that an extreme event is more likely than usual, the values do not represent probabilities. Any forecasts or warnings must be based on a careful study of probabilistic and deterministic information in addition to the EFI.

Since potentially extreme situations (wind storms, for example) are characterized by high dynamical instability in the atmosphere and large spread, EFI users should be aware that it is not uncommon for an extreme event to be preceded by wide-ranging shallow slope CDFs, yielding EFI values that are not particularly high. CDFs should be directly referenced. If, for example, the EFI indicates to forecasters that anomalous wind speeds or rainfall rates are more likely than normal, they have to find out from the CDF diagram what this means for a specific threshold, e.g. 5 mm/12 hours. If the climatological risk is 5% and the predicted probability is 20%, the risk is four times larger than normal. Any action will, however, depend on whether this 20% is high enough for a specific end-user to undertake protective action.

Finally, another key issue of the EFI is that members well beyond M-climate extremes contribute no more to the EFI than members matching the M-climate extreme. Recently the ‘Shift of Tails’ has been developed to address this, and is offered as an additional product (Tsonevsky and Richardosn 2012).

5.4.5. EFI maps

On the ECMWF web site, the EFI is presented in maps, either for each parameter separately or on a composite map for temperature, precipitation and wind (see Figure 55)

Anomalous weather predicted by EPS: Wednesday 17 August 2011 at 00 UTC
1000 hPa Z ensemble mean (Friday 19 August 2011 at 12 UTC)
and EFI values for Total precipitation, maximum 10m wind gust and mean 2m temperature (all 24h)
valid for 24 hours from Friday 19 August 2011 at 00 UTC to Saturday 20 August 2011 at 00 UTC

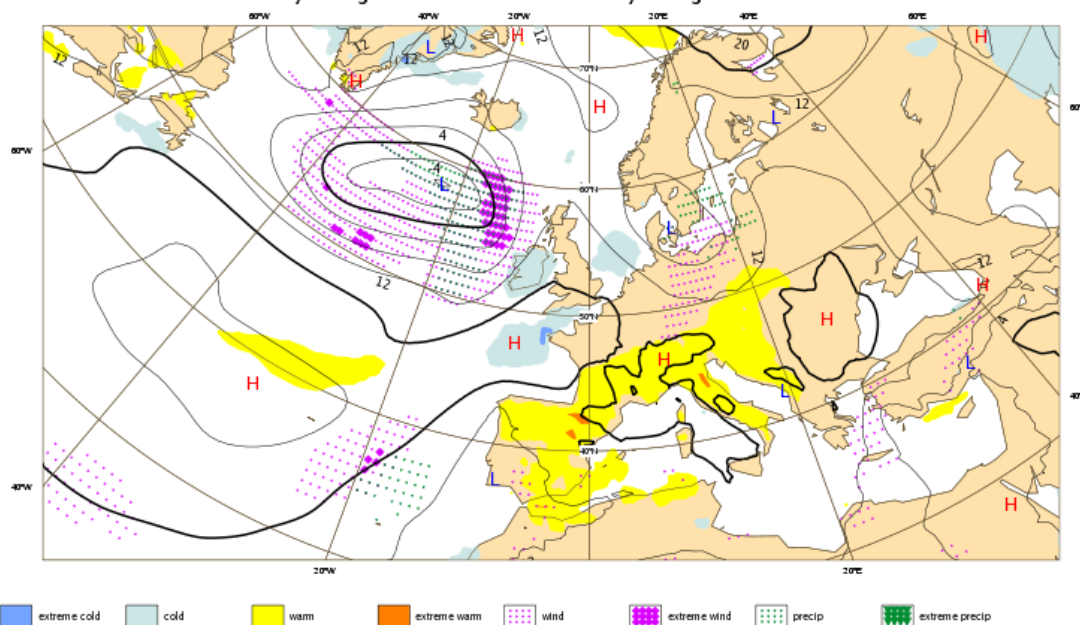


Figure 55: The global “anomalous weather” or “interactive EFI” chart from 17 August 2011, 00 UTC between +48 and +72 hours. It shows the geographical distribution of the EFI of the principal weather parameters: maximum wind gust, 24 h precipitation and 2 m temperature, overlaid with the ensemble mean of the 1000 hPa geopotential field.

Attached to each grid point of the global EFI maps there is a CDF diagram for each of the EFI parameters, with information on climate at the grid point and the available forecast distributions, including the corresponding EFI values. These diagrams can be displayed interactively by clicking on the desired location.

5.5. Tropical cyclone diagrams

The ECMWF tropical cyclone forecast products are designed to provide both deterministic and probabilistic information on the movement and intensity of individual tropical cyclones.

- a) **Cyclone position:** Once official reports signify the existence of a tropical cyclone, it is automatically tracked. The tracking algorithm is based on the extrapolation of past movement and of the mid-tropospheric steering flow to obtain a first-guess position. The *actual position* is determined by searching for mean sea level (MSL) pressure and 850 hPa vorticity extremes around the first-guess position. In some circumstances the thickness maximum, the central MSL pressure and the orography are also considered in the evaluation.
- b) **Strike probability charts:** Strike probability is defined as the proportion of members that predict that the tropical cyclone will pass within a 120 km radius of a given location at

any time during the next five days. In other words, the time dimension is integrated over the forecast range (see Figure 56). This allows for a quick assessment of high-risk areas, regardless of the exact timing. A 40% probability at a specific location means that, within a circular area of 120 km, 40% of members have a tropical cyclone centre during the coming five days.

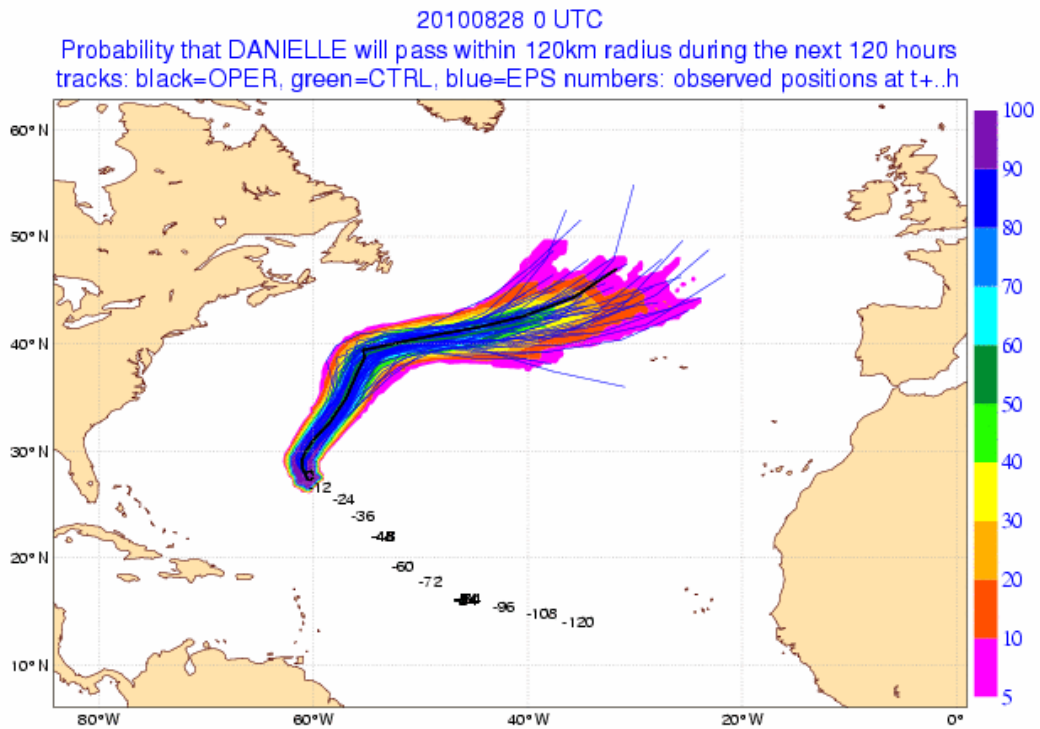


Figure 56: Strike probability map for tropical storm Danielle from the 28 August 2010, 00 UTC.

- c) **Lagrangian meteograms** are a convenient way of evaluating the forecast for a specific tropical cyclone. They contain time series of the central pressure and of the 10 m wind speed maximum predicted within a 7° x 7° lat-long box, centred on the cyclone and following its motion in each forecast member. The symbols are similar to those used on the EPSgrams. The number of members which contain the tropical cyclone is also presented in the diagram at the top of Lagrangian meteograms; the other parameters need to be interpreted with this number in mind (see Figure 57).

EPS Lagrangian Meteogram
Tropical Cyclone DANIELLE (06L) starting from 27.7 N 60.4 W
Deterministic Forecast and EPS Distribution 28 August 2010 0 UTC

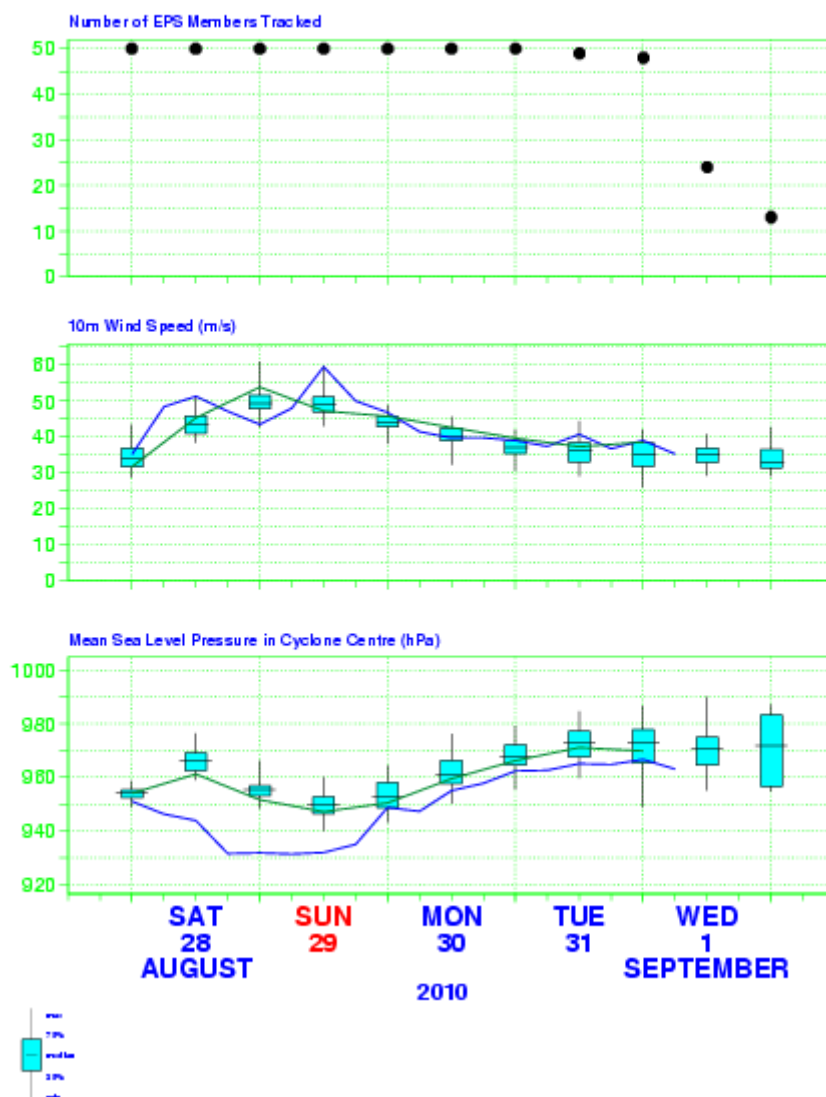


Figure 57: Corresponding Lagrangian meteogram for Tropical Cyclone Danielle, 28 August 2010. Note the decreasing number of members which forecast any tropical cyclone at the end of the ten-day period. Although there is no marked difference between the ENS and the HRES wind speed (blue line), the latter forecasts deeper central pressure. The green line indicates the Control.

Both the strike probability charts and the Lagrangian meteograms are dependent on observations from various tropical cyclone centres around the world and do not take TC genesis into account.

A specific product has been developed to show the potential tropical cyclone activity at different time ranges in the forecast. It includes both tropical cyclones that are present at analysis time and those that develop during the forecast but have not yet come into existence. The maps show the "strike probability", based on the number of members that predict a tropical cyclone, each member having equal weight. To be counted, the tropical cyclone

centre must track within a 300 km radius of the location within a time window of 48 hours (see Figure 58).

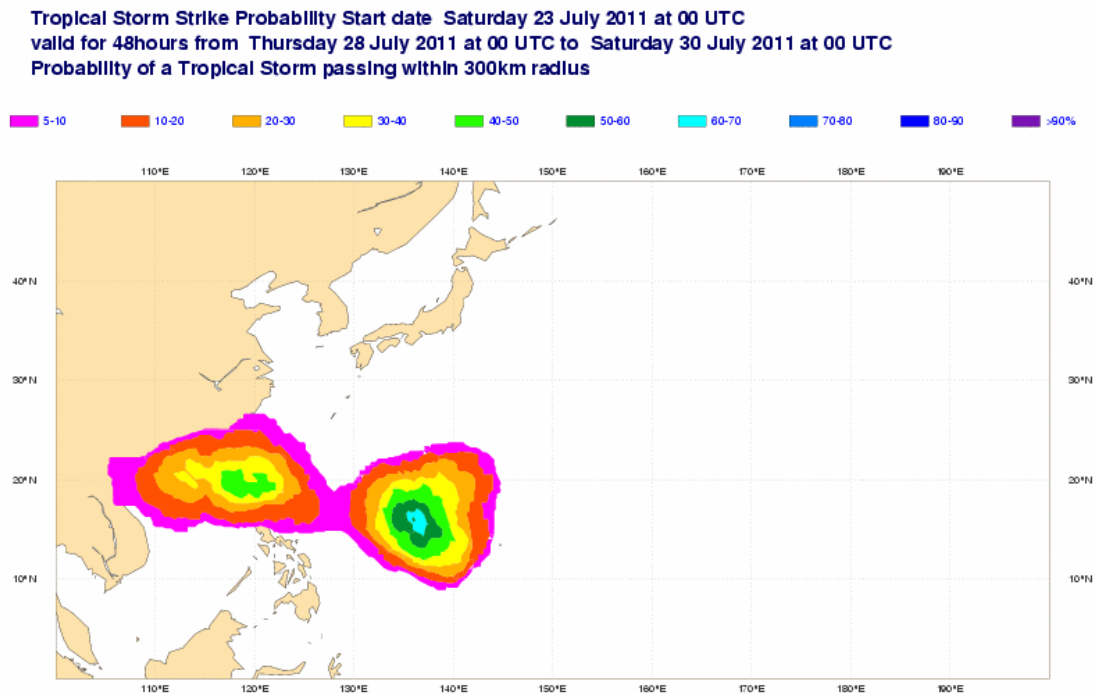


Figure 58: The Tropical Storm Strike Probability chart from Saturday 23 July 2011, indicating the probability of the passage of two not yet developed storms, within a 300 km radius, between 5 and 7 days ahead, i.e. during the 48 hours between Thursday and Saturday 28-30 July 00 UTC. The western system developed into tropical storm NOCK-TEN and briefly reached typhoon status with maximum sustained winds of 75 mph late on Tuesday evening. The eastern system developed into a tropical depression on the 25th, a tropical storm, named MUIFA, on the 28th and a typhoon on the 30 July.

This product provides a quick assessment of high-risk areas, allowing for some uncertainty in the exact timing or position. The strike probabilities are generated for three storm categories: all tropical cyclones (wind speeds $>8\text{m/s}$), tropical storms and above ($>17\text{ m/s}$) and hurricanes/typhoons ($> 32\text{m/s}$). Wind assignment is tuned on the $7^\circ \times 7^\circ$ latitude/longitude box maximum, as represented on Lagrangian meteograms.

5.6. Cyclone track maps

Through a new, feature-based approach to post-processing ECMWF is developing a suite of products that provide synoptic insights into ensemble handling. These web page products aim to represent, objectively and in a variety of ways, the location and behaviour of near-surface, synoptic-scale features, such as fronts, frontal waves, cyclonic features and cyclonic feature tracks, in the ensemble forecasts. The features represented are those typically associated with adverse weather: barotropic lows, frontal systems and frontal waves.

Co-location masking, using a feature-type hierarchy and a minimum separation threshold, helps to keep all cyclonic features 300 km or more apart. Mean sea level pressure, as estimated from 1000 hPa geopotential height and temperature, is also shown as a reference point on many plots. A tracking algorithm has been used to follow the cyclonic features as they evolve in each ensemble member. As a severe weather event approaches, the new

products can indicate that there is an increasing risk of a major storm system in the area of interest, they highlight the track that the system is likely to take and they also suggest the degree of confidence that can be placed in that track (see Figure 59).

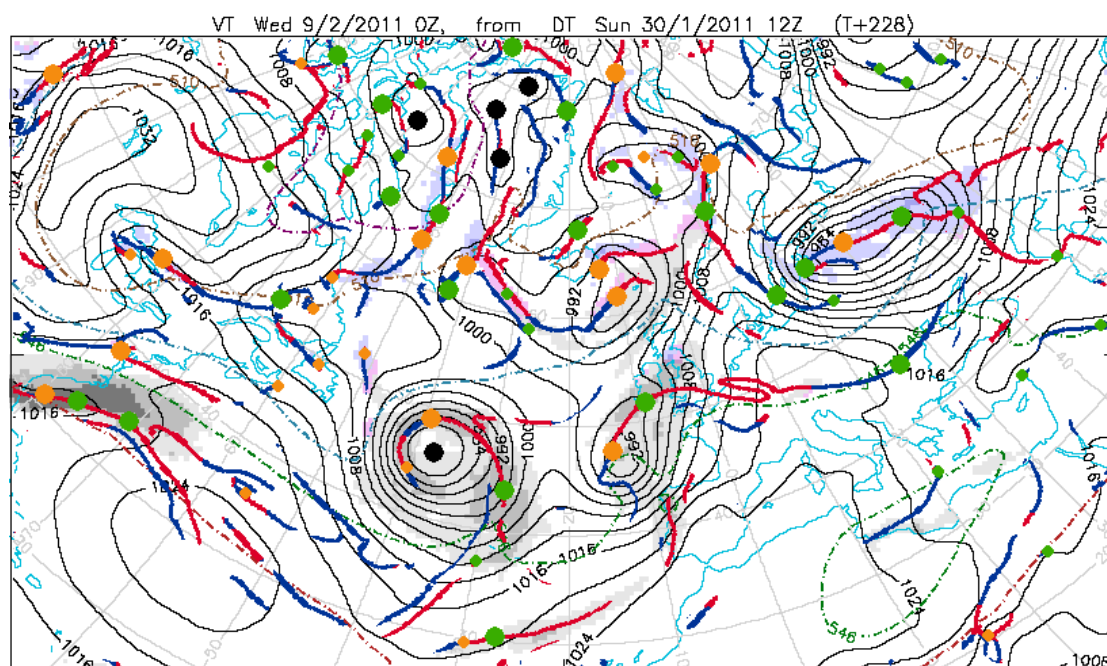


Figure 59: A still image of ensemble member 15 on 30 January 2011, 12 UTC + 228 hour forecast. Automatically diagnosed positions of fronts and troughs are indicated by lines and important synoptic features by filled circles.

The inherent automation should vastly reduce the amount of time forecasters need to spend analysing the ENS and HRES outputs. Since synoptic ‘features’ have historically been used, in part, to highlight the likelihood of severe weather occurring, these products inherently focus, by proxy, on this potential (see further Hewson, 2009; Hewson and Titley, 2010).

5.7. Clustering

To compress the amount of information being produced by the ensemble and highlight the most predictable parts, individual members that are "similar" according to some measure (norm) are grouped together. The norm for measuring which members are “similar” can be defined in different ways. Cluster means (average over all members in the cluster) or representative members provide a convenient overview of the ensemble forecast information.

Clustering can be performed over different geographical areas and for different parameters; it can be done for each forecast time or for different forecast intervals. Every possible clustering is a compromise: the advantage of condensing information is balanced by the disadvantage of losing information that, on some occasions, could have been important to retain.

At ECMWF two types of clustering are currently applied, one is based on “weather scenarios” and the other on “weather regimes”; another variant, “tubing”, is a combination of a “refined” ensemble mean and ensemble outliers.

5.7.1. Weather scenario clustering

Since the emphasis is on large-scale developments, the 500 hPa geopotential forecast field was chosen for the clustering of *daily weather scenarios*. The clustering is performed over an area that covers Europe and its immediate surroundings, including the northeast Atlantic (75N-30N, 20W-40E).

Clustering is performed over four predefined time windows: 3-4 days, 5-7 days, 8-10 days and 11-15 days, with the root mean square (RMS) metric as the norm. To ensure synoptic consistency, each individual ensemble member must belong to the same cluster through the time window. For two members to be assigned to the same cluster, they must display similar synoptic 500 hPa development over the whole time window. Weak gradients in 500 hPa forecasts can lead to synoptically rather different members being assigned to the same cluster because of the RMS norm.

Clustering in this way, rather than on individual forecast days, has the advantage that the temporal continuity and synoptic consistency are retained. Since all members are regarded a priori as equally likely, the number of members in each cluster could define its probability or, rather, “weight”. The clustering scheme is designed to create no more than six clusters (Ferranti and Corti, 2011).

A cluster is represented not by the mean of its members but by its most representative member (MRM), which is selected by a pattern-matching algorithm, based on minimizing the distance between the cluster’s “centre of gravity” and the member, using the RMS norm. The MRM is chosen to symbolize the cluster; it should not be seen as a substitute for the cluster average and should not be used as a deterministic forecast.

The number of cluster scenarios is related to the characteristics of the ensemble forecast distribution. If the distribution is made up of few, well separated groups of “similar forecasts” (“multi-modal distribution”) the cluster scenarios will represent the range of possible weather conditions (see Figure 60).

Saturday 23 April 2011 12UTC ECMWF EPS Cluster scenario - 1000 hPa Geopotential
Reference step t+120-168 Based on the 500hPa Geopotential Clustering

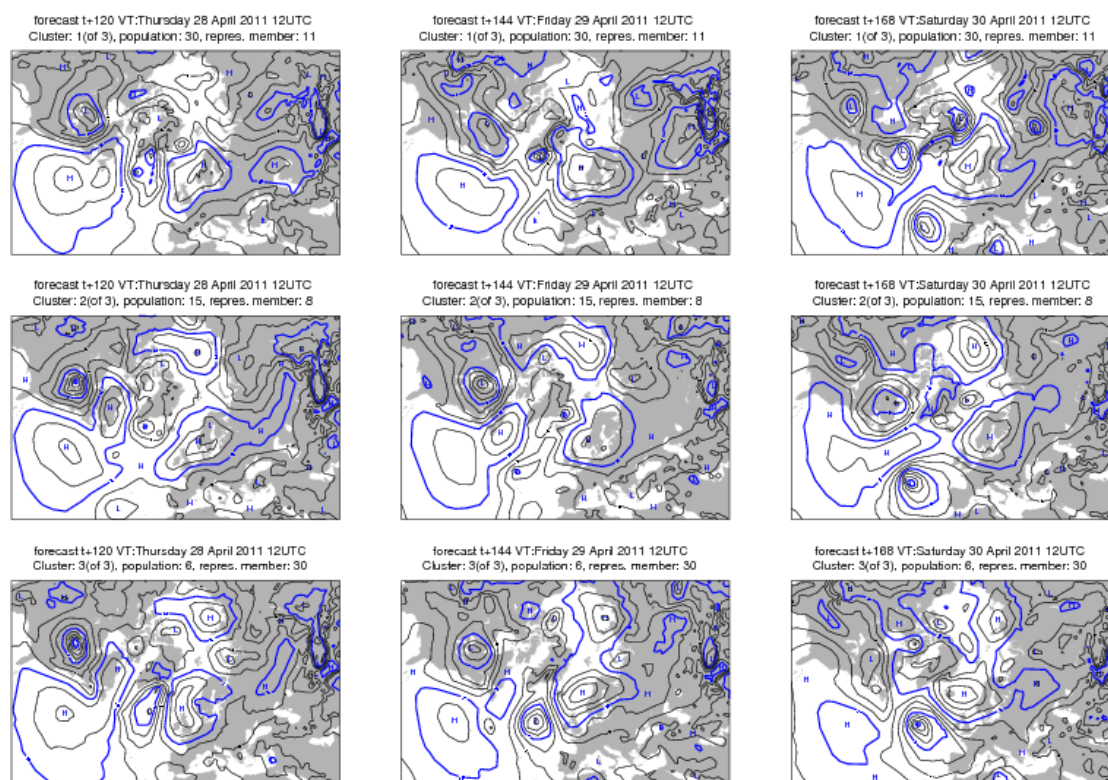


Figure 60: The most representative 1000 hPa members selected to describe the clustering of the forecast 23 April 2011, 12 UTC +120 to +168 hours.

If the ensemble distribution is very homogeneous and the cluster algorithm cannot partition the ensemble, no significant clusters are detected and the ensemble median is presented as the sole cluster MRM. The existence of a large spread does not therefore mean that a cluster will necessarily be created. On the other hand, even if the spread is small, clusters will be created, provided that a partition is possible. *Large ensemble spread does not automatically lead to more clusters, or vice versa.*

The clusters are intended to give an overview of the ensemble forecast information and should not be over-interpreted. The differences between two clusters will be mainly related to genuine differences in the 500 hPa flow pattern, in particular if the differences are large scale. Minor differences may partly be due to the choice of MRM for each of the two clusters. For the MSL clusters, major differences might also be due to the relation between the flow at 500 hPa and the MSL pressure; fairly similar 500 hPa patterns might be linked to quite different MSL pressure patterns.

5.7.2. Climatological weather regimes

The clustering described above is flow-dependent; there are no a priori prescribed regimes. Pre-defined climatological weather regimes are used for another type of clustering. Four common large-scale flow patterns have been computed from 29 years of reanalysis data (ERA-Interim and ERA-40): Euro-Atlantic blocking (regime 2); the positive (regime 1) and negative (regime 3) phases of the North Atlantic Oscillation and a pronounced ridge over the

Atlantic (regime 4). One set of fixed climatological regimes is valid for the cold (October to April) and another for the warm (May to September) seasons.

A pattern-matching algorithm is used to assign each of the cluster representative members to the closest climatological weather regime, sometimes called “Grosswetterlage” (German for large-scale weather regime). This is associated with a specific colour: positive NAO pattern is associated with blue, negative NAO with green, Euro-Atlantic blocking with red and the Atlantic ridge pattern with violet. The simplification into “Grosswetterlagen” increases the predictability and usefulness of the system.

5.7.3. *Tubing*

All ensemble members which, in RMS terms, are “close to” the EM are averaged to provide a more “refined” EM: the central cluster mean (CCM). Members which are significantly different, “outliers”, are grouped together in a number of *tubes* (maximum 9). Each tube is represented not by an average of the members in the tube but by its most extreme member; this allows better visualization of the different scenarios in the ensemble.

The CCM and the tubes are computed for the whole forecast range. For each reference step (+96 h, +144 h, +168 h, +192 h and +240 h), tubing products are generated over a 48-hour sequence, finishing on the reference step. For example +48/+72/+96 h are used for the +96 h tubing, the +120/+144/+168 h for the +168 h tubes.

The tubes are not intended to serve as probability alternatives, only to give an indication of what is not included in the central cluster mean. They show the “direction” towards which tube members deviate from the main central cluster mean. Synoptic experience suggests, however, that every tube has a 10% chance of verifying, which leaves the central cluster with a typical probability of 60-90% of verifying, depending on the number of tubes. Forecast experience also suggests that 2-3 tubes represent normal large-scale predictability; fewer tubes yield higher predictability and more tubes lower predictability. Forecasters should not use the CCM as the basis for a categorical forecast, if it contains unusually few members and there are an unusually high number of “tubes”.

6. Epilogue: how to increase the public's trust in medium-range weather forecasts

At the time when ECMWF was founded, it was estimated that medium-range weather forecasts would lead to large economic gains for society. Currently, forecasts are, on average, synoptically useful for up to a week or more, with extreme weather events generally forecast three to four days in advance. Nevertheless, medium-range forecast information is not always used to its full potential; when decisions on the protective action to be taken against extreme weather are made, medium-range forecasts too often serve only as background information.

6.1. How can trust in medium-range forecasts be increased?

Increasing the trust in medium-range weather forecasts would make them an even more essential part of core meteorological activities at the meteorological services, in particular for warnings of extreme events.

6.1.1. Improving the forecast system

One way to increase the trust in medium-range forecasts is, of course, to further improve the skill of the ECMWF deterministic forecast system. Its skill has increased by a day per decade since 1979 and it is likely that this trend will continue, thanks to improvements to the deterministic forecast system planned for the next ten years:

- Systematic increase in the resolution of the assimilation and forecasting systems
- Enhancement of the representation of physical processes in the model
- Exploitation of better data and their assimilation, in particular from satellites

However, an overall improvement of the deterministic forecasts may not be enough to increase the use of the medium-range forecasts. It is not enough that the forecasts are high quality, they must also be trusted.

6.1.2. Trust in individual forecasts

The ultimate criterion of a good forecast system is the quality of the decisions based on it. Although decision-makers have always had high confidence in the skill of the forecasts *in general*, there is less confidence in the skill of *specific* forecasts for a particular event, for example, when extreme weather is likely. It is therefore essential that every single forecast is so trusted that it can be used for decision-making. *A good forecast that is not trusted is a forecast without value, irrespective of how well it verifies retrospectively.* A fourth planned improvement is therefore:

- Better ways to quantify the forecast uncertainty by means of the ENS.

The ENS is able to pinpoint which deterministic forecasts can be relied on and thereby increase end-users' willingness to make decisions based on these good forecasts.

6.1.3. When the deterministic forecast cannot be trusted.

It is self-evident that useful decisions can be made when there is high confidence in the skill of deterministic forecasts. However, it is less obvious that useful decisions can also be made

when the deterministic forecast is likely to be wrong – *provided that forecasters are aware of this uncertainty!* As shown in the example in Appendix A-8, most users are in this case better served by not receiving a forecast at all, rather than receiving one with misleading certainty. The optimum solution in such cases is to present the uncertainties in probabilistic or similar terms. This brings to the fore the role of human forecasters.

6.2. The role of the forecaster in the medium-range

What is and will be the role of the human forecaster, given the steadily increasing skill of NWP? The demise of weather forecasters “within 5 - 10 years” has been prophesied almost since the start of NWP. However, human forecasters obviously serve a purpose because there are more of them in operational duty today than ever before, increasingly so in the commercial sector. What function do they really serve?

The proportion of freely available, automatically generated weather forecasts has increased tremendously because of the expansion of the Internet. Such forecasts might satisfy needs during normal weather conditions but not in situations of extreme or high-impact weather. A decision to evacuate an area will never be made purely on the basis of automated NWP output nor is there, and might never be, one single source of NWP information with a concerted message, in particular in situations threatening extreme or high-impact weather.

Weather forecasting has never been primarily about getting it “right” or “wrong”, as in some quiz show, but, rather, about providing information for decision-making, maximizing advantages and minimizing disadvantages.

It is here, in the decision-making process, that professional weather forecasters can really “add value”, thanks to their education, their unique position in the centre of the information flow and their experience in the skill and characteristics of different forecast systems.

6.3. How the forecaster can “add value”

What distinguishes professional meteorologists is their ability to make use of uncertainty. In highly predictable weather situations anybody can confidently report “what the weather is going to be” just by reading off the computer output, but in difficult weather situations it is only the professionals who can cleverly express uncertainty: “This cold air might arrive over our area later in the week”...”The rain might exceed 50 mm in places”...”We cannot exclude hurricane force wind gusts.” *It is this uncertainty information that adds “extra value” to the forecast.*

Appendix A Some statistical concepts to facilitate the use and interpretation of deterministic medium-range forecasts

Introduction

An NWP system can be evaluated in at least two ways. *Validation* measures the realism of the model with respect to its ability to *simulate* the atmosphere's behaviour whereas *verification* measures the system's ability to *predict* atmospheric states.

Only the most commonly used validation and verification methods will be discussed here, mainly with respect to upper air variables, 2 m temperature and 10 m wind. Verification of binary forecasts will be discussed in relation to utility. For a full presentation the reader is referred to Nurmi (2003; Joliffe and Stephenson, 2003; Wilks, 2006).

A-1 Forecast validation

A forecast system that perfectly simulates the behaviour of the atmosphere has the same degree of variability as the atmosphere with no systematic errors.

A-1.1 The mean error

The mean error (ME) of forecasts (f) relative to analyses (a) can be defined as

$$ME = \overline{f - a}$$

where the over-bar denotes an average over a large sample in time and space. A perfect score, $ME=0$, does not exclude very large errors of opposite signs which cancel each other out. If the mean errors are independent of the forecast and vary around a fixed value, this constitutes an "unconditional bias". If the ME is flow dependent i.e. if the errors are dependent on the forecast itself or some other parameter, then we are dealing with systematic errors of "conditional bias" type; in this case, variations in the ME from one month to another might not necessarily reflect changes in the model but in the large-scale flow patterns (see Figure 61 below).

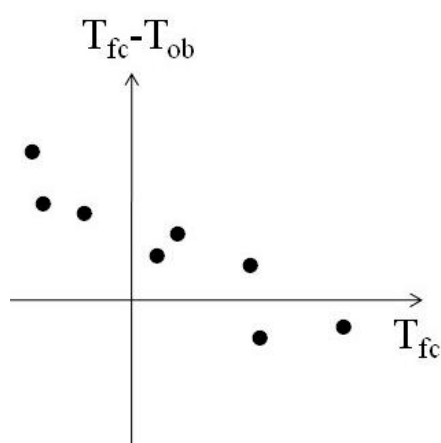


Figure 61: A convenient way to differentiate between "unconditional" and "conditional" biases is to plot scatter diagrams, with forecasts vs. forecast errors or observations (analyses) vs. forecast error. From the slope and direction of the scatter in these diagrams it is also possible to find out if the forecasts are over- or under-variable. In this case the colder the forecasts the larger the positive error, the warmer the forecast the larger the negative error. This implies that cold anomalies are not cold enough and warm anomalies not warm enough, i.e. the forecasts are under-variable.

A-1.2 Forecast variability

The ability of a NWP model to forecast extremes with the same frequency as they occur in the atmosphere is crucial for any ensemble approach, either lagged, multi-model or EPS. If the model has a tendency to over- or under-forecast certain weather elements, their probabilities will, of course, also be biased.

More generally, the forecast variability over time and space should be equal to at least the analysed, ideally the observed variability. There are different variance measures to monitor this variability:

- Variability around the climatological average, which measures the model’s ability to span the full climatological range
- The averaged analysed and forecast *spatial* variance over a specified area at a specific time e.g. a day; it may be presented as a time series
- The averaged *temporal* variability over a specified area, calculated over a sufficiently long time period. The variance can be computed for every grid point or as the change over 12 or 24 hours. It may be presented as geographical distributions (see Figure 62).

For all three methods the level of variability averaged over many forecasts in the medium range should be the same as for the initial analysis or a short-range forecast.

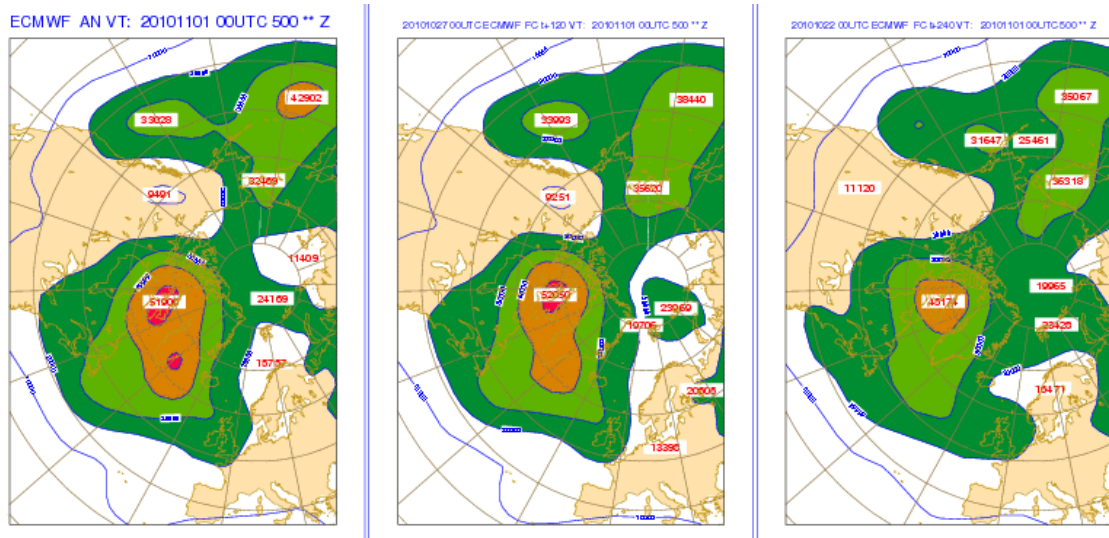


Figure 62: 500 hPa geopotential variability, October 2010 - March 2011. The standard deviation over the period is calculated for every grid point. The analysis (left) shows maximum variability between Greenland and Canada and in the North Pacific. This is well captured by the D+5 forecast (centre) and D+10 forecast (right) but with slightly decreasing values.

If a *perfect* model has, by definition, no systematic errors, then a *stable* model might have systematic errors which do not change their characteristics during the forecast range. Most state-of-the-art NWP models are fairly stable in the medium range but start to display some model drift, such as gradual cooling or warming, moistening or drying, in the extended ranges.

A-1.3 False systematic errors

One of the complexities of interpreting the ME is that apparent systematic errors might, in fact, have a non-systematic origin. If this is the case, *a perfect model appears to have systematic errors; a stable model appears to suffer from model drift*. This is a reflection of a general statistical artefact, the “regression to the mean” effect ¹.

The fact that a perfect model forecasts anomalies with the same intensity and frequencies as observed does not mean that they will be correct in time and place. Due to decreasing predictive skill it will, with increasing lead time, have less success in getting the forecast anomalies right in intensity, time and place. If the forecast is wrong for a specific forecast anomaly, in particular for a strong anomaly, the verifying truth might be more anomalous but in most cases will be less anomalous. Even if the forecast anomaly has the right intensity, phase errors will tend to displace it rather towards less anomalous patterns than towards even more anomalous configurations (see Figure 63).

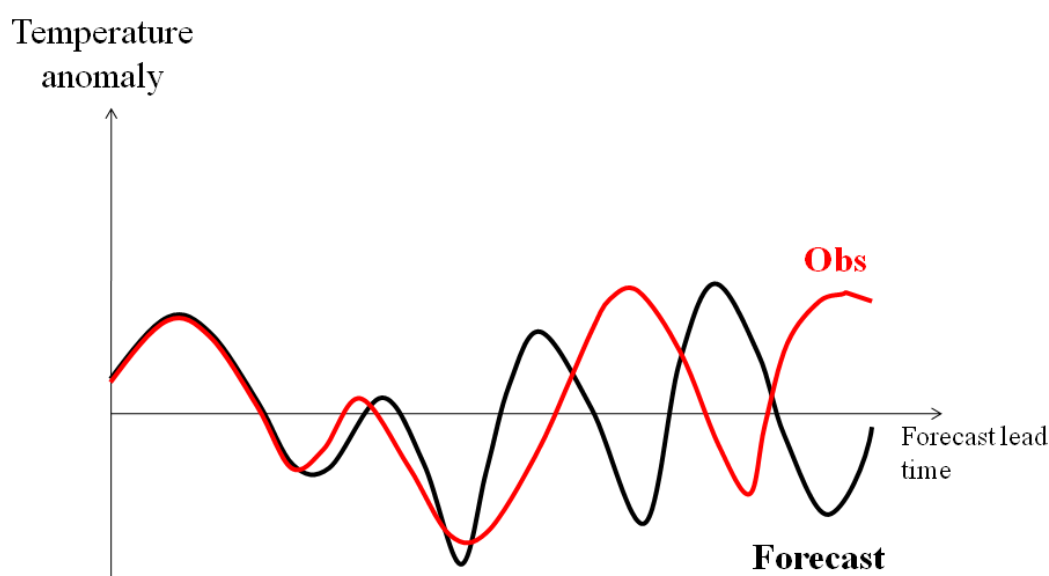


Figure 63: A schematic picture of a medium range forecast (black) and the verifying analysis. The forecast anomalies have about the same magnitudes as the verifying anomalies, but they are out of phase. This will yield a tendency for positive anomalies to verify against less positive or even negative anomalies, negative anomalies to verify against less negative or even positive anomalies.

Anomalies will therefore appear as if they have been systematically exaggerated, increasingly so as skill decreases with increasing lead time. Plotted in a scatter diagram, these non-systematic forecast errors therefore give a misleading impression that positive anomalies are systematically over-forecast and negative anomalies systematically under-forecast (see Figure 64).

¹ The “regression to the mean” effect was first discussed by Francis Galton (1822-1911) who found that tall (short) fathers tended to have tall (short) sons, but on average slightly shorter (taller) than themselves.

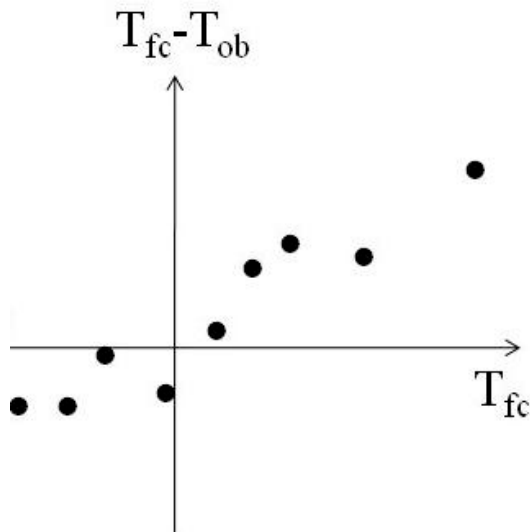


Figure 64: A scatter diagram of forecasts versus forecast error. Warm forecasts appear too warm, cold forecasts appear too cold. If the forecasts are short range, it is reasonable to infer that the system is over-active, overdeveloping warm and cold anomalies. If, on the other hand, the forecasts are well into the medium range, this might not be the case. Due to decreased forecast skill, predicted anomalies tend to verify against less anomalous observed states.

A-1.4 False model climate drift

This “regression to the mean” effect gives rise to another type of false systematic error. Forecasts produced and verified over a period characterized by on average anomalous weather will display a false impression of a model climate drift. A perfect model will produce natural looking anomalies, independent of lead time, but since the initial state is already anomalous, the forecasts are, with decreasing skill, more likely to be less anomalous than even more anomalous. At a range where there is no longer any predictive skill, the mean error will be equal to the observed mean anomaly with the opposite sign (see Figure 65).

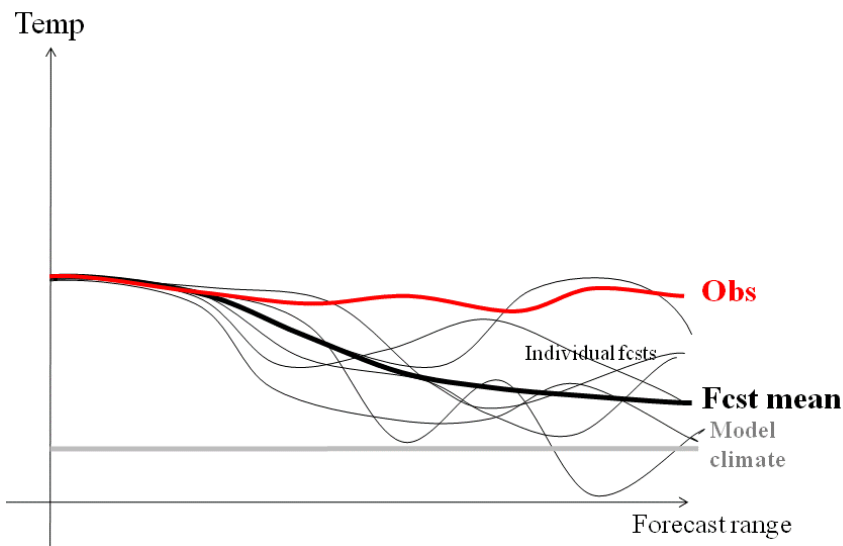


Figure 65: A sequence of consecutive NWP forecasts (thin black lines, their mean (thick black line) and the observations (red line). Forecasts starting in an anomalous state are less likely to forecast even more extreme conditions. With increasing lead time and decreasing skill the forecasts will tend to cluster increasingly around the climate average and give an impression of increasing ME. The mean error will therefore give the false impression of a drift in the model climate.

The ME can be trusted to reflect the properties of the model's performance only during periods with no or small average anomalies.

A-2 Forecast verification

Objective weather forecast verification can be performed from at least three different perspectives: *accuracy* (the difference between forecast and verification), *skill* (comparison with some reference method, such as persistence, climate or an alternative forecast system) and *utility* (the economic value or political consequences of the forecast). They are all "objective" in the sense that the numerical results are independent of who calculated them, but not necessarily objective with respect to what is considered "good" or "bad". The skill measure depends on a subjective choice of reference and the utility measure depends on the preferences of the end-user. Only the first approach, the accuracy measure, can be said to be fully "objective", but, as seen in 4.3.4, in particular Figure 31 and Figure 32, the *purpose* of the forecast might influence what is deemed "good" or "bad".

A-2.1 Measures of accuracy

The most common accuracy measure is the Root Mean Square Error (RMSE):

$$RMSE = \sqrt{\overline{(f - a)^2}}$$

which measures the distance between the forecast and the verifying analysis or observation. The RMSE is negatively orientated, i.e. increasing numerical values indicate increasing "failure".

The mean absolute error:

$$MAE = \overline{|f - a|}$$

is also negatively orientated. Due to its quadratic nature, the RMSE penalizes large errors more than the non-quadratic MAE and thus takes higher numerical values. This might be one reason why MAE is sometimes preferred, although the practical consequences of forecast errors are probably better represented by the RMSE. We will concentrate on the RMSE, or rather the squared version, the mean square error:

$$MSE = \overline{(f - a)^2}$$

which is more convenient to analyse mathematically.

A-2.2 The effect of mean, analysis and observation errors on the RMSE

If the forecasts have a mean error (ME), $f = f_o + ME$, where f_o is a forecast with no systematic errors. If $(f_o - a)$ is uncorrelated to ME, then the MSE is their quadratic sum:

$$MSE = \overline{(f_o - a + ME)^2} = \overline{(f_o - a)^2} + ME^2$$

If the analysis or observation errors (ERR) have to be taken into account and they are non-correlated with $(f_o - a)$, the MSE is their quadratic sum:

$$MSE = \overline{(f_o - a + ERR)^2} = \overline{(f_o - a)^2} + ERR^2$$

Systematic forecast errors, as well as analysis and observational errors, have their highest impact in the short range, when the non-systematic error level is still relatively low (see Figure 66).

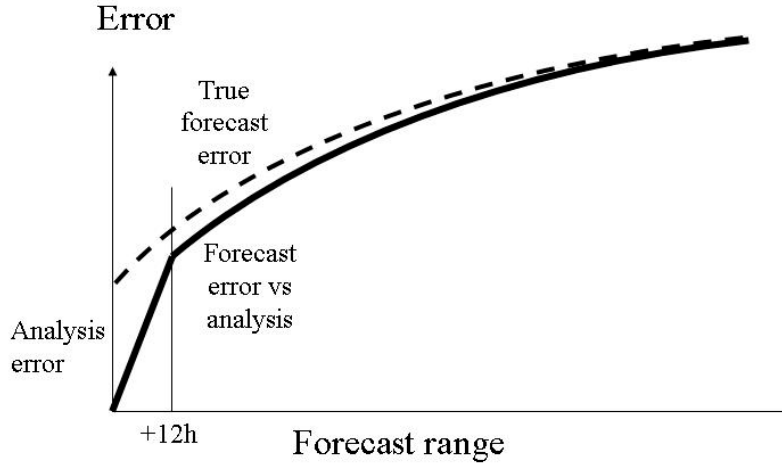


Figure 66: Forecasts verified against analyses often display a “kink” for the first forecast interval. This is because the error curve starts from the origin, where the forecast at $t=0$ is identical to the analysis. However, the true forecast error (forecasts vs. correct observations) at initial time ($t=0$) represents the analysis error and is rarely zero. The true error curve with respect to the correct observations lies at a slightly higher level than the error curve with respect to the analysis, in particular initially.

Any improvement of the NWP output must, therefore, with increasing forecast range, increasingly address the non-systematic errors (see Appendix B-6 on the statistical post-processing of NWP output).

A-2.3 The decomposition of MSE

The MSE can be decomposed around c , the climate of the verifying day:

$$MSE = \overline{(f - c + c - a)^2} = \overline{(f - c)^2} + \overline{(a - c)^2} - 2\overline{(f - c)(a - c)}$$

which can be written:

$$MSE = A_f^2 + A_a^2 - 2cov[(f - c)(a - c)]$$

where A_a and A_f are the atmospheric and model variability respectively around the climate. Hence the level of forecast accuracy is determined not only by the predictive skill, as reflected in the covariance term, but also by the general variability of the atmosphere, expressed by A_a , and how well the model simulates this, expressed by A_f .

A-2.4 Forecast error baseline

When a climatological average replaces the forecast ($f = c$), the model variability A_f and the covariance term become zero and

$$RMSE = E_{\text{climate}} = A_a$$

which is the accuracy of climatological weather information used as forecasts. Since climatological averages can be found in tourist brochures, any deterministic medium-range forecast to an end-user should be more accurate than them (see 4.3.4. for a discussion of why

errors of user-orientated forecasts *should not* exceed the E_{climate} level whereas forecasts from good NWP models at some range *must*.

A-2.5 Error saturation level

Forecast errors do not grow indefinitely but asymptotically approach a maximum, the “Error Saturation Level” (ESL).

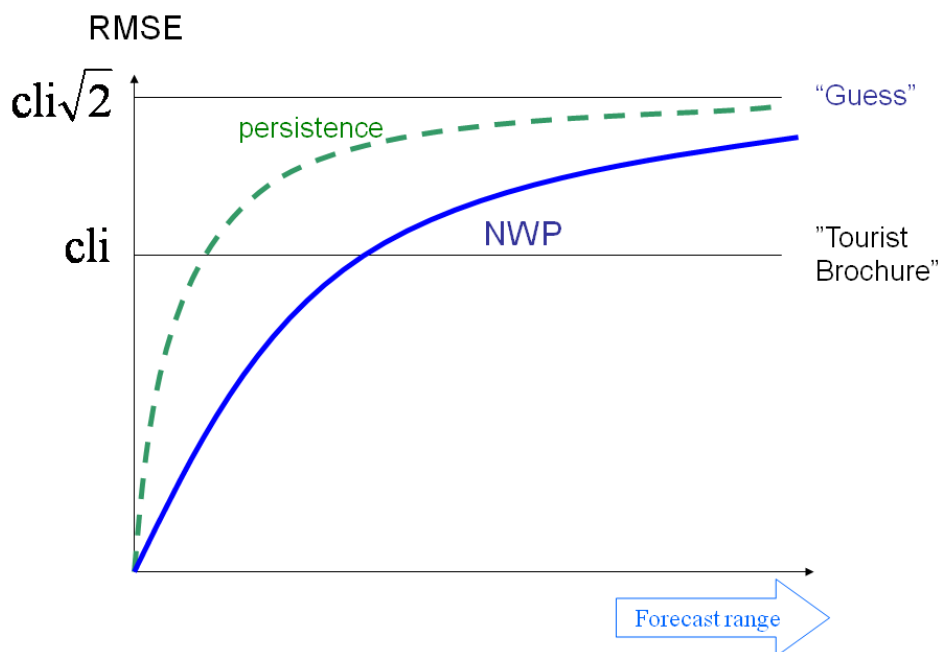


Figure 67: The error growth in a state-of-the-art NWP forecast system will at some stage display larger errors than a climatological average used as forecast and will, as do the errors of persistence forecasts and guesses, asymptotically approach an error level 41% above that of a forecast based on a climatological average

For extended forecast ranges, with decreasing correspondence between forecast and observed anomalies, the covariance term approaches zero. For $A_f=A_a$ this yields an ESL at

$$RMSE = E_{\text{saturation}} = A_a\sqrt{2}$$

which is 41% larger than E_{climate} , the error when a climatological average is used as a forecast (see Figure 67). The value $A_a\sqrt{2}$ is also the ESL for persistence forecasts or guesses based on climatological distributions.

A-2.6 Measure of skill - the anomaly correlation coefficient

Another way to measure the quality of a forecast system is to calculate the correlation between forecasts and observations. However, correlating forecasts directly with observations or analyses may give misleadingly high values because of the seasonal variations. It is therefore established practice to subtract the climate average from both the forecast and the verification and to verify the forecast and observed *anomalies* according to the anomaly correlation coefficient (ACC), which in its most simple form can be written:

$$ACC = \frac{\overline{(f - c)(a - c)}}{\sqrt{\overline{(f - c)^2} \overline{(a - c)^2}}}$$

The WMO definition also takes any mean error into account:

$$ACC = \frac{[(f - c) - \overline{(f - c)}][\overline{(a - c)} - (a - c)]}{\sqrt{\left(\overline{(f - c) - \overline{(f - c)}}\right)^2 + \left(\overline{(a - c) - \overline{(a - c)}}\right)^2}}$$

The ACC can be regarded as a *skill score relative to the climate*. It is positively orientated, with increasing numerical values indicating increasing “success”. It has been found empirically that ACC=60% corresponds to the range up to which there is synoptic skill for the largest scale weather patterns. ACC=50% corresponds to forecasts for which the error is the same as for a forecast based on a climatological average, i.e. RMSE = A_a. An ACC of about 80% would correspond to a range where there is still some skill in large-scale synoptic patterns.

A-3 Interpretation of verification statistics

The mathematics of statistics can be relatively simple but the results are often quite difficult to interpret, due to their counter-intuitive nature: what looks “good” might be “bad”, what looks “bad” might be “good”. As we have seen in A-1.3, seemingly systematic errors can have a non-systematic origin and forecasts verified against analyses can yield results different from those verified against observations. As we will see below, different verification scores can give divergent impressions of forecast quality and, perhaps most paradoxically, improving the realism of an NWP model might give rise to *increasing* errors.

A-3.1 Interpretation of RMSE and ACC

Both A_f and A_a and, consequently, the RMSE vary with geographical area and season. In the mid-latitudes they display a maximum in winter, when the atmospheric flow is dominated by large-scale and stronger amplitudes, and a minimum in summer, when the scales are smaller and the amplitudes weaker.

For a forecast system that realistically reflects atmospheric synoptic-dynamic activity A_f=A_a. If A_f < A_a the forecasting system *underestimates* atmospheric variability, which will contribute to a decrease in the RMSE. As discussed in Chapter 4, this is “bad” if we are dealing with a NWP model but “good”, if we are dealing with post-processed deterministic forecasts to end-users. On the other hand, if A_f > A_a the model *overestimates* synoptic-dynamic activity, which will contribute to increasing the RMSE. This is normally “bad” for all applications.

Comparing RMSE verifications of different models or of different versions of the same model is most straightforward when A_f=A_a and the models have the same general variability as the atmosphere.

A-3.2 Effect of flow dependency

Both RMSE and ACC are flow dependent, sometimes in a contradictory way. In non-anomalous conditions (e.g. zonal flow) the ACC can easily take low (“bad”) values, while in anomalous regimes (e.g. blocking flow) it can take quite high (“good”) values. The opposite is true for RMSE, which can easily take high (“bad”) values in meridional or blocked flow regimes and low (“good”) values in zonal regimes. Conflicting indications are yet another

example of “what looks bad is good”, as they reflect different virtues of the forecasts and thereby provide the basis for a more nuanced overall assessment.

A-3.3 The “double penalty effect”

A special case of the flow dependence of the RMSE and ACC is the “double penalty effect”, where a bad forecast is “penalised” twice: first for *not* having a system where there is one and second for *having* a system where there is none. It can be shown that, if a wave is forecast with a phase error of half a wave length or more, it will score worse in RMSE and ACC *than if the wave had not been forecast at all* (see Figure 68).

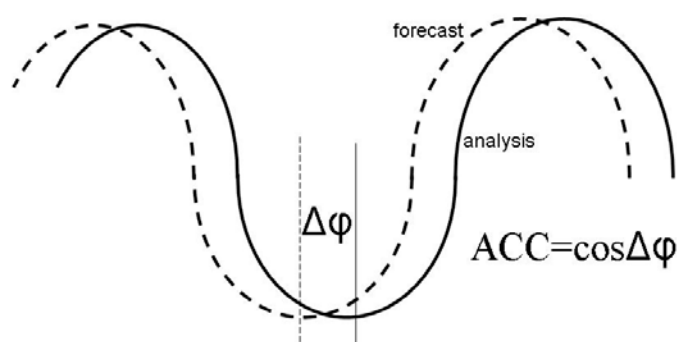


Figure 68: When the phase error $\Delta\phi$ is larger than half a wave length, the scores will be worse than if there was no wave forecast at all.

The double penalty effect often appears in the late medium range, where phase errors become increasingly common. At this range they will strongly contribute to false systematic errors (see A-1.3).

A-3.4 Subjective evaluations

Considering the many pitfalls in interpreting objective verification results, purely subjective verifications should not be dismissed. They might serve as a good balance and check on the interpretation of the objective verifications. This applies in particular to the verification of extreme events, where the low number of cases makes any statistical verification very difficult or even impossible.

A-4 Graphical representation

The interpretation of RMSE and ACC outlined above may be aided by a graphical vector notation, based on elementary trigonometry. The equation for the decomposition of the MSE is mathematically identical to the “cosine law”. From this it follows that the cosine of the angle β between the vectors (f-c) and (a-c) corresponds to the ACC (see Figure 69).

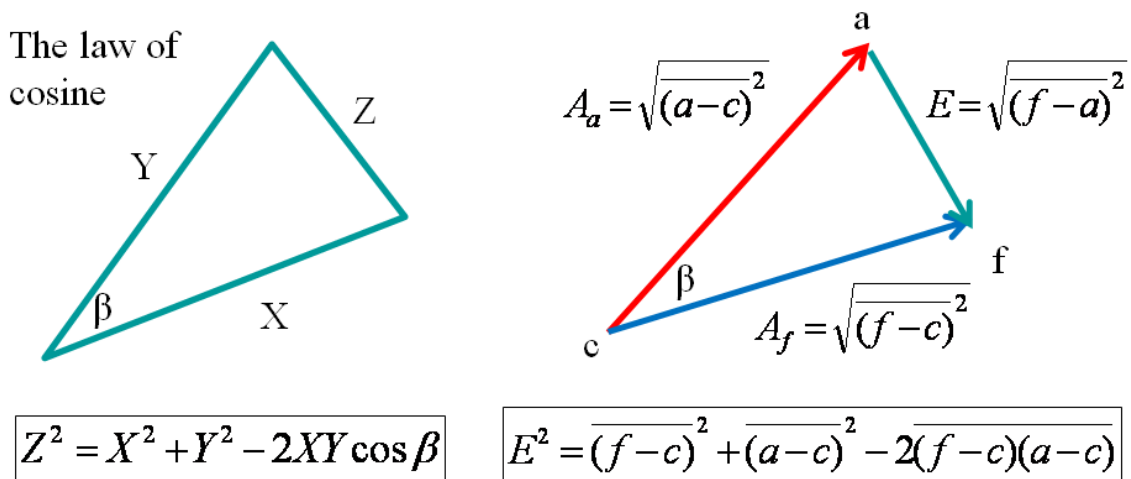


Figure 69: The relationship between the cosine theorem and the decomposition of the RMSE.

A-4.1 Forecast errors

When the predicted and observed anomalies are uncorrelated, i.e. there is no skill in the forecast, they are in a geometrical sense orthogonal and the angle β between vectors $(a-c)$ and $(f-c)$ is 90° and the error is on average $\sqrt{2}$ times the atmospheric variability around climate.

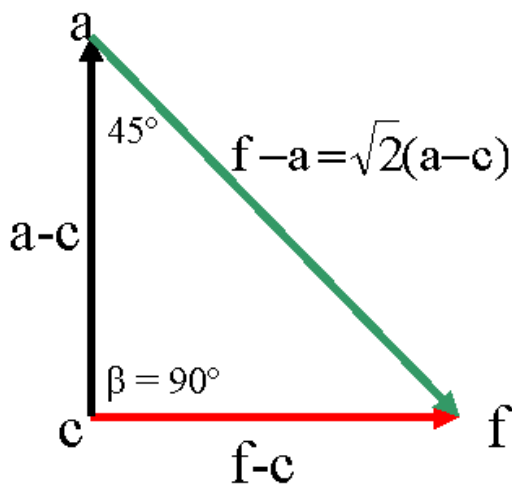


Figure 70: When the forecast and observed anomalies are orthogonal (i.e. uncorrelated) $\beta=90^\circ$ and the forecasts $(f-c)$ have on average errors equal to $\sqrt{2}$ times A_a (the atmospheric variability) or the error of a climatological average.

From Figure 70 it can also be seen that the climate average (c) is more accurate than the forecast at extended or infinite range. From vector-geometrical arguments it is easy to understand why $ACC=50\%$ when the $RMSE=E_{climate}$ and $RMSE < E_{climate}$ for higher ACC, for example 60%, which is the empirically determined limit for useful predictions (see Figure 71).

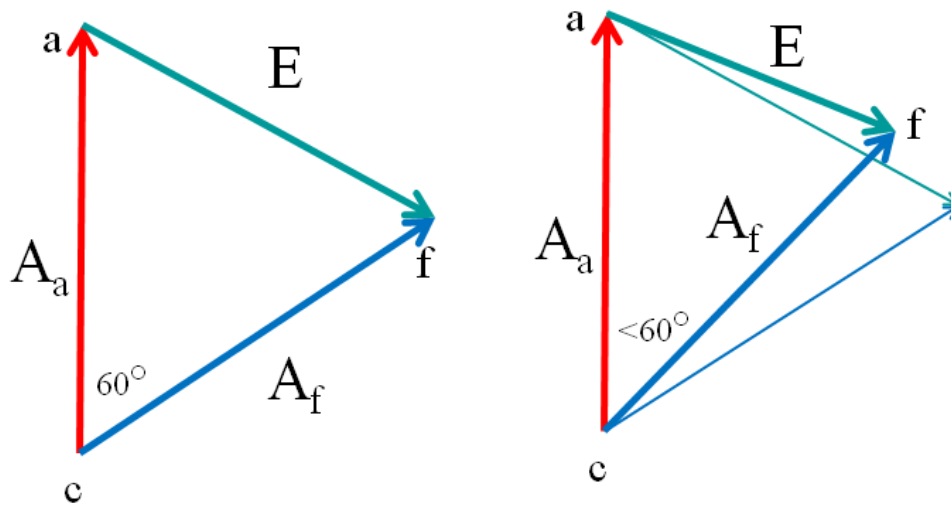


Figure 71: When the ACC=50%, i.e. the angle between the anomalies (a-c) and (f-c) =60°, the RMSE=A_a, the atmospheric variability (left). When ACC>50% the RMSE is smaller. An ACC=60% is agreed to indicate the limit of useful synoptic forecast skill.

A-4.2 Flow dependence

The flow dependence of RMSE and ACC is illustrated in Figure 72, for (left) a case of, on average, large anomaly, when a large RMS error is associated with a large ACC (small angle β), and (right) a less anomalous case, when a smaller RMS error is associated with a small ACC (large angle β).

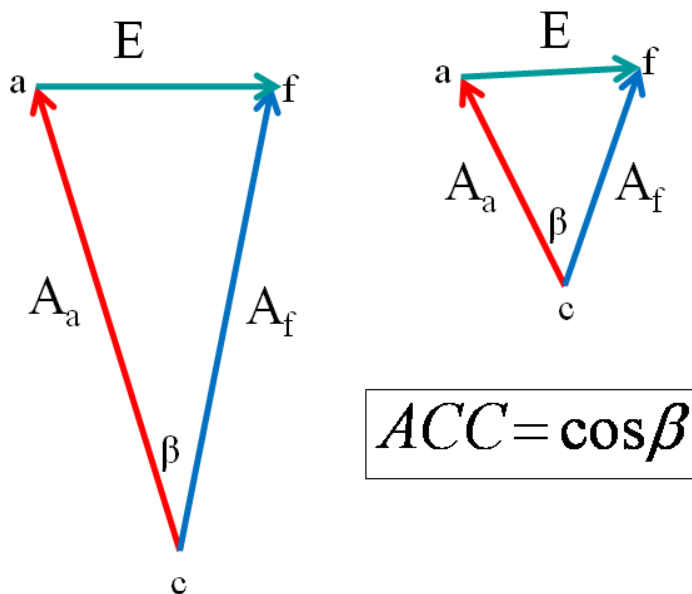


Figure 72: In situations with large variability around the climate average (left) relatively large RMSE can be associated with relatively large ACC (small β) and (right) in situations with relatively small variability around the climate relatively small RMSE can be associated with small ACC (larger β). For these cases the RMSE and ACC will give conflicting signals.

If the RMSE is used as the norm, it would in principle be possible, at an extended range, to pick out those “Members of the Day” that are better than the average, just by selecting those members which are less anomalous. If, however, the ACC is used as the norm, the “Members of the Day” may turn out to be those members which are *more* anomalous.

A-4.3 Damping of forecast anomalies

As discussed in Chapter 4., dampening the variability of the forecasts increases their accuracy. It can be shown, see Figure 73, that optimal damping is achieved when the variability is reduced by a proportion that is equal to cosine (β) or the ACC.

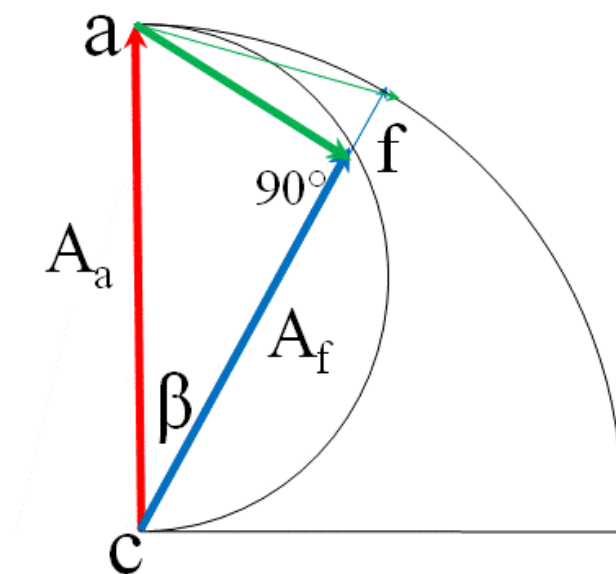


Figure 73: Damping the forecast variability A_f will minimize the RMSE, if it becomes orthogonal to the forecast. This happens when $A_f = ACC \cdot A_a$ and the forecast vector $f-c$ varies along a semi-circle with a radius equal to half A_a .

A-4.4 Forecast error correlation

At an extended forecast range, when there is low skill in the forecast anomalies and weak correlation between them, there is still a fairly high correlation between the forecast errors. This is because the forecasts are compared with the same analysis. Consider (see Figure 74) two consecutive forecasts f and g , from the same model or two different models, with errors $(f-a)$ and $(g-a)$. Although the angles between $(f-c)$, $(g-c)$ and $(a-c)$ at an infinite range are 90° and thus the correlations zero, the angle between the errors $(f-a)$ and $(g-a)$ is 60° , which yields a correlation of 50%. For shorter ranges the correlation decreases when the forecast anomalies are more correlated and the angle between them $<60^\circ$. The perturbations in the analyses are constructed to be uncorrelated.

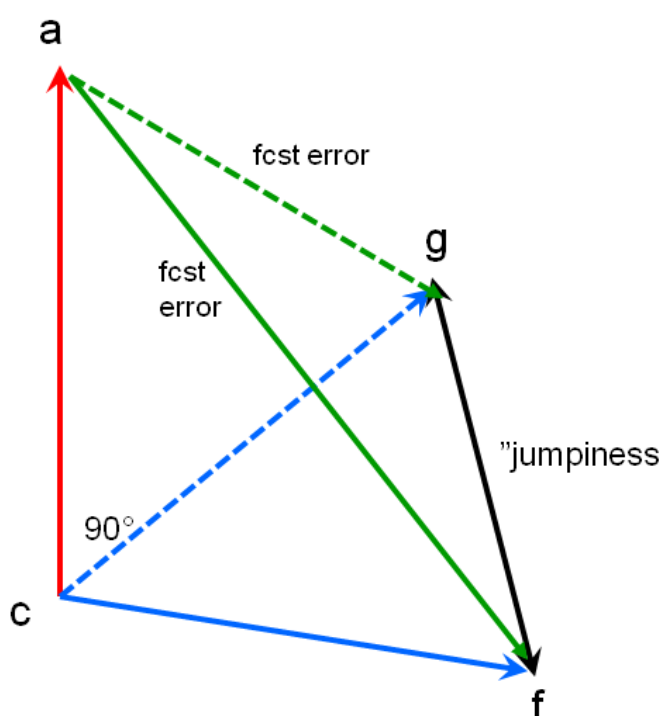


Figure 74: A 3-dimensional vector figure to clarify the relation between forecast jumpiness and error. Two forecasts, f and g , are shown at a range when there is no correlation between the forecast and observed anomalies ($f-c$), ($g-c$) and ($a-c$). The angles between the three vectors are 90° . The angles in the triangle $a-f-g$ measure up to 60° which means that there is a 50% correlation between the “jumpiness” ($g-f$) and the errors ($f-a$) and ($g-a$). The same is true for the correlation between ($f-a$) and ($g-a$).

A-4.5 Forecast jumpiness and forecast skill

From the same Figure 74 it follows that since the angle between the forecast “jumpiness” ($f-g$) and the error ($f-a$) is 60° , the correlation at an infinite range between “jumpiness” and error is 50%. For shorter forecast ranges the correlations decrease because the forecast anomalies become more correlated, with the angle between them $<60^\circ$.

A-4.6 Combining forecasts

Combining different forecasts into a “consensus” forecast either from different models (“the multi-model ensemble”) or from the same model (“the lagged average forecast”) normally yields higher forecast accuracy (lower RMSE). The forecasts should be weighted together with respect not only to their average errors but also to the correlation between these errors (see Figure 75).

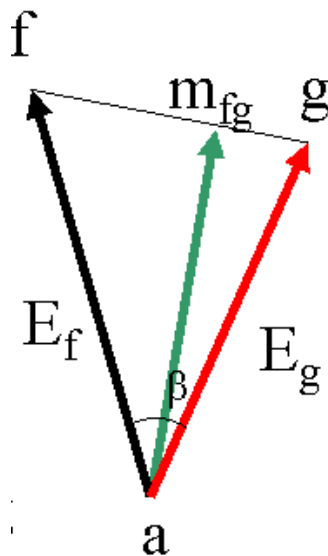


Figure 75: Forecasts f and g , either from two different NWP systems or from the same, but with different lead times, verifying at the same time. The errors $E_f=(f-a)$ and $E_g=(g-a)$ correlate cosine (β). Weighted together they yield a forecast m_{fg} with a RMSE which is lower than the errors E_f and E_g of the two averaged forecasts. The smaller the β , the larger their error correlation and the less m_{fg} will yield an error reduction.

However, when E_f and E_g correlate less than their fraction E_g/E_f , combining forecasts does not yield a reduction in errors (see Figure 76).

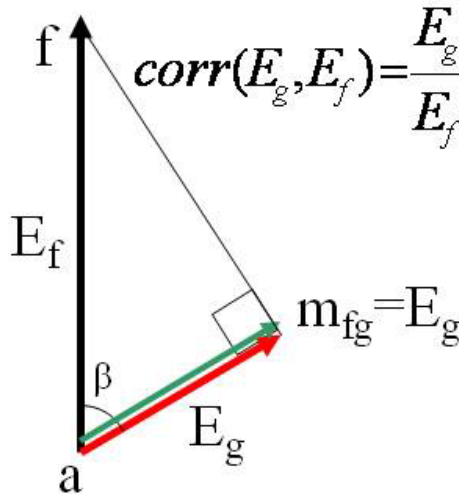


Figure 76: For certain relations between forecast accuracy and forecast error correlation no combination will be able to reduce the RMSE.

The discussion can be extended to any number of participating forecasts. In ensemble systems the forecast errors are initially uncorrelated but slowly increase in correlation over the integration period, though never exceeding 50%.

A-5 The usefulness of statistical know-how

Statistical verification is normally associated with forecast product control. Statistical know-how is not only able to assure a correct interpretation but also to help add value to the medium-range NWP output. The interventions and modifications performed by experienced

forecasters are to some extent statistical in nature. Modifying or adjusting a short-range NWP in the light of later observations is qualitatively similar to “optimal interpolation” in data assimilation. Correcting for systematic errors is similar to linear regression analysis and advising end-users in their decision-making involves an understanding of cost-loss analysis. Weather forecasters are not always aware that they make use of Bayesian principles in their daily tasks, even if the mathematics is not formally applied in practice (Doswell, 2004).

Investigations have shown that forecasters who have a statistical education and training do considerably better than those who do not have such understanding (Doswell, 2004). Forecasters should therefore keep themselves informed about recent statistical validations and verifications of NWP performance.

A-6 Utility verification

The ultimate verification of a forecast service is the value of the decisions that end-users make based on its forecasts, providing that it is possible to quantify the usefulness of the forecasts; this brings a subjective element into weather forecast verification.

A-6.1 The contingency table

For evaluating the utility aspect of forecasts it is often convenient to present the verification in a contingency table with the corresponding hits (H), false alarms (F), misses (M) and correct no-forecasts (Z). If N is the total number of cases then $N=H+F+M+Z$. The sample climatological probability of an event occurring is then $P_{\text{clim}}=(H+M)/N$.

Table 2

	Event obs	Event not obs
Event forecast	H	F
Event not forecast	M	Z

A wide range of verification scores² can be computed from this table, but here we will only mention the *Hit Rate* $HR=H/(H+M)$ and the *false alarm rate* $FR=F/(Z+F)$ ³.

A-6.2 The “expected expenses”

The *expected expenses* (*EE*) are defined as the sum of the costs due to protective actions and the losses endured:

$$EE=c \cdot (H+F) + L \cdot M$$

²Note that the terminology here may be different from that used in other books. We refer to the definitions given by Nurmi (2003) and the recommendations from the WWRP/WGNE working group on verification.

³ The FR should not be confused with the false alarm ratio $FAR=F/(H+F)$, i.e. the proportion of false alarms, given the event was forecast, which is one of the main parameters, together with the HR, in ROC diagrams.

where c is the cost of protective action, when warnings have been issued, and L is the loss, if the event occurs without protection. Always protecting makes $EE=c \cdot N$ and never protecting $EE=L \cdot (M+H)$. The break-even point, when protecting and not protecting are equally costly, occurs when $cN = L(H+M)$ which yields $c/L = (H+M)/N = P_{clim}$. Whenever the “cost-loss ratio” $c/L < P_{clim}$, it is advantageous to protect, if P_{clim} is the only information available.

A-7 Practical examples

The following set of examples is inspired by real events in California in the 1930s (Lewis, 1994, p.73-74).

A-7.1 A situation with no weather forecast service

Imagine a location where, on average, it rains 3 days out of 10. Two enterprises, X and Y, each lose €100, if rain occurs and they have not taken protective action. But whereas X only has to invest €20 for protection, Y has to pay €60.

Thanks to his low protection cost, X protects every day, which costs on average €20 per day over a longer period. Y, on the other hand, chooses never to protect, due to the high cost, and suffers an average loss of €30 per day over an average 10-day period, owing to the three rain events (see Figure 77).

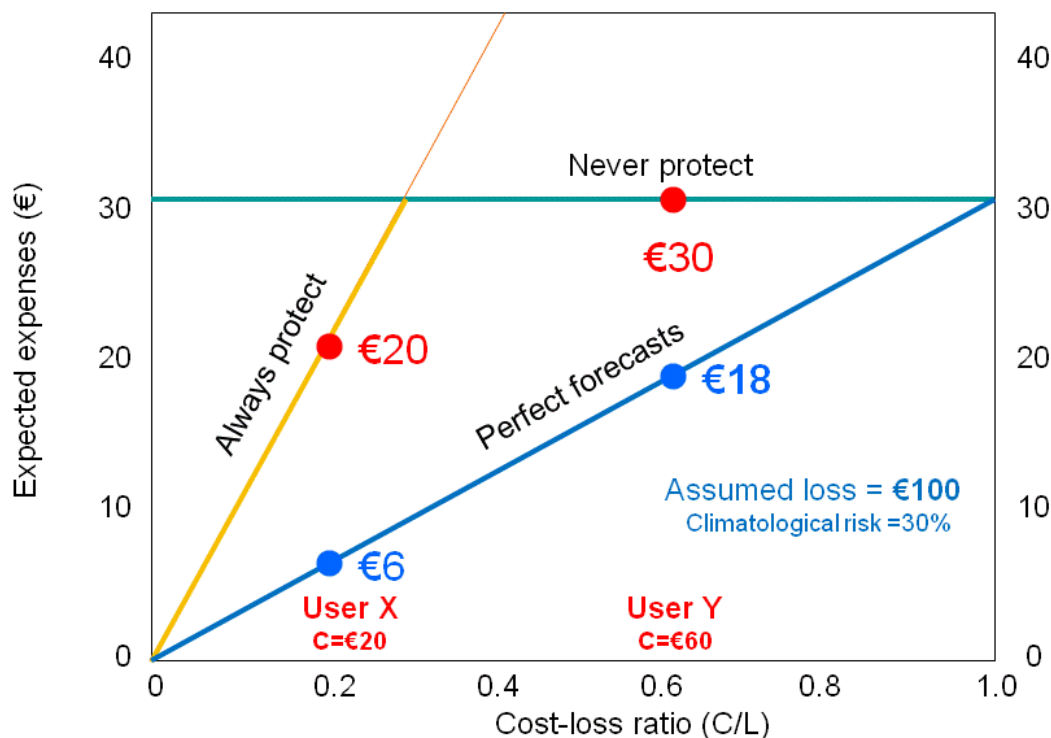


Figure 77: The triangle defined by the expected daily expenses for different costs (c), when the loss (L) is 100€. End-users who always protect increase their expenses (yellow), end-users who never protect lose on average 30 € per day. Even if perfect forecasts were supplied, protection costs could not be avoided (blue line). The triangle defines the area within which weather forecasts can reduce the expected expenses.

Note that the baseline is not a lack of expenses but the cost of the protection necessary, if perfect knowledge about the future weather is available, in X's case €6 and in Y's €18 per day.

A-7.2 The benefit of a local weather service

The local weather forecast office A issues deterministic forecasts. They are meteorologically realistic in that rain is forecast *with the same frequency as it is observed*. The overall forecast performance is reflected in a contingency table (overleaf):

Table 3

A	Obs rain	Obs dry
Fcst rain	2	1
Fcst dry	1	6

Relying on these forecasts over a typical 10-day period, both X and Y protect three times and are caught out unprotected only once. X is able to lower his loss from €20 to €16, and Y from €30 to €28 (see Figure 78).

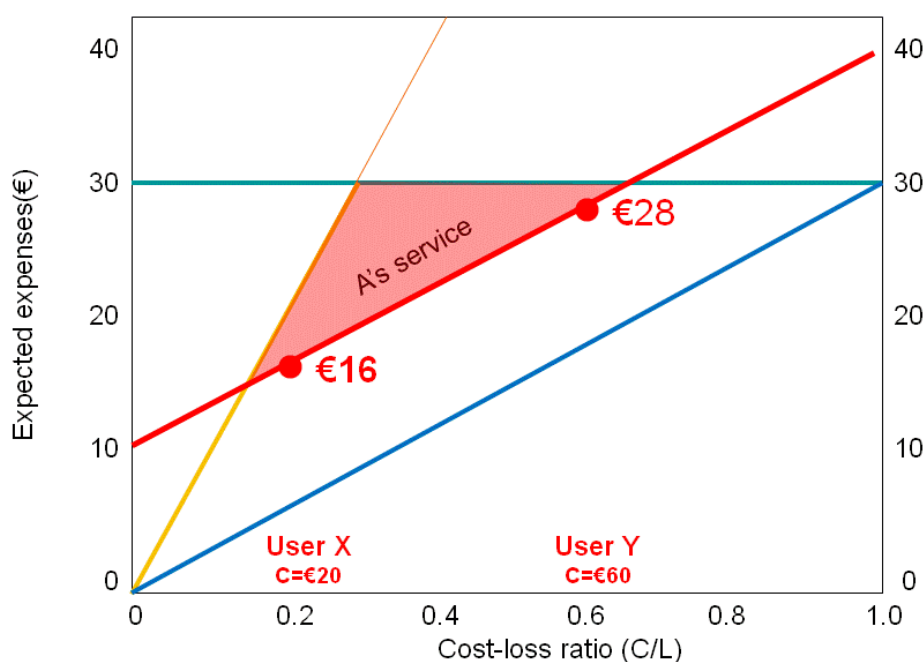


Figure 78: The same as above, but with the expected expenses for end-users served by forecast service A. The red area indicates the added benefits for X and Y from basing their decisions on deterministic weather forecasts from service A.

Note that end-users with very low or very high protection costs do not benefit from A's forecast service.

A-7.3 The establishment of two new weather services

Two new weather agencies, B and C, start to provide forecasts to X and Y. The newcomers B and C have forecast performances in terms of H, F, M and Z:

Table 4

B	Obs rain	Obs dry
Fcst rain	1	0
Fcst dry	2	7

Table 5

C	Obs rain	Obs dry
Fcst rain	3	3
Fcst dry	0	4

Agency B heavily under-forecasts rain and agency C heavily over-forecasts. Both give a distorted image of atmospheric behaviour - but what might seem “bad” is actually “good”.

By following B’s forecasts, which heavily under-forecast rain, end-user Y, who has high protection costs, reduces his expenses from €28 to €26.

By following C’s forecasts, which heavily overforecast rain, end-user X, who has low protection costs, reduces his expenses from €16 to €12 (see Figure 79).

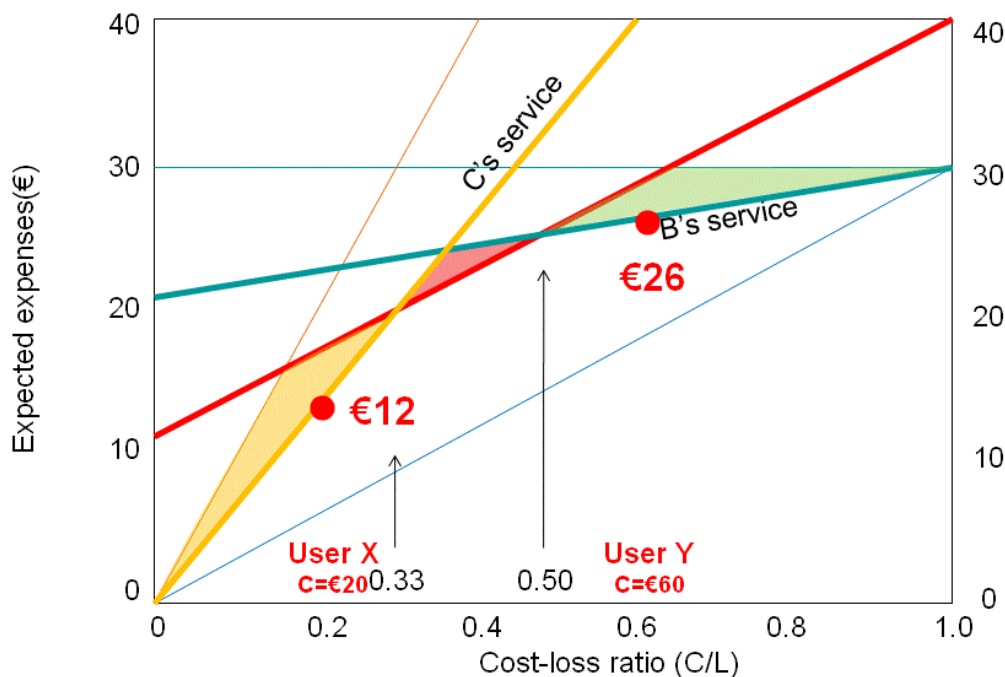


Figure 79: The cost-loss diagram with the expected expenses according to forecasts from agencies B and C for different end-users, defined by their cost-loss ratios. Weather service A is able to provide only a section of the potential end-users, the ones with C/L-ratios between 33 and 50%, with more useful forecasts than B and C. The green and yellow areas indicate where X and Y benefit from the forecasts from agencies B and C respectively.

B has also managed to provide a useful weather service to those with very low protection costs, C to those with very high protection costs. In general, any end-user with protection costs $<€33$ benefits from C's services, any end-user with protection costs $>€50$ benefits from B's services. Only end-users with costs between $€33$ and $€50$ benefit from A's services more than they do from B's and C's.

There seem to be only two ways in which weather service A can compete with B and C:

- It can improve the deterministic forecast skill – this would involve NWP model development, which takes time and is costly
- It can “tweak” the forecasts in the same way as B and C, thus violating its policy of well tuned forecasts

There is, however, a third way, which will enable weather service A to quickly outperform B and C *with no extra cost and without compromising its well tuned forecasts policy.*

A-8 An introduction to probabilistic weather forecasting

The late American physicist and Nobel Laureate Richard Feynman (1919-88) held the view that it is better not to know than to be told something that is wrong or misleading. This has recently been re-formulated thus: it is better to know that we do not know than to believe that we know when we don't.

A-8.1 Uncertainty - how to turn a disadvantage into an advantage

Local forecast office A in its competitive battle with B and C starts to make use of this insight. It offers a surprising change of routine service: *it issues a categorical rain or no-rain forecast only when the forecast is absolutely certain.* If not, a “don't know” forecast is issued. If such a “don't know” forecast is issued about four times during a typical ten-day period, the contingency table might look like this (assuming “don't know” equates to “50-50” or 50%):

Table 6

	Obs rain	Obs dry
Fcst rain	1	0
??	2	2
Fcst dry	0	5

This does not look very impressive, rather the opposite, *but, paradoxically, both X and Y benefit highly from this special service.* This is because they are now free to interpret the forecasts in their own way.

User X, with low protection costs, can afford to interpret the “don't know” forecast as if it could rain and therefore takes protective action. By doing so, X drastically lowers his costs to $€10$ per day, $€20$ cheaper than following C's forecasts.

Y, on the other hand, having expensive protection, prefers to interpret “don't know” as if there will be no rain and decides not to protect. By doing so, Y lowers his costs to $€6$ per day, on a par with following service B's forecasts (see Figure 80).

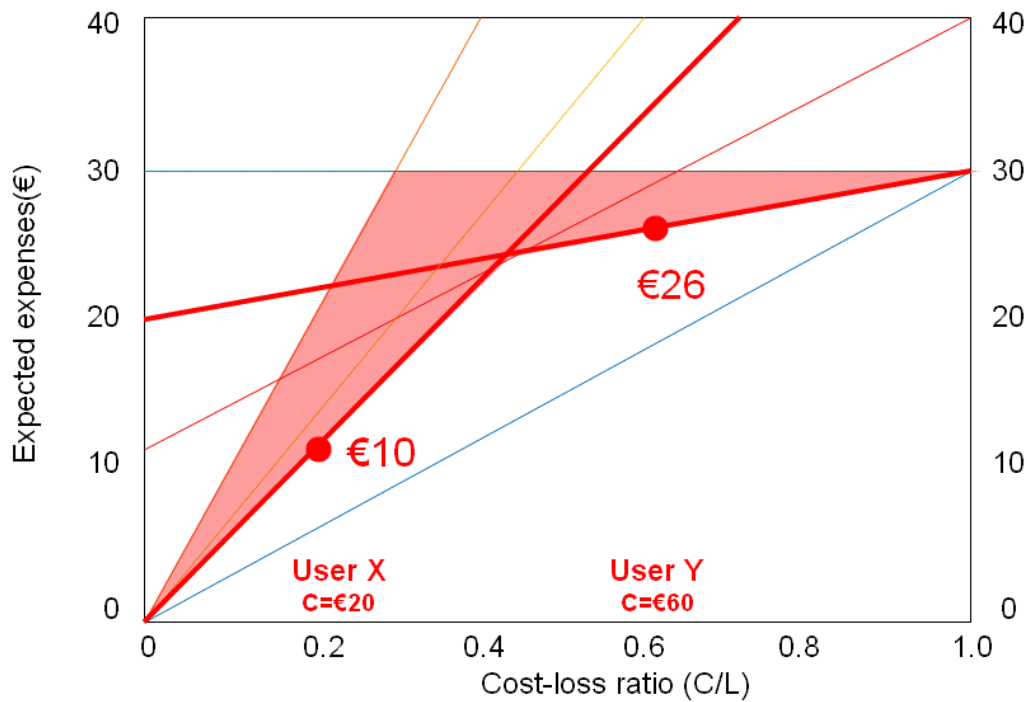


Figure 80: The expected daily expenses when the end-users are free to interpret the “don’t know” forecast either as “rain”, if they have a low c/L ratio, or as “no rain”, if their c/L ratio is high.

So what might appear as “cowardly” forecasts prove to be more valuable for the end-users! If forecasters are uncertain, they should say so and thereby gain respect and authority in the longer term.

A-8.2 Making even more use of uncertainty - probabilities

However, service A can go further and quantify *how* uncertain the rain is. This is best done by expressing the uncertainty of rain in probabilistic terms. If “don’t know” is equal to 50%⁴ then 60% and 80% indicate less uncertainty, 40% and 20 % larger uncertainty. Over a 10-day period the contingency table might, on average, look like this, where the four cases of uncertain forecasts have been grouped according to the degree of uncertainty or certainty:

⁴ A “do not know” forecast does not necessarily mean “50-50”. It could mean the climatological probability. In fact, unless the climatological rain frequency is 50% a “50-50” statement actually provides the non-trivial information that the risk is higher or lower than normal.

Table 7

	Obs rain	Obs dry
100%	1	0
80%	.8	.2
60%	.6	.4
40%	.4	.6
20%	.2	.8
0%	0	5

The use of probabilities will allow other end-users, with protection costs different from X's and Y's, to benefit from A's forecast service. They should take protective action if the forecast probability exceeds their cost/loss ratio ($P > c/L$). Assuming possible losses of €100, someone with a protection cost of €30 should take action when the risk > 30%, someone with costs of €75, when the forecast is of >75% probability (see Figure 81).

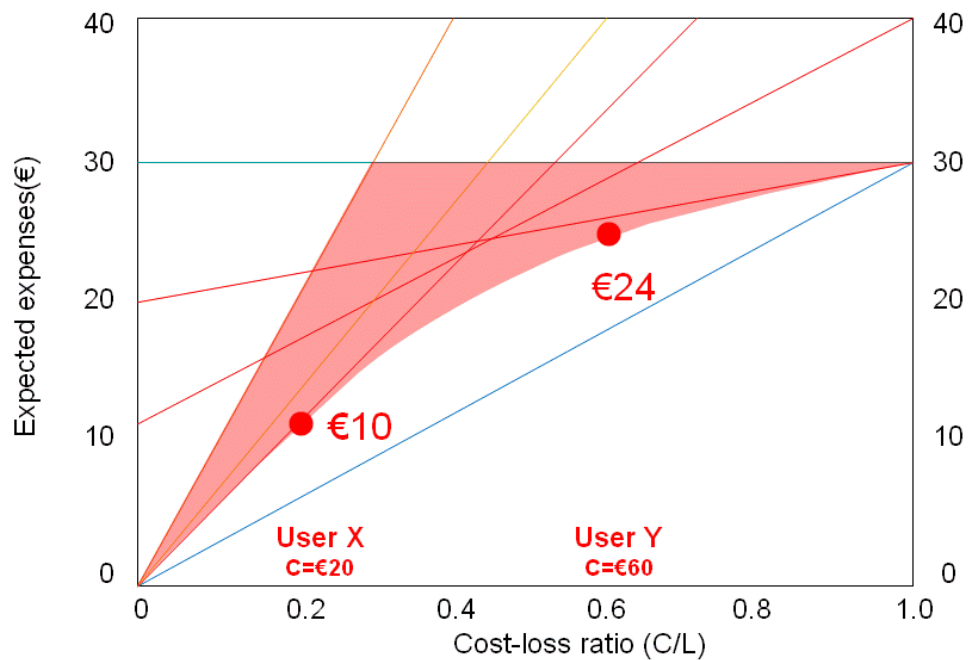


Figure 81: The same figures but with the expected expenses indicated for cases where different end-users take action after receiving probability forecasts. The general performance (thick blue line) is now closer to the performance for perfect forecasts.

X lowers his expenses to €10 and Y to €24.

A-8.3 Towards more useful weather forecasts

What looks “bad” has indeed been “good”. Refraining from giving a forecast, vague phrasing or expressing probabilities is often regarded by the public as a sign of professional incompetence. As Edward Lorenz once noted:

“Unfortunately, a segment of the public tends to look upon probability forecasting as a means of escape for the forecaster” (Lorenz, 1970).

Instead, it has been shown that what looks like “cowardly” forecast practice is, in reality, more beneficial to the public and end-users than perceived “brave” forecast practice. Lorenz:

“What the critics of probability forecasting fail to recognize or else are reluctant to acknowledge is that a forecaster is paid not for exhibiting his skill but for providing information to the public, and that a probability forecast conveys more information, as opposed to guesswork, than a simple [deterministic] forecast of rain or no rain.”(Lorenz, 1970)

Although the ultimate rationale of probability weather forecasts is their usefulness, which varies from end-user to end-user, forecasters and developers also need verification and validation measures which are objective, in the sense that they do not reflect the subjective needs of different end-user groups.

A-8.4 Quality of probabilistic forecasts

The forecast performance in Table 7 exemplifies skilful probability forecasting. In contrast to categorical forecasts, probability forecasts are never “right” or “wrong” (except when 0% or 100% has been forecast). They can therefore not be verified and validated in the same way as categorical forecasts. This will be further explained in Appendix B.

A-8.5 When probabilities are not required

If an end-user does not appreciate forecasts in probabilistic terms and, instead, asks for categorical “rain” or “no rain” statements, the forecaster must make the decisions for him. Unless the relevant cost-loss ratio is known, this restriction puts forecasters in a difficult position.

If, on the other hand, they have a fair understanding of the end-user’s needs, forecasters can simply convert their probabilistic forecast into a categorical one, depending on whether the end-user’s particular probability threshold is exceeded or not. The forecasters are, in other words, doing what the end-user should have done. So, for example, to an end-user with a 40% threshold weather service A would issue categorical forecasts which during a 100 day period would verify like this:

Table 8

A	Obs rain	Obs dry
Fcst rain	28	12
Fcst dry	2	58

Note that for this particular end-user the rain has been over-forecast: 40 forecasts against 30 occurrences. For an end-user with a threshold of 60% the contingency table would look like

Table 9 below.

Table 9

A	Obs rain	Obs dry
Fcst rain	18	2
Fcst dry	12	68

In the example in Table 9, the rain is under-forecast: 18 forecasts against 30 occurrences. *Generally, categorical forecasts have to be biased, either positively i.e. over-forecasting the event, for end-users with low cost-loss ratios or negatively, i.e. under-forecasting, for end-users with high cost-loss ratios*⁵.

A-8.6 An extension of the contingency table – the “SEEPS” score

The “SEEPS” score (Stable Equitable Error in Probability Space) has been developed to address the task of verifying deterministic precipitation forecasts. In contrast to traditional deterministic precipitation verification, it makes use of three categories: “dry”, “light precipitation” and “heavy precipitation”. “Dry” is defined according to WMO guidelines as ≤ 0.2 mm per 24 hours. The “light” and “heavy” categories are defined by local climatology, so that light precipitation occurs twice as often as “heavy” precipitation. In Europe the threshold between “light” and “heavy” precipitation is generally between 3 and 15 mm per 24 hours.

⁵ As discussed in Section 4.3.4 a good NWP model should not over- or under-forecast at any forecast range. This is yet another example of how computer -based forecasts differ from customer -orientated forecasts.

Appendix B Some statistical concepts to facilitate the use and interpretation of ensemble forecasts

This chapter discusses only the most commonly used probabilistic validation and verification methods. For a full presentation the reader is referred to Nurmi (2003).

Introduction

The distinction between *validation* (forecast system's characteristics) and *verification* (forecast system's predictive skill) is as relevant in probabilistic as in deterministic forecasting. As with the deterministic forecasting system, probability verification can address the *accuracy* (how close the forecast probabilities are to the observed frequencies), the *skill* (how the probability forecasts compare with some reference system) and *utility* (the economic or other advantages of the probability forecasts).

Sceptics of probability forecasts argue that forecasters might exaggerate uncertainty “to cover their backs”. However, as will be shown, the verification of probabilistic forecasts takes the “reliability” of the probabilities into account and will detect any such misbehaviour. Indeed, one of the most used verification scores, the Brier score, is mathematically constructed in a way that encourages forecasters to state the probability they really believe in, rather than some misperceived “tactical” probability.

B-1 The reliability diagram

The most transparent way to illustrate the performance and characteristics of a probabilistic forecast system is the reliability diagram, where the x-axis is the predicted probability and the y-axis the frequency with which the forecasts verify. It serves both as a way to validate the system and to verify its forecasts (see Figure 82).

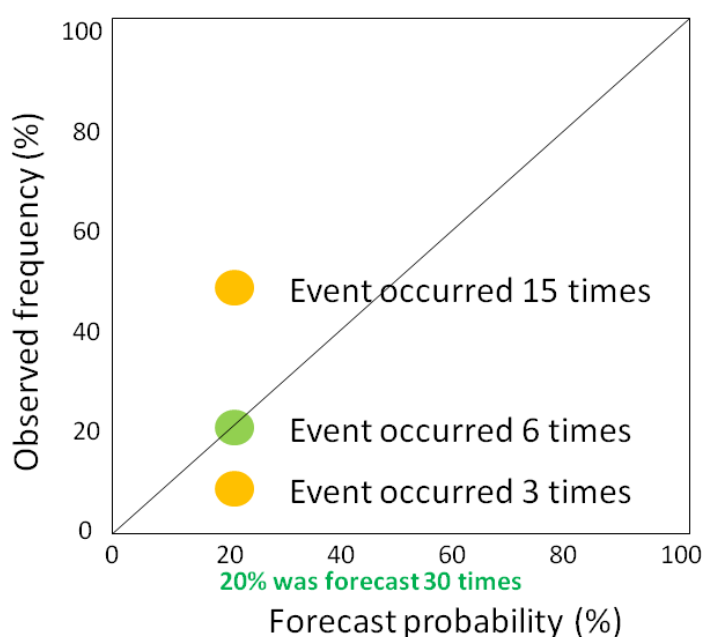


Figure 82: Schematic explanation of the reliability diagram. Out of thirty 20% probability forecasts, the predicted event should verify six times, i.e. in 20% of the time, not more, not less.

B-1.1 Reliability

When the forecast probabilities agree with the frequency of events for this particular probability the distribution should lie along the 45° diagonal. In such a case the probability forecasts are considered reliable. The frequency of forecast probabilities is represented by green circles of varying sizes (see Figure 83).

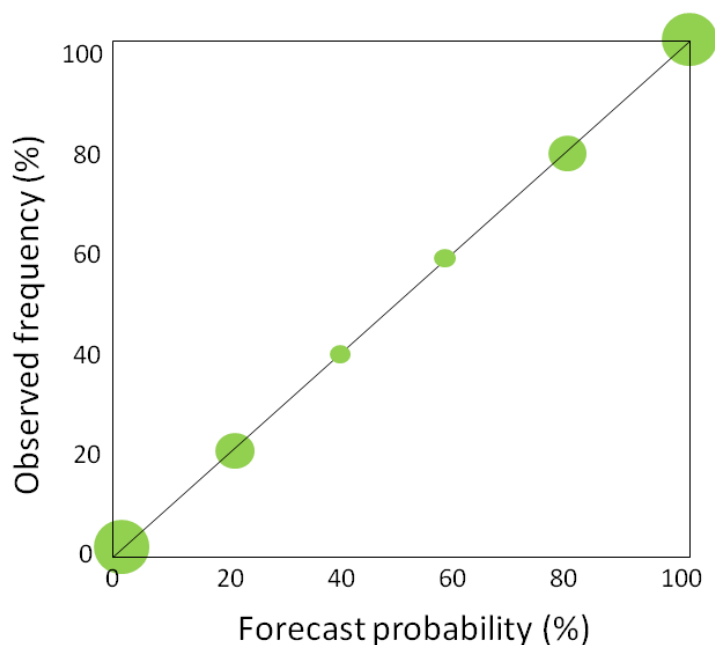


Figure 83: Probabilities with good sharpness. The probabilities cluster as far away as possible from the climatological frequency, here assumed to be 50%.

B-1.2 Sharpness

Climatological probability averages used as forecasts would yield perfect reliability, since the distribution would be exactly on the 45° diagonal, but would not be very useful. Ideally, we want the forecast system, while mainly reliable, to span as wide a probability interval as possible, with as many forecasts as possible away from the climatological average and as close to 0% and 100% as possible. The property of a probabilistic forecast system to spread away from the climatological average is called *sharpness*. The distribution in Figure 83 has good sharpness, whereas it is poor in Figure 84.

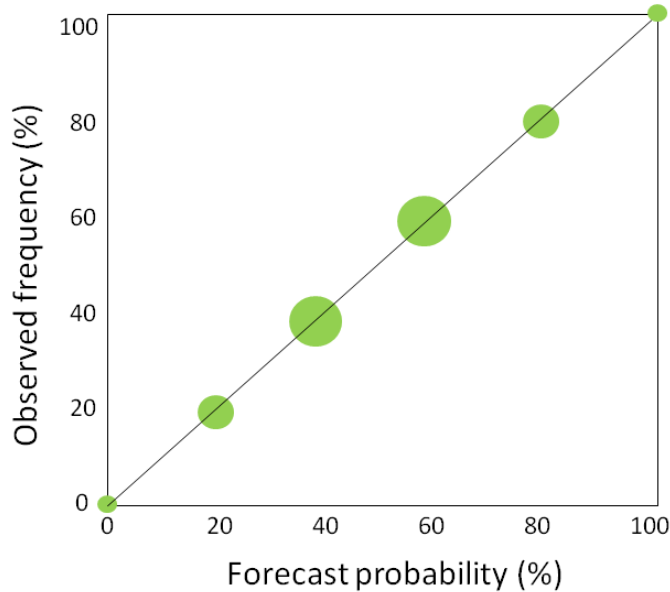


Figure 84: An example of a reliable forecast system with poor sharpness. When the predictability of a certain weather parameter is low, the forecasts might still be reliable but will tend to cluster around the climatological average.

Improvements in probability forecasts will, provided they are reliable, be accompanied by improved sharpness until, ultimately, only 0% and 100% forecasts are issued and verify, corresponding to a perfect deterministic forecast system. However, an improvement in sharpness does not necessarily mean that the forecast system has improved.

B-1.3 Under- and overconfident probability forecasts

Most probabilistic forecast systems, both subjective and objective, tend to give distributions flatter than 45°. This means that low risks are underestimated and high risks overestimated - the forecast system is *overconfident*. Figure 85 shows an example of overconfidence.

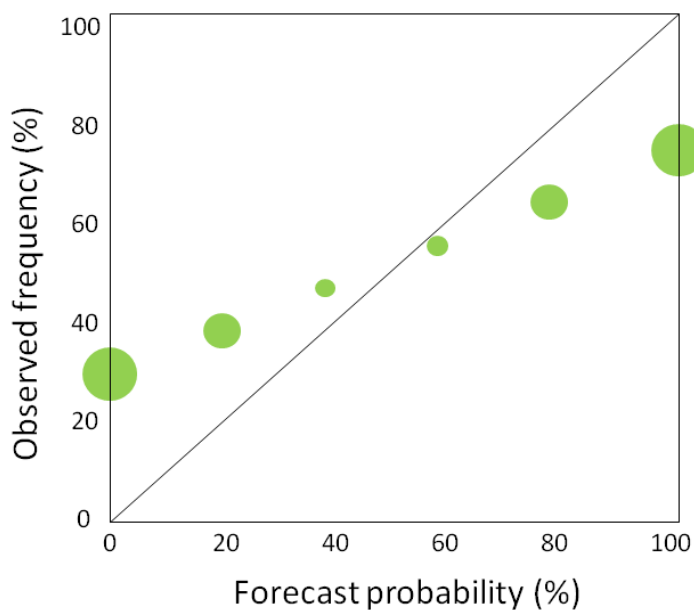


Figure 85: Probability forecasts with good sharpness but overconfident, since 0% forecasts are not always followed by dry weather, 100% forecasts not always followed by rain.

The less common case: the distribution is steeper than 45°, low risks have been overestimated and high risks underestimated. The forecast systems are then *under-confident* (see Figure 86).

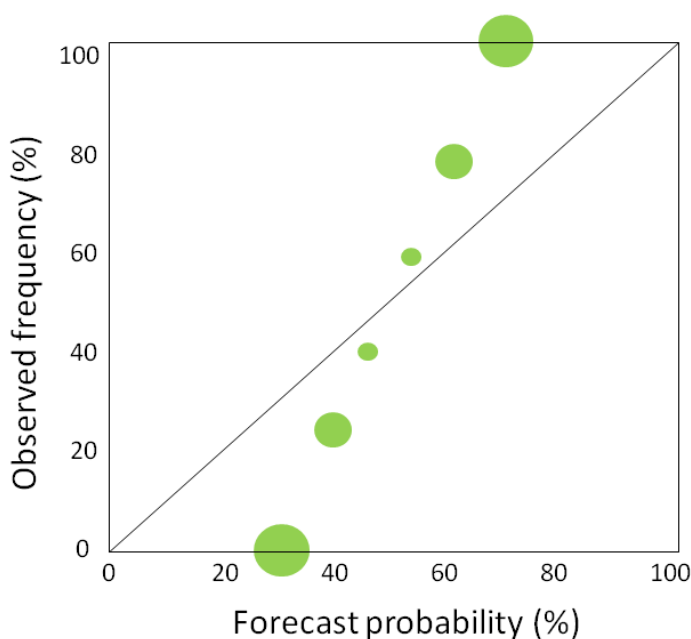


Figure 86: Probabilities indicating reluctance to use very high or low probabilities. The probability forecasts are under-confident.

Under- or overconfidence can be corrected by the calibration of probabilities (see B-5).

B-2 Rank histogram (Talagrand diagram)

A more detailed way of validating the spread is by a *rank histogram* (sometimes called a *Talagrand diagram*). It is constructed from the notion that in an ideal ensemble system the

verifying analysis is equally likely to lie in any “bin” defined by any two ordered adjacent members, including when the analysis is outside the ensemble range on either side of the distribution. This can be understood from induction, if we consider an ideal ensemble with one, two or three members:

With one ensemble member (**I**) verifying observations (●) will always (100%) fall “outside”
●I●

With two ensemble members (**I I**), verifying observations will for this ideal ensemble fall outside in two cases out of three **●I●I●**

With three ensemble members (**I I I**), verifying observations will fall for this ideal ensemble outside in two cases out of four **●I●I●I●**

In general, if N = number of members, the verification will in two cases out of $N + 1$ always fall outside, yielding a proportion of $2/(N+1)$ outside. For the same reasons the HRES and the ENS Control should lie outside the ensemble $2/(N+1)$ of the time. For a 50-member ensemble system this means 4%. This is consistent with the discussion in Section 4.4.8, that due to the limited number of ensemble members, it would be unrealistic to assume that the probability was 0% or 100% just because none or all of the members forecast the event.

In an ideal ensemble, the rank histogram distribution should, on average, be flat with equal numbers of verifying observations in each interval. If there is a lack of spread, this will result in a U-shaped distribution with an over-representation of cases where the verifications fall outside the ensemble and under-representation of cases when they fall within the ensemble centre. If the system has a bias with respect to the verifying parameter, the U-shape might degenerate into a J-shape.

An ideal ensemble system might, however, display a U-shape distribution due to observation uncertainties. For example, with 50 ensemble members an ensemble spread of 20°C yields an average bin width of 0.4°C, an ensemble spread of 5°C yields an average bin width of only 0.1°C, smaller than the observation uncertainty (see Figure 87).

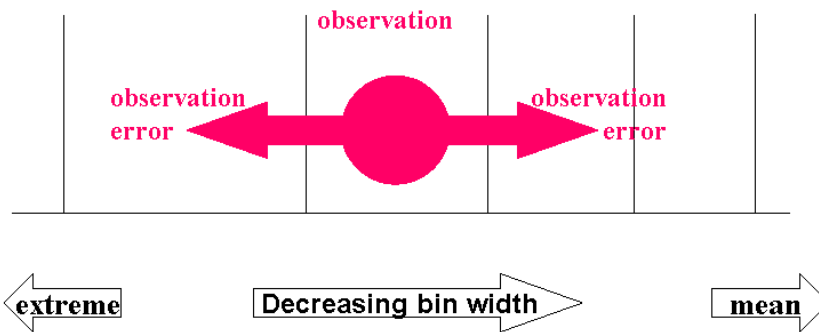


Figure 87: An observation (a filled circle) and its uncertainty assumed symmetric (the arrows). Since the forecast bins widen their intervals away from the centre (the mean of the distribution), an observation is more likely, for random reasons, to fall into an outer and wider bin than an inner and narrower one.

The small bin size introduces an element of chance with respect to which bin the observation will fall into. Since the bin sizes due to the normal distribution will increase with increasing

distance from the centre, an observation is more likely to end up in a bin further away from the centre than closer to the centre. This will result in a misleading U-shaped distribution.

B-3 Verification measures

In contrast to deterministic forecasts, an individual probabilistic forecast can never be “right” or “wrong” except when 0% or 100% have been stated. Probability forecasts can therefore, only be verified from large samples of forecasts.

B-3.1 The Brier score - the MSE of probability forecasts

The most common verification method for probabilistic forecasts, the Brier score (BS), has a mathematical structure similar to the MSE

$$BS = \overline{(p - o)^2}$$

BS measures the difference between the forecast probability of an event (p) and its occurrence (o), expressed as 0 or 1, depending on whether the event has occurred or not. As with RMSE, the BS is negatively orientated, i.e. the lower, the “better”.

B-3.2 Decomposition of the Brier score

Similarly to the MSE the BS can be decomposed into three terms, the most often quoted was suggested by Allan Murphy (1973, 1986) who used “binned” probabilities:

$$BS = \overline{\overline{n_k(p_k - \bar{o})^2}} - \overline{\overline{n_k(\bar{o} - o_k)^2}} + \bar{o}(1 - \bar{o})$$

where n_k is the number of forecasts of the same probability category k . The first term on the right hand side measures how much the forecast probabilities can be taken at face value, their *reliability*. On the reliability diagram this is the n_k weighted sum of the distance (vertical or horizontal) between each point and the 45° diagonal (see Figure 88).

The second term measures how much the predicted probabilities differ from a climatological average and therefore contribute information, the *resolution*. On the reliability diagram this is the weighted sum of the distances to a horizontal line defined by the climatological probability reference.

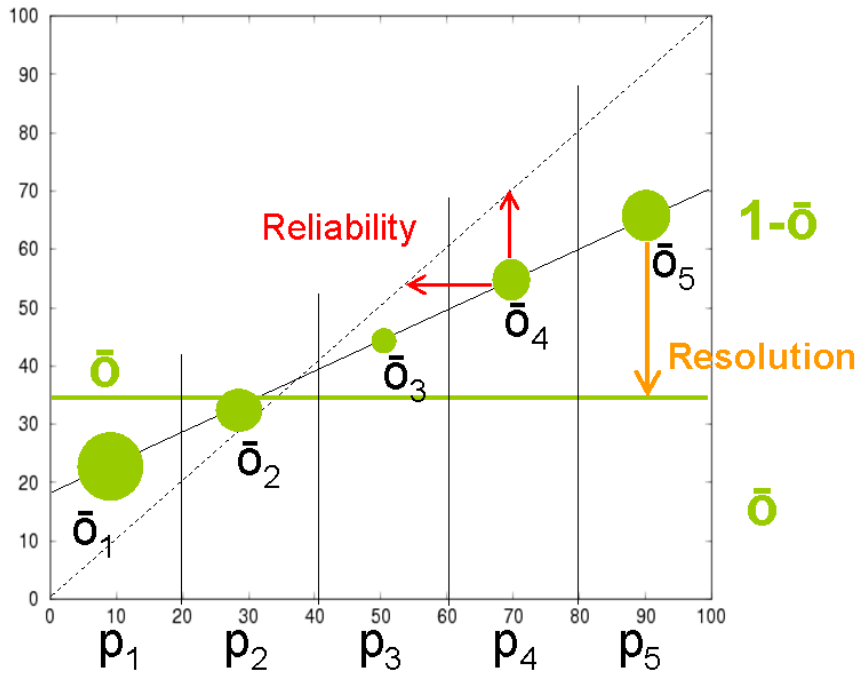


Figure 88: Summary of Allan Murphy’s reliability and resolution terms

Resolution, the degree to which the forecasts can discriminate between more or less probable events, should not be confused with sharpness, the tendency to have predictions close to 0% and 100%. They are also independent of one another.

The final term in the decomposition, called *uncertainty*, is the variance of the observations. It takes its highest, most “uncertain”, value when $\bar{o}=0.5$ (see Figure 89).

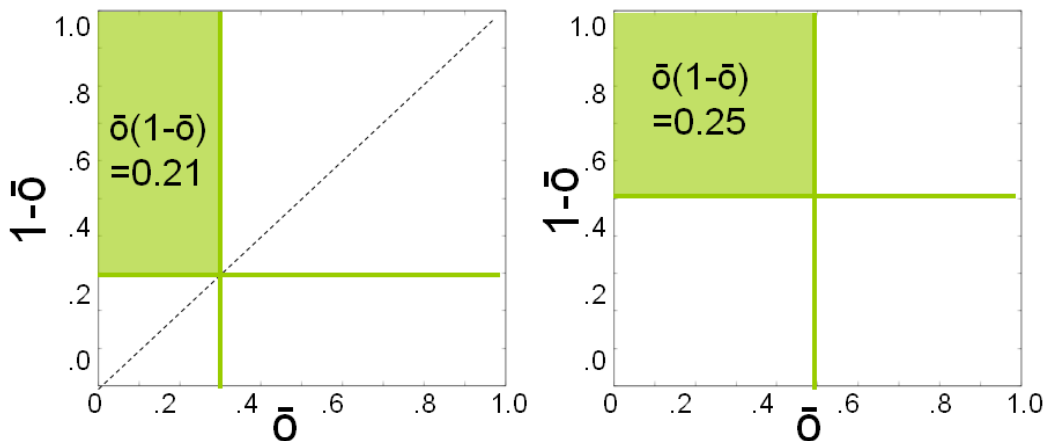


Figure 89: Uncertainty is at its maximum for a climatological observed probability average of 50%.

The name “uncertainty” can be understood from the familiar fact that it is easier to predict the outcome of tossing a coin if it is heavily biased. In the same way, if it rains frequently in a region and rarely stays dry, forecasting can be said to be “easier” than if rain and dry events occur equally often,

The uncertainty is purely dependent on the observations, just as the A_a -term in the RMSE decomposition. It is also the BS of the sample climatology forecast and plays the same role with the BS as the A_a term with the RMSE (see Section A-2.4). Comparisons of Brier scores for different forecast samples can only be made if the uncertainty is the same.

B-3.3 The Brier score is a “proper” score

The Brier score is strictly “proper”, i.e. it encourages forecasters to really try to find out the probability, without thinking about whether the forecast value is “tactical” or not. Indeed, if forecasters deviate from their true beliefs, the BS will “punish” them! *This sounds strange.* How can an abstract mathematical equation know someone’s inner beliefs?

Assume forecasters honestly think the probability of an event is p but have, for misguided “tactical” reasons, instead stated r . If the event occurs, the contribution to the BS will be $(1-r)^2$, if the event does not occur $(r-0)^2$ weighted by the probabilities of the outcomes to occur. But for this, the “honest” probability p respectively $1-p$ must be used. This is where the forecaster’s true beliefs are revealed!

The expected contribution to the BS is therefore:

$$\Delta BS = (1-r)^2 p + (r-0)^2 (1-p)$$

Differentiating with respect to r yields

$$\frac{d\Delta BS}{dr} = -2p + 2r$$

with a minimum for $r = p$, i.e. to minimize the expected contribution to the Brier score, the honestly believed probability value should be stated.

B-3.4 The Brier skill score

A Brier skill score (BSS) is conventionally defined as the relative probability score compared with the probability score of a reference forecast.

$$BSS = \frac{BS_{ref} - BS}{BS_{ref}}$$

“Uncertainty” plays no role in the BSS.

B-3.5 The rank probability score (RPS)

Probabilities often refer to the risk that some threshold might be exceeded, for example that the precipitation >1 mm/12h or that the wind >15 m/s. However, when evaluating a probabilistic system, there are no reasons why these thresholds are particularly significant. For the rank probability score (RPS) the BS is calculated for different (one-sided) discreet thresholds and then averaged over all thresholds. A generalization is the continuous rank probability score (CRPS) where the thresholds are continuous (see Nurmi, 2003; Jolliffe and Stephenson, 2003; Wilks, 2006).

B-4 The relative operating characteristics (ROC) diagram

A powerful way to verify probability forecasts and in particular to compare their performance with deterministic forecast systems, is the two-dimensional “relative operating characteristics” or “ROC” diagram. These categorical forecasts will produce a set of pairs of “hit rate” and “false alarm rate” values to be entered into the ROC diagram: false alarm rate

(FR) on the x-axis and hit rate (HR) value on the y-axis. The upper left corner of the ROC diagram represents a perfect forecast system (no false alarms, only hits). The closer any verification is to this upper left corner, the higher the skill. The lower left corner (no hits or false alarms) represents a system which never warns of an event. The upper right corner represents a system where the event is always warned for (see Figure 90).

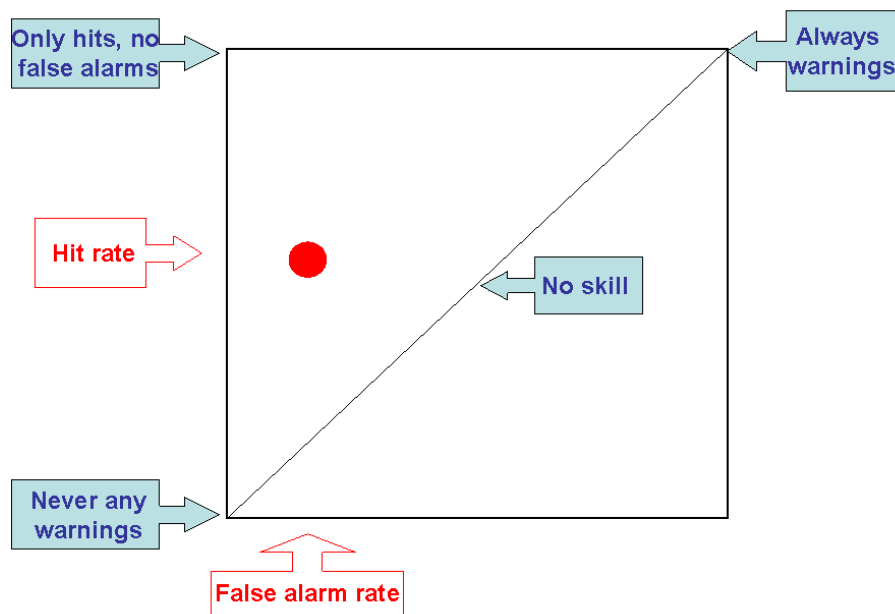


Figure 90: The principle of the ROC diagram: a large number of probability forecasts are turned into categorical forecasts depending on whether the probability values of individual forecasts are above or below a certain threshold. The false alarm rate and the hit rate are calculated, thus determining the position in the diagram (red filled circle).

Probabilistic forecasts are transformed into categorical yes/no forecasts defined by thresholds varying from 0% to 100% (see Figure 91).

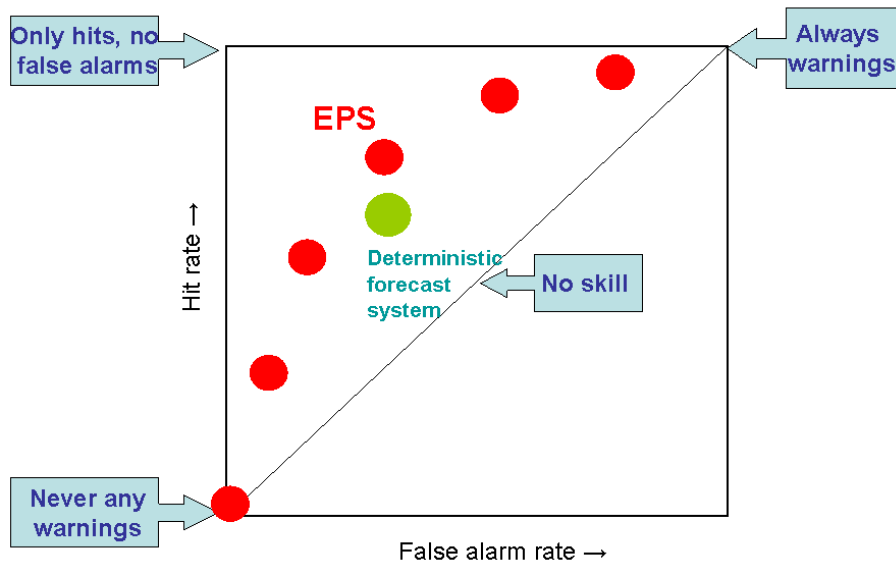


Figure 91: The same as above, but repeated for several thresholds between 0 and 100%, including the hit rates and false alarm rates of the deterministic model; although not providing probabilistic predictions it can be represented on the diagram by its typical hit rate and false alarm rate (green filled circle).

The ROC score is the area underneath the forecast curve (see Figure 92).

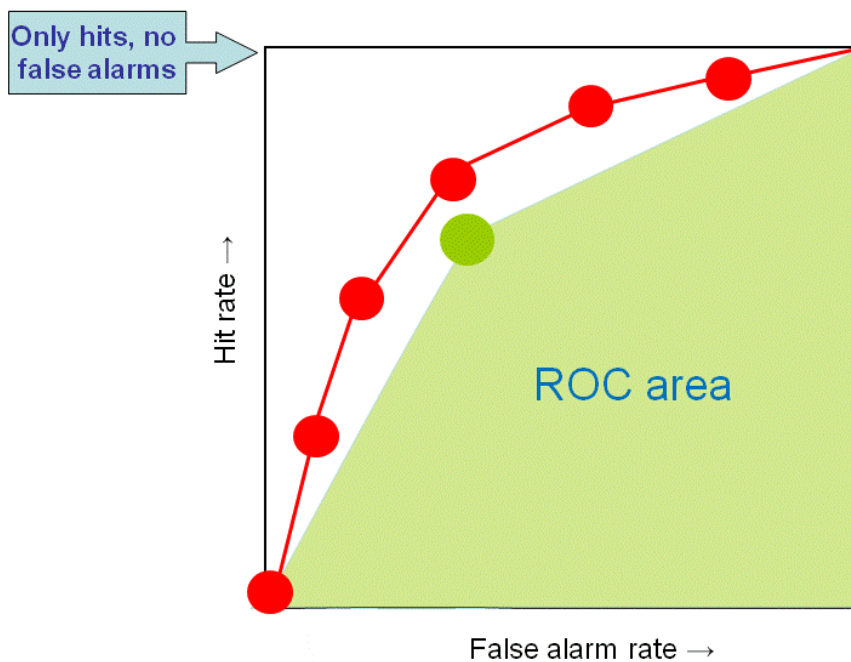


Figure 92: The area underneath the points, joined by straight lines, defines the ROC area, which is, ideally, 1.0 and at worst 0.0. Random forecasts yield 0.5, the triangular area underneath the 45° line.

There are two schools on how to calculate this: either with a smooth spline or linearly, connecting the points.

B-5 Calibration of probabilities

For operational purposes the reliability can be improved by calibration using verification statistics. For instance, if it is found that in cases when 0% has been forecast, the event tends to occur in 30% of the cases, and when 100% has been forecast, only in 70% of the cases. If the misfit is linearly distributed in between these two extremes, the reliability can be made perfect by calibration - but at the expense of reduced sharpness, since very low and very high probabilities are never forecast (see Figure 93).

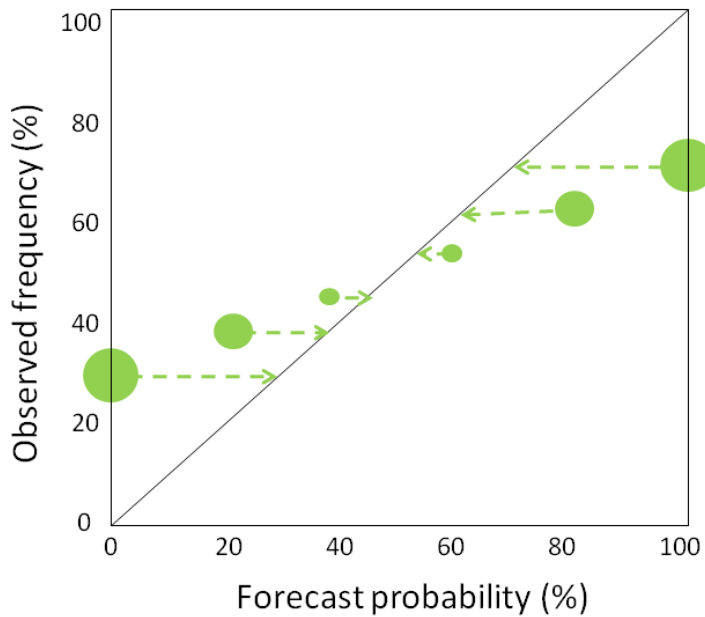


Figure 93: The probability distribution from an overconfident forecast system is calibrated, limiting the range from 0% - 100% to 30% - 70%.

On the other hand, when the probability forecasts are under-confident, calibration might restore the reliability without giving up the sharpness (see Figure 94).

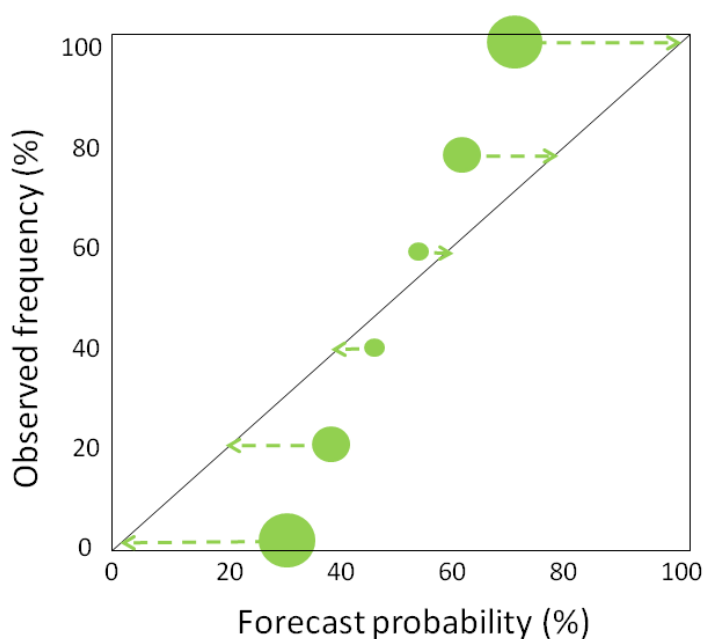


Figure 94: The probabilities from an under-confident forecast system are calibrated, widening the range from 30% to 70% to 0% to 100%.

This means that there is some “hidden skill” in probability forecasts biased in this way.

B-6 Statistical post-processing – model output statistics

An efficient way to improve the ensemble forecast, both the EM and the probabilities, is by statistical post-processing (SPP), which is an advanced form of calibration of the output from the deterministic ensemble members. The most commonly used SPP method is “model output statistics” (MOS).

B-6.1 The MOS equation

Deterministic NWP forecasts are statistically matched against a long record of verifying observations through a linear regression scheme. The predictand (Y) is normally scalar (for example 2 m temperature) and the predictors (X) one or several forecast parameters, selected by a linear regression system as the parameters which provide the most information (for example forecasts of 2 m temperature, 850 hPa temperature, 500 hPa geopotential etc):

$$Y = X_1 + X_2 \cdot T_{2m} + X_3 \cdot T_{850hPa} + X_4 \cdot Z_{500} + \dots \text{etc}$$

where the coefficients $X_{i=1, 2, 3 \dots n}$ are estimated by the regression scheme. For this discussion it is sufficient to consider the simple MOS equation:

$$Y = X_1 + X_2 \cdot T_{2m}$$

where X_1 and X_2 have been estimated from a large amount of representative historical material. This is often quite an effective correction equation, since the errors in many meteorological forecast parameters in a first approximation tend to be linearly dependent on the forecast itself (except perhaps precipitation and cloudiness).

B-6.2 Simultaneous corrections of mean error and variability

The MOS equation not only minimizes the RMSE, it also corrects simultaneously for both systematic mean errors and for the variability. In the above equation X_1 represents the mean

error correction and X_2 the variability correction. There is therefore no necessity to apply two different schemes, one for reducing the systematic error (“bias”) and one for correcting the spread.

B-6.3 Short-range MOS

However, the corrections imposed by MOS have different emphases in the short and medium range. In the short range, where most synoptic features are forecast with realistic variability, the MOS equation mainly corrects true systematic errors and representativeness errors.

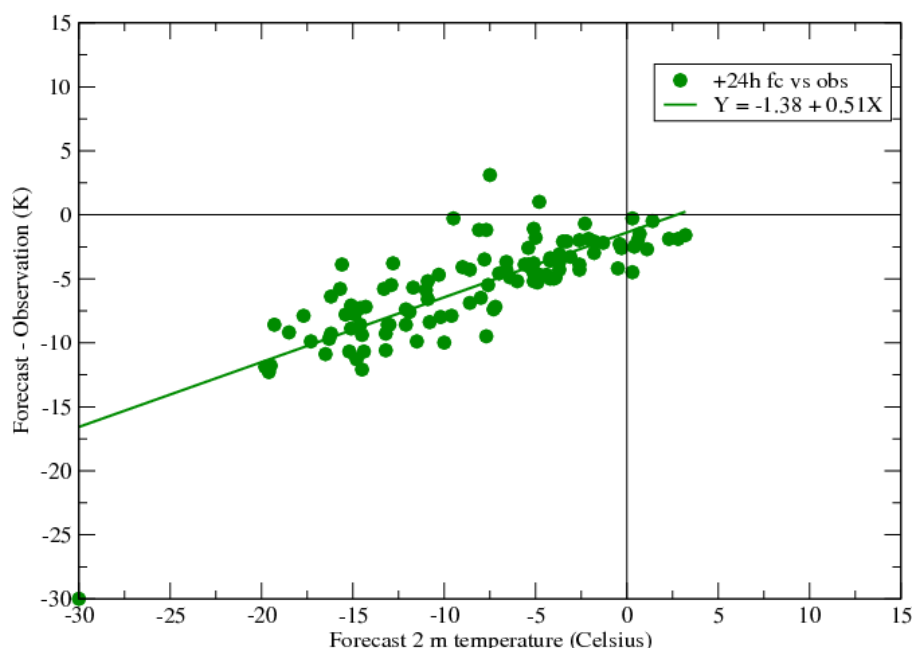


Figure 95: A scatter diagram of forecast errors versus forecast for Tromsø in northern Norway, November 2010 - February 2011. Cold temperatures are too cold and, as a whole, the forecasts overestimate the variability of the temperature.

The scatter diagram in Figure 95 depicts the errors at D+1 and therefore shows *true systematic errors*: the colder the forecast, the larger the mean error, which is equivalent to over-forecast variability.

B-6.4 Medium-range MOS

MOS also improves forecasts in the medium range but, with increasing forecast range, less and less of this improvement is due to the MOS equation’s ability to remove systematic errors.

In the medium range, the dominant errors are non-systematic. As discussed in A-1.43, these non-systematic errors can appear as *false systematic errors* (see, for example, Figure 64). They will thus be “corrected” by the MOS in the same way as true systematic errors. By this means MOS is essentially dampening the forecast anomalies and thereby minimizing the RMSE.

This might be justified in a purely deterministic context but not in an ensemble context, where the most skilful damping of less predictable anomalies is achieved by ensemble averaging through the EM.

It is therefore recommended that MOS equations are calculated in the short range, typically at D+1, based on forecasts from the Control, and then applied to all the members in the ensemble throughout the whole forecast range, as long as any genuine model drift can be discarded.

B-6.5 Adaptive MOS methods

About every few years, NWP models undergo significant changes that make the MOS regression analysis obsolete. There are, however, techniques whereby the MOS can be updated on a regular (monthly or quarterly) basis, although this does not completely eliminate the drawback of historic inertia.

Alternatively, adaptive methods have increasingly come into use. Here the coefficients X_1 and X_2 in the error equation are constantly updated in the light of daily verification (Persson, 1991).

Figure 96 shows forecasts and observations for the location with severe systematic 2 m temperature errors depicted in Figure 95. It is not a case of “plain bias” but of “conditional bias”, since mild forecasts are less at error than cold forecasts. A simple mean-error correction would therefore not be optimal.

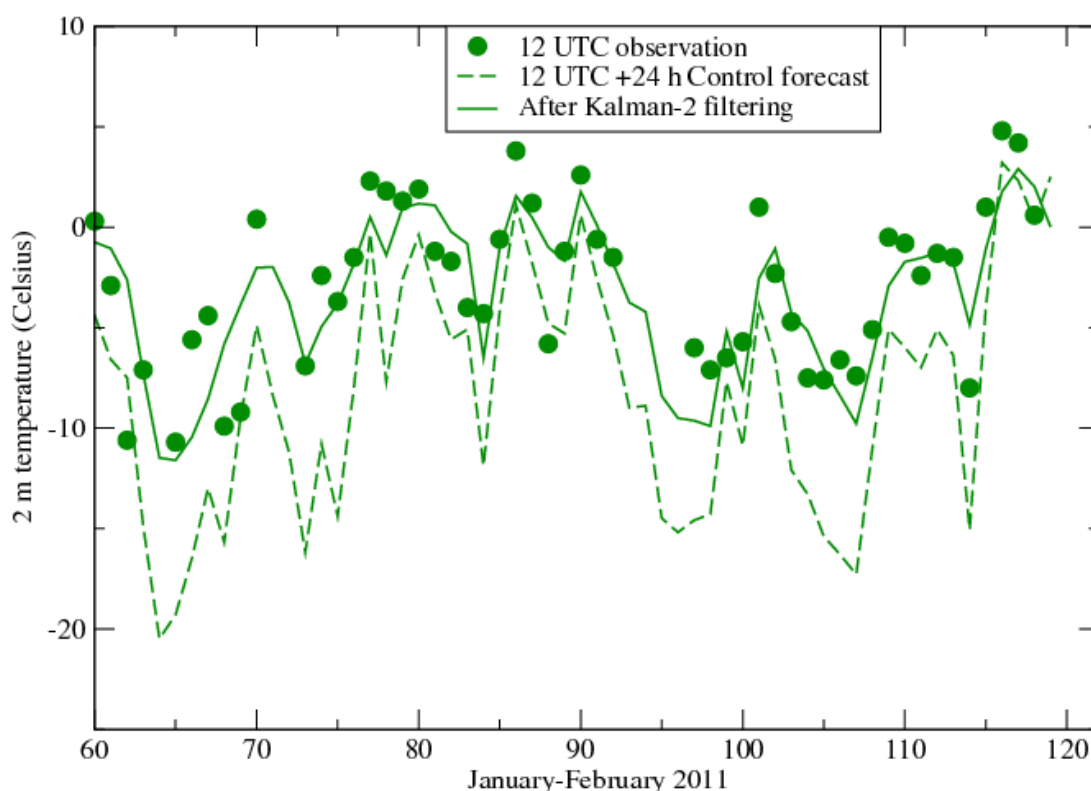


Figure 96: Adaptive Kalman filtering of 2-metre temperature forecasts for Tromsø in northern Norway during winter 2011. The forecasts are too cold and over-variable, both of which are remedied by X_1 and X_2 in a 2-parameter error equation.

By a daily verification, the Kalman filter estimates the coefficients X_1 and X_2 in the error equation:

$$\text{Err} = X_1 + X_2 \cdot T_{fc}$$

where T_{fc} is the verified forecast. The coefficients are updated from a variational principle of “least effort”, whereby the equation line is translated (by modifying X_1) and rotated (by modifying X_2), so that it takes the verification into account, considering the uncertainties in the verification and the coefficients (see Figure 97).

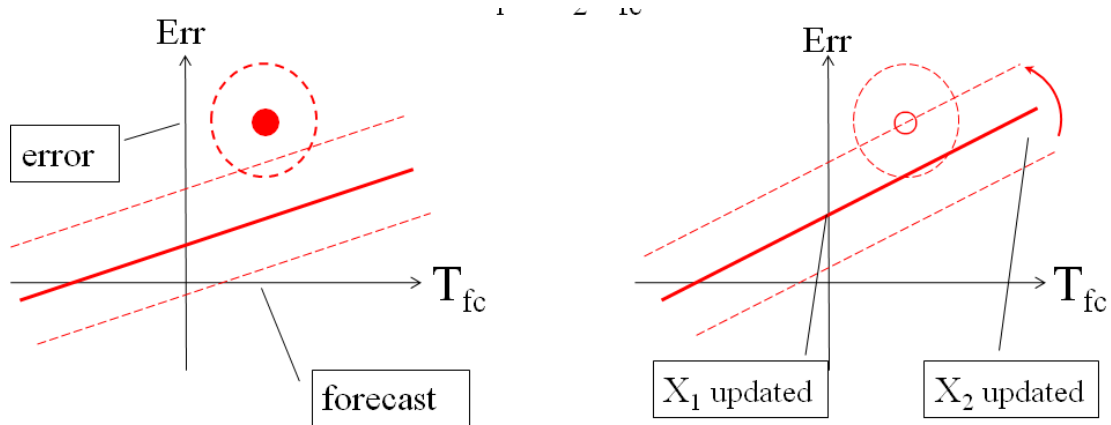


Figure 97: A schematic illustration of the workings of an adaptable MOS by Kalman filtering. At a given time the error equation has a certain orientation (full red line) with a certain estimated uncertainty (red dashed lines). A forecast is verified and yields an error (red filled circle) that does not normally fall on the error line. Depending on the interplay between the equation uncertainty and the verification uncertainty (dashed red circle), the error equation line is translated and rotated to take the new information into account, after which this information is discarded.

Note that the system keeps information only about the error equation and its uncertainty and the last, not yet verified forecast. When the forecast is verified and the verification has affected the error equation, the verifying observation is discarded.

Figure 98 shows an ensemble forecast for the same location with severe systematic 2 m temperature errors.

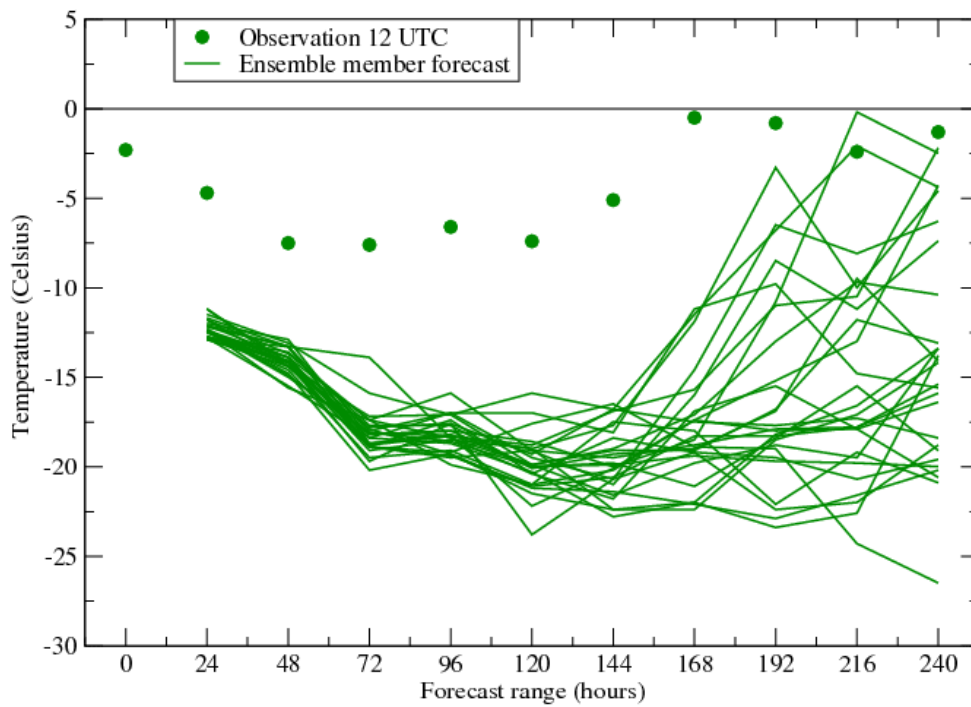


Figure 98: A plume diagram for Tromsø, 12 February 2011. The forecast is too cold with 50-100% probabilities of temperatures $< -15^{\circ}\text{C}$.

The two-dimensional error equation is able to apply corrections which are different for different forecast temperatures and thus take the flow dependence into account to some degree. The error equation is applied to all ensemble members at all ranges, assuming no significant model drift (see Figure 99).

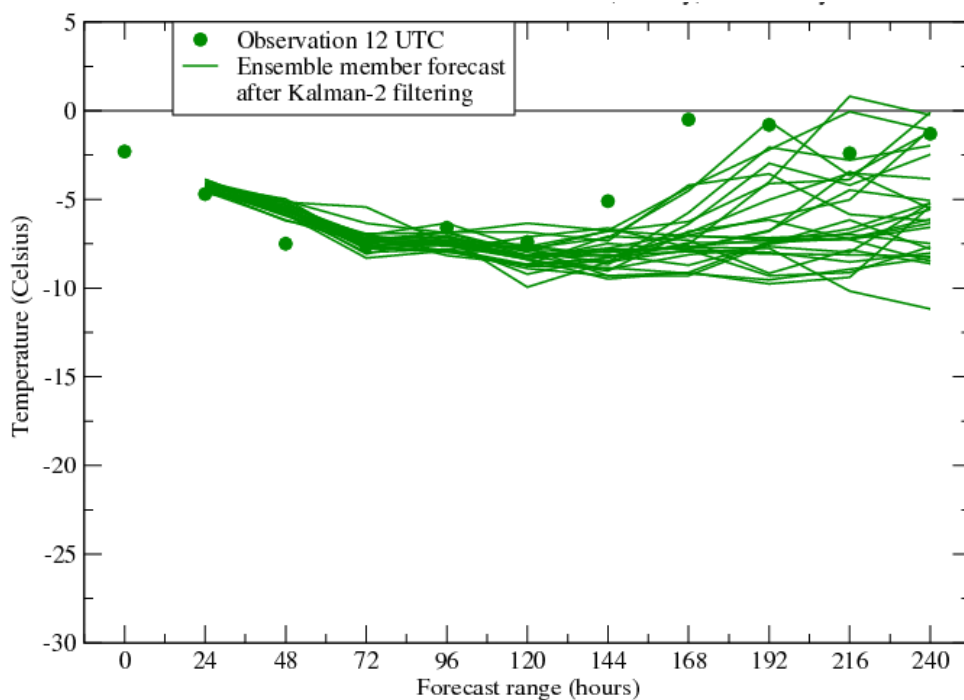


Figure 99: The same as Figure 98 but after the Kalman-filtered errors equation has been applied. Mild forecasts have hardly been modified, whereas cold ones have been substantially warmed, leading to less spread and more realistic probabilities with, for example, 0% probabilities for 2 m temperature < -15°C.

A two- or multi-dimensional error equation is able not only to correct for mean errors, but also systematic over- and under-forecasting of the variability, thereby providing realistic probabilities.

References and further literature

An **ECMWF Newsletter** is published quarterly. It covers topics in meteorology and the operational activities at the Centre, including short descriptions of operational changes to the analysis and forecasting system. The Newsletter is widely distributed and is available at the ECMWF web site <http://www.ecmwf.int/publications/newsletters/>

Proceedings from the Centre's annual seminar and workshops are distributed widely to national weather services and scientific institutions of the meteorological community.

The ECMWF web site www.ecmwf.int is the main repository for its documentation. Comprehensive information on the analysis and forecasting system, the archive and dissemination can be found there. Proceedings from the Centre's annual seminar and workshops are published there, as is ECMWF's series of Technical Memoranda, describing scientific and technical aspects of the Centre's work. Please refer to:

www.ecmwf.int/publications

Useful references mentioned in the User Guide:

www.ecmwf.int/products/forecasts/seasonal/documentation/system4/index.html (Seasonal forecast documentation and User Guide)

Andersson, E. J-N Thépaut, 2008: ECMWF's 4D-Var data assimilation system –the genesis and ten years in operations, ECMWF Newsletter 115, 8-12

Balsamo, G., S. Boussetta, E. Dutra, A. Beljaars, P. Viterbo, B. Van den Hurk, 2011: Evolution of land surface processes in the IFS, ECMWF Newsletter, 127, 17-22.

Bechtold, P., M. Köhler, T. Jung, F. Doblas-Reyes, M. Leutbecher, M. J. Rodwell, F. Vitart, G. Balsamo, 2008: Advances in simulating atmospheric variability with the ECMWF model: from synoptic to decadal time-scales. Q.J.R.Meteorol. Soc., 134, 1337-1351, also available as ECMWF Tech. Memo. 556

Bright, D. and P.A.Nutter, 2004: On the challenges of identifying the "best" ensemble member in operational forecasting, 20th Conference on Weather Analysis and Forecasting/16th Conference on Numerical Weather Prediction, J11.3

Buizza, R., M.Leutbecher, L.Isaksen, J.Haseler, 2010: Combined use of EDA- and SV-based perturbations in the EPS, ECMWF Newsletter 123, 22-28.

Doswell, C.A. III, 2004: Weather forecasting by humans - Heuristics and decision making. Wea. Forecasting, 19, 1115-1126.

Ferranti, L. and S. Corti 2011: New clustering products, ECMWF Newsletter 127, 6-12, Spring 2011

Göber, M., E. Zsótér, D. Richardson, 2008: Could a perfect model ever satisfy a naïve forecaster? On grid box mean versus point verification, Meteorological Applications 15:3, 359–365,

Hamill, T.M., 2003: Evaluating Forecasters' Rules of Thumb: A Study of $d(\text{prog})/dt$, Weather and Forecasting, vol. 18:5, 933-37

Hersbach, H. P. Janssen, 2007: Operational assimilation of surface wind data from the MetOp ASCAT scatterometer at ECMWF, ECMWF Newsletter, 113, 6-8.

Hewson, T.D., 2009: Tracking fronts and extra-tropical cyclones. ECMWF Newsletter. 121, 9-19.

Hewson, T.D. & H.A. Tittley, 2010: Objective identification, typing and tracking of the complete life-cycles of cyclonic features at high spatial resolution. Meteorol. Appl., 17, 355-381.

Isaksen, L., J.Haseler, R. Buizza, M. Leutbecher, 2010: The new Ensemble of Data Assimilations, ECMWF Newsletter 123, 15-21

Jolliffe, I.T. and D.B. Stephenson, D.B. Eds, 2003: Forecast Verification: A Practitioner's Guide in Atmospheric Science, Wiley and Sons, Chichester

Jung, T., G. Balsamo, P. Bechtold, A. Beljaars, M. Köhler, M. Miller, J.-J. Morcrette, A. Orr, M. Rodwell, A. Tompkins, 2010 : The ECMWF model climate: Recent progress through improved physical parametrizations. Quart. J. Roy. Meteor. Soc., 136(650), 1145-1160, doi: 10.1002/qj.63 also available as ECMWF Tech. memo. 623.

Lalaurette F. 2003: Early detection of abnormal weather conditions using a probabilistic extreme forecast index. Quarterly Journal of the Royal Meteorological Society, Volume 129, Issue 594, 3037–3057, Part A

Lewis, J., 1994: Cal Tech's program in meteorology: 1933 – 1948. Bull. Amer. Meteor. Soc., 75, 69 -81, in particular 73-74

Lorenz, E.N., 1970: Forecast for another century of weather progress. A Century of Weather Progress. Amer. Meteor. Soc., 18-24.

Murphy, A.H. 1973: A new vector partition of the probability score. Journal of Applied Meteorology 12 (4): 595–600. <http://ams.allenpress.com/archive/1520-0450/12/4/pdf/i1520-0450-12-4-595.pdf>.

Murphy, A. H. 1986: A New Decomposition of the Brier Score: Formulation and Interpretation, Monthly Weather Review, 114:12, 2671-2673

Miller M., R. Buizza, J. Haseler, M. Hortal, P. Janessen and A. Untch, 2010: Increased resolution in the ECMWF deterministic and ensemble prediction systems, ECMWF Newsletter No. 124 pp.10-16,

Nurmi, P., 2003: Recommendations on the verification of local weather forecasts. ECMWF Tech. Mem. 430.

Palmer, T., R. Buizza, R. Hagedorn, A. Lawrence, M. Leutbecher, and L. Smith, 2006: Ensemble prediction: A pedagogical perspective. ECMWF Newsletter, 106, 10–17.

Persson, A., 1991: Kalman filtering - a new approach to adaptive statistical interpretation of numerical forecasts. Lectures and papers presented at the WMO training workshop on the interpretation of NWP products in terms of local weather phenomena and their verification, WMO, Wageningen, the Netherlands, XX-27-XX-32.

Persson, A and B. Strauss, 1995: On the skill and consistency in medium-range weather forecasts, ECMWF Newsletter 70, 12-15.

Tsonevsky, I and D Richardson, 2012: Application of the new EFI products to a case of early snowfall in Central Europe, ECMWF Newsletter 133, 4.

Wilks, D., 2006: Statistical Methods in the Atmospheric Sciences. 2nd ed. Elsevier, 627 pp.

Zsoter, E., R. Buizza & R. Richardson, 2009: 'Jumpiness' of the ECMWF and UK Met Office EPS control and ensemble-mean forecasts. Mon. Wea. Rev., 137, 3823-3836.

Zsótér, E. 2006: Recent developments in extreme weather forecasting, ECMWF Newsletter 107, 8-1